CHEMICAL MODIFICATIONS OF CORE HISTONES DURING EXIT OF STATIONARY PHASE IN *SACCHAROMYCES CEREVISAE*

Mzwanele Ngubo

SUBMITTED IN ACCORDANCE WITH THE REQUIREMENTS FOR THE DEGREE

MASTER OF SCIENCE

IN THE FACULTY OF AGRICULTURE AND NATURAL SCIENCES

DEPARTMENT OF BIOTECHNOLOGY

UNIVERSITY OF THE FREE STATE

FEBRUARY 2011

Prof. Hugh-George Patterton

ACKNOWLEDGEMENTS

I would like to thank Yaweh, the living God for the grace, wisdom and sanity He has given me throughout the duration of this study. For “I would have lost heart, unless I had believed that I would see the goodness of the Lord in the land of the living.”

To my parents for their unconditional love, support and understanding and allowing me this opportunity – I am forever grateful.

I would also like to express my uninhibited gratitude to my supervisor, Prof. H-G. Patterton, for his support, advice, guidance and the freedom he gave me.

To all my friends and members of the Lab of Epigenomics and DNA Function, thank you for your support, kindness and sometimes counsel. I really appreciate it.

This research was supported by the NRF (National Research Foundation, South Africa) and ABRC (Advance Biomolecular Research Cluster, University of the Free State).

INDEXES

CONTENTS

ABSTRACT

The involvement of histone acetylation in facilitating gene expression is well-established, particularly in the case of histones H3 and H4. It was previously shown in *Saccharomyces cerevisiae* that gene expression was significantly down-regulated and chromatin more condensed in stationary phase compared to exponential phase. We were therefore interested in establishing the acetylation state of histone H3 and H4 in stationary and in exponential phase, since the regulation of this modification could contribute to transcriptional shut-down and chromatin compaction during semi-quiescence. We made use of nano-spray tandem mass spectrometry to perform a precursor ion scan to detect an *m/z* 126 immonium ion, diagnostic of an N^{ε}-acetylated lysine residue that allowed unambiguous identification of acetylated as opposed to tri-methylated lysine. The fragmentation spectra of peptides thus identified were searched with Mascot against the Swiss-Prot database, and the y-ion and b-ion fragmentation series subsequently analyzed for mass shifts compatible with acetylated lysine residues. We found that K9, K14 and K36 of histone H3 and K12 and K16 of histone H4 were acetylated in exponential phase (bulk histones), but could not detect these modifications in histones isolated from stationary phase cells. The corresponding un-acetylated peptides were, however, observed. This result was confirmed by Western analysis (work not presented here). H4K16 acetylation was previously shown to disrupt formation of condensed chromatin *in vitro*.

Keywords: histone tail modifications; lysine acetylation; chromatin compaction; stationary phase; *Saccharomyces cerevisiae*; nuclei isolation; mass spectrometry.

CHAPTER 1

The Role of the Core Histone Tails in Chromatin Compaction.

1.1. Introduction

In the nucleus of invariably all eukaryotes DNA is packaged in a complex of protein and DNA to form chromatin. Compaction of eukaryotic genomes into chromatin is required to fit over a meter of DNA into the limited volume of the cell nucleus. This compacted structure is inherently repressive to the processes that require access to the DNA molecule. The role of higher-order chromatin folding in transcriptional control received significant interest in the early 1980s, but recently this key issue has been seriously revisited (Horn and Peterson, 2002). The total length of genomic DNA is approximately 100,000 times longer than a nucleus' diameter. Therefore, how DNA is packaged and successfully unpackaged, and how this process is regulated, is critical.

Conventional wisdom held that all heredity was specified by the genetic information encoded in the sequence of DNA base pairs, and that fundamental and heritable changes in cell biochemistry required changes in DNA sequence. However, with a more significant understanding of chromatin function, this is now realized not to be the case. The past years have seen the understanding of the role of nucleosomes go beyond their involvement in genomic compaction to more complex functions as the regulatory units of the genome. While there has been considerable evidence that isolated genes can be regulated at the DNA level, there is now strong evidence that genes have additional regulatory switches at the chromatin level. The latter switches are comprised, mostly, by targeted covalent

modifications to the exposed tails of the histone proteins. The recognition of these marks by proteins and multi-subunit complexes in turn influences DNA expression, replication, recombination, and repair (Venkitaraman, 2010; Kwon *et al*., 2000; Schübeler *et al*., 2002).

The misregulation of chromatin structure and concomitant association of non-histone proteins with chromatin was shown to be central to many serious diseased states in humans (Hendrich and Bickmore, 2001). For instance, the chromatin associated tumour suppressor p53 was investigated as one of the possible causes of oesophageal cancer that is predominant among the South African male population in the Eastern Cape (Rheeder *et al*., 1992). It was shown that over-expressed oncogenic Mdm2 directed histone ubiquitination modifications by binding to chromatin in a complex with p53, and in this way may repress p53-activated transcription during oncogenic transformation (Minsky and Oren, 2004). Thus, the importance of histone tail modifications in the maintenance of a healthy physiological homeostasis is clear.

1.2. Histone Structure

The central region of all four core histone proteins share a similar structural motif, constructed from three α-helices connected by two loops, L1 and L2, and is denoted as α1-L1-α2-L2-α3. This “histone-fold” motif is highly conserved, as was seen in structures obtained from organisms as diverse as archaea (Starich *et al*., 1996), insects (Xie *et al*., 1996), birds (Arents *et al*., 1991) and amphibians (Luger *et al*., 1997), presumably because of its unique dimerisation and DNA binding properties. The histones form crescent-shaped (“hand-shake”) heterodimers [H3-H4 and H2A-H2B] that bind 1.7 turns of DNA double helix, which arcs over each dimer of the histone pair to generate a 140 base-pair bend. As the contact surfaces of the heterodimers offset towards the N terminus by one helical turn, the C

terminus of each α2 helix extends further along the long axis than the adjacent N terminus of the paired histone, as is depicted in Figure 1.

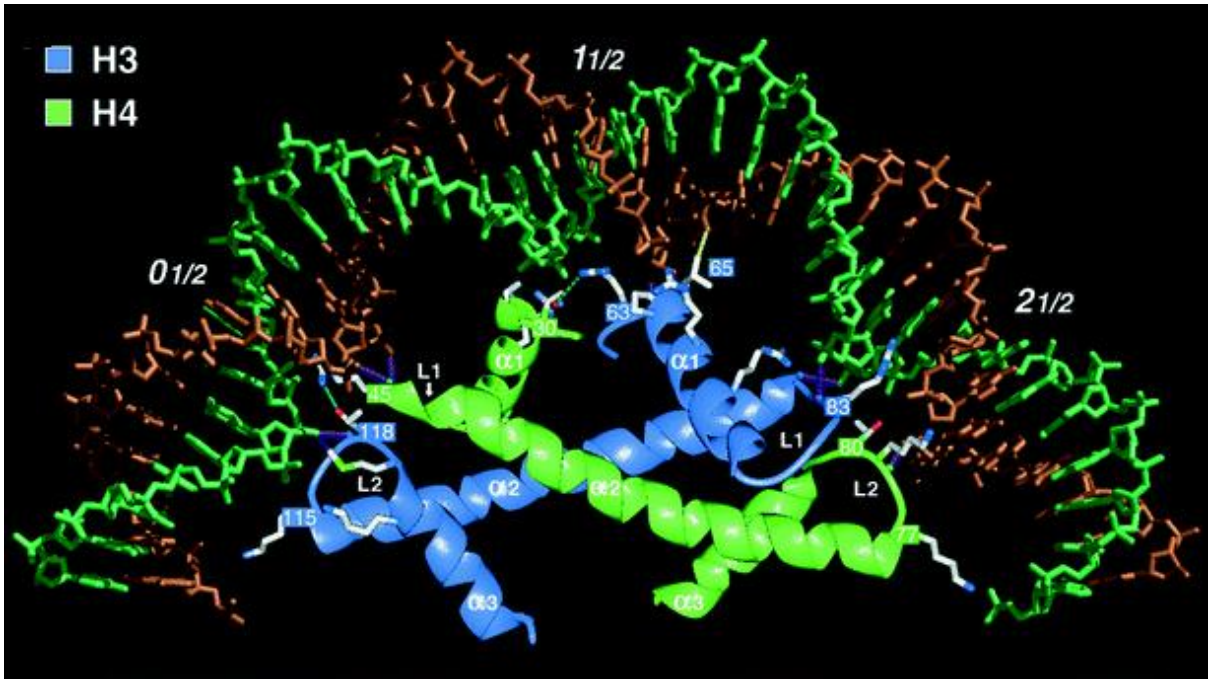

Figure 1. The histone fold domains (α1-L1-α2-L2-α3) of histones H3 and H4, and the cresent-shaped "handshake" of the H3-H4 heterodimer. (Adapted from Luger *et al*., 1997).

The full N-terminal tails do not have a distinct structure in the crystal (Luger *et al*., 1997), suggesting that they are highly flexible. The X-ray crystal structures did, however, show that the H3 and H2B amino-terminal tails passed over and between the gyres of the DNA superhelix in the nucleosome. These tails may contact neighbouring nucleosomes (Luger *et al*., 1997; Davey *et al*., 2002).

1.3. Assembly of Histones into Nucleosomes

Eukaryotic DNA is organized in subunits called nucleosomes, the basic repeating structural element of chromatin. These subunits are formed by the association of about 146 bp of duplex DNA with two copies of each of the core histones H2A, H2B, H3 and H4 (Kornberg, 1974). DNA is bound to the histones through electrostatic forces between the negatively charged phosphate groups on the DNA backbone and positively charged amino acids (e.g., lysine and arginine) in the histone proteins (Wolfe and Grimes, 1993). As the DNA double helix spools around the histone octamer to create a nucleosome core, it contacts the histone surface at 14 sites with clusters of hydrogen bonds and salt links (Luger and Richmond, 1998). Communally, these weak interactions render the nucleosome a stable particle.

Previous work has shown that chromatin assembly is a step-wise process involving the association of a tetramer of histone H3-H4 with the DNA followed by the incorporation of H2A-H2B dimers to form the nucleosome (van Holde, 1988). Additionally, linker histone H1 binds to approximately 20bp of DNA in between nucleosomes augmenting the compaction of the chromatin polymer (Garcia *et al*., 2007). Through an ill-defined hierarchical series of compaction steps involving histone tails, nucleosome-nucleosome interactions are formed both within and between individual nucleosomal arrays. This results in the formation of the 30 nm chromatin fibre. The nucleosome, in its role as the principal packaging element of DNA within the nucleus, is the primary determinant of DNA accessibility (Belmont and Bruce, 1994).

1.4. Chemical Modifications of the Core Histone Tails

1.4.1. Enzymes Involved in Histone Modifications and their Physiological Roles

The post-translational modifications of the core histone tails are catalyzed by numerous different enzymes, such as kinases, histone methyltransferases (HMTases), protein R methyltransferase (PMRT) and histone acetyltransferases (HATs) (McManus and Hendzel, 2006). There are at least 35 different residues within the tails that serve as substrates for at least 31 post-translational modifications (Bonaldi *et al*., 2004; Zhang *et al*., 2003). The chemical modifications may function by two characterized mechanisms: the first is the disruption of the interactions between nucleosomes in order to ‘‘unravel’’ chromatin, and the second is the provision of molecular surfaces recognized by other proteins, thereby recruiting non-histone proteins. A large number of papers have suggested that numerous proteins, thus far considered to be transcriptional activators, co-activators, or repressors, were actually enzymes that covalently modified the histone N-termini (Wade and Wolffe, 1997; Pazin and Kadonaga, 1997). It was also shown that a number of transcriptional regulators had high homology to the subunits of both HATs and HDACs (Brownell, 1996). To date, the most studied modifications of histones are acetylation, ubiquitination, methylation, phosphorylation, sumoylation and ADP-ribosylation.

1.4.2. Lysine Acetylation

A number of acetylation sites in yeast histones have been identified by mass spectrometry and the use of specific antibodies against specific sites of acetylation (Kouzarides, 2007;Suka *et al*., 2001). In euchromatin H4 lysines 5, 8 and 12 are predominantly bound by a bromodomain of a transcriptional activation factor. This has strengthened the long held belief that acetylation enhances transcription (Johnson *et al*., 1998). Acetylation of histone H4 lysine 16 was found to regulate both chromatin structure and the physiological cooperation between recruited non-histone proteins and the chromatin fibre (Shogren-Knaak *et al*., 2006).

Histone acetylation is catalyzed by a class of enzymes known as histone acetyltransferases (HATs), which use acetyl-CoA as a substrate to acetylate specific lysine residues within histones. Numerous multi-protein complexes have been identified that possess HAT activity. These complexes generally consist of one protein that serves as the catalytic subunit, and supporting proteins that serve to potentiate, regulate, or target the HAT activity to specific locations within the genome. In *Saccharomyces cerevisiae* the typical example is the 1.8-MDa SAGA complex which has a Gcn5-dependent HAT activity, and contains at least three distinct groups of gene products (Bonenfant *et al*., 2006; Turner, 2000). The first of these are the Ada proteins isolated as proteins that interact functionally with the transcription factor Gcn4 and the activation domain. The second group comprises all members of the TBP-related set of Spt proteins, except Spt15. The third group within SAGA includes a subset of TBP- associated factors (Clayton *et al*., 2000; Grant *et al*., 1998). Nuclear HATs (Brown *et al*., 2000; Marmostein, 2001) generally function to regulate chromatin structure and gene transcription by neutralizing the positive charge associated with lysine residues at physiological pH.

The reverse reaction is carried out by histone deacetylases (HDACs), which mediate transcriptional repression (Kouzarides, 2002). Moreover, acetylation in a specific manner can also regulate DNA replication, histone deposition, and DNA repair by recruiting proteins that have an acetyl-lysine binding module, the bromodomain (Khorasanizadeh, 2004).

Studies in animal cells have shown that equilibrium between acetylation and deacetylation can tilt rapidly in response to stimuli that switches genes off or on (Imai *et al*., 2000). Acetyl groups are repeatedly introduced and taken off histones, with turnover half-lives ranging in the order of minutes to hours when different chromatin fractions are studied by radioactive acetate incorporation in cultured cells (Hendzel and Davie, 1991).

1.4.3. Lysine and Arginine Methylation

Previous studies have demonstrated that several lysine residues, including lysines 4, 9, 27, and 36 of H3 and lysine 20 of H4, are predominant sites of methylation (van Holde, 1988; Strahl *et al*., 1999). Different histone methylation states are associated with different chromatin functions, and early experiments proposed that H3 Lys4 methylation was linked to active genes, whereas H3 Lys9 methylation was linked to inactive genes (Lachner and Jenuwein, 2002). However, in budding yeast, Set1-mediated methylation of H3 Lys4 is involved in rDNA silencing and H3 Lys4 methylation is enriched in silenced regions (Briggs *et al*., 2001; Bryk *et al*., 2002).

The SET domain contains the enzymatic activity responsible for lysine methylation of histone tails, and was shown to be responsible for methyl transfer from *S*-adenosylmethionine

(AdoMet) to the histone lysine side-chain nitrogen (ε-NH_2) (Rea *et al*., 2000). Histone methylation has important roles in regulating gene expression and forms part of the epigenetic memory system that regulates cell fate and identity. Lysine methylation is directly implicated in epigenetic inheritance. Methylation of specific arginines in histones H3 and H4 correlate with the active state of transcription (Zhang and Reinberg, 2001).

The catalytic module that methylates specific arginines is known as a protein R methyltransferase (PRMT) domain, and was linked to transcriptional activation. Methylation of histone H3 arginine residue 3 by PMRT1 allowed subsequent acetylation of histone tails by p300 (Wang *et al*., 2001). In another publication, Rice and colleagues showed that mono-methylation (me1) and di-methylation (me2) at histone H3 lysine 9 (H3 K9me1 and H3 K9me2) were localized to silenced euchromatin, whereas tri-methylation (H3 K9me3) was predominantly found at pericentric heterochromatin. Although, the functional importance of mono-, di-, and tri-methylation of lysine residues is poorly understood, it is tempting to speculate that the elevated levels of H3 lysine 9 methylation may function to stabilize the silenced regions of heterochromatin (Rice *et al*., 2003).

1.4.4. Serine and Threonine Phosphorylation

The proper segregation of chromosomes is an essential step in the accurate execution of each cell cycle and requires the precise coordination of a large number of events governing chromosome and microtubule dynamics (Nurse, 2000). One of these events is the ordered inter-conversion between extended interphase chromatin and highly compacted mitotic chromosomes. Phosphorylation of histone H3 and linker histone H1 has long been known to correlate with chromosome condensation during mitosis (Bradbury *et al*., 1973; Gurley *et al*., 1974). In fact, mutational studies have shown that the phosphorylation of histone H3 at

Ser10 and at Ser28 correlated with mitosis and chromosome condensation (Hsu *et al*., 2000). Recent data even suggest that one of the mechanisms by which H3 Ser10 phosphorylation may function is via the displacement of HP1, which recognizes Lys9 methylation in H3, which is normally associated with condensed chromatin (Fischle *et al*., 2003). Other serine phosphorylation sites were also identified on histones H4, H2A, and H2B (Cheung *et al*., 2000). Serine 10 phosphorylation on histone H3 is also linked to the activation of transcription. When mammalian cells were exposed to a mitogen or stress, the time course of this phosphorylation corresponded to the transient expression of activated "immediate-early" genes (Thomson *et al*., 1999). The kinases that phosphorylate H3 are Aurora-B/Ipl1, PKA, Rsk-2, and Msk1, which tend to add a phospate group to the targeted Ser/Thr sites that are surrounded by basic residues (Hsu *et al*., 2000). Phosphorylation is reversed by the protein phosphatase 1 (PP1) family of enzymes (Hsu *et al*., 2000).

1.4.5. Lysine Ubiquitination

The linking of ubiquitin or a small ubiquitin-related modifier, sumo, to a specific lysine residue in histones plays an important role in regulating transcription either through proteosome-dependent degradation of transcription factors or other mechanisms related to the recruitment of modification complexes. While histone ubiquitination has typically been attributed to the positive control of transcription (Bonaldi *et al.,* 2004), recent studies indicated that sumoylation of histone H4 was important for transcriptional repression (Shiio and Eisenman, 2003).

The ubiquitin attachment is a three step process involving E1 activating, E2 conjugating and an E3 ligase enzyme. In general, ubiquitination is initiated when ubiquitin-activating enzyme E1 first activates ubiquitin. Activated ubiquitin is then transferred to a cysteine residue of the

ubiquitin-conjugating enzymes (E2). In the last step, an iso-peptide bond is formed between ubiquitin and a lysyl ε-amino group within a substrate protein. This step can be catalyzed either directly by the E2, or is facilitated by a third enzyme called the ubiquitin-protein ligase (E3). Proteins targeted for poly-ubiquitination commonly contain a degradation motif termed a degron, which is recognized by the E3 (Caron *et al*., 2005). Poly-ubiquitinated protein targets are recognized and degraded by the 26S proteasome. Additionally, H2B ubiquitination has been illustrated through mutational studies to be important for methylation of lysines 4 and 79 in histone H3 (Sun and Allis, 2002).

1.4.6. ADP Ribosylation

The functional role of the ADP ribosylation of histones is not well understood. Proteins can be singly (mono) or multiply (poly) ADP ribosylated. Enzymes that mediate the modification are Mono-ADP ribosyltransferases (MARTs) and poly-ADP-ribose polymerases (PARPs) (Hassa *et al*., 2006). Poly-ADP-ribosylation of histones and several other nuclear proteins seem to participate in nuclear processes involving the repair of DNA strand breaks, replication or recombination. PARPs, for instance, are activated by DNA strand breaks. It was also proposed that the PARP-associated polymers may recruit proteins that act as molecular "flags" to sites of DNA breaks. In addition, the Sir family of NAD-dependent histone deacetylases was shown to have low levels of ADP ribosyltransferase activity. There are many reports of ADP ribosylation of histones, but only one site was definitively mapped: H2B ADP ribosylation at Glu2 (Oraga *et al*., 1980). Experimental evidence that may link ADP-ribosyltransferase catalytic activity to transcription is sparse. Nonetheless, recently a role for PARP-1 activity in transcription was demonstrated under conditions where DNA repair was induced (Kraus and Lis, 2003).

1.5. Histone Code

The histone code hypothesis proposes that the combinatorial pattern of N-terminal modifications of histones provides an identity to each nucleosome that the cell interprets as a code from the genome to regulate various cellular processes (Nowak and Corces, 2004). These modifications occur on multiple and specific residues, and the combinatorial modification profiles of histones suggest that the modification sites can act as binding surfaces for specific proteins that recognize these particular marks, leading to active or silenced genomic regions (Jenuwein and Allis, 2001). The hypothesis predicts that (i) distinct modifications of the histone tails will change the affinities of non-histone proteins for chromatin, and (ii), modifications on the same or different histone tails may be inter-dependent and generate various combinations on any one nucleosome. The enzymes that recognise and act upon these histone tail modifications are highly specific for particular amino acid positions (Strahl and Allis, 2000; Turner, 2000), thereby extending the information content of the genome beyond simply the sequence of nucleotides in the genome. This additional level of information associated with chromatin is known as epigenetics, and includes chemical modifications of the DNA molecule such as methylation of cytosines as well.

Mechanical communication between modifications may occur at several different levels. For example, the histone H3 N-terminus appears to exist in two distinct modification states that are likely to be regulated by a “switch” between Lys9 methylation and Ser10 phosphorylation. Ser10 phosphorylation inhibits Lys9 methylation (Rea *et al*., 2000) but is synergistically coupled with Lys9 and/or Lys14 acetylation during mitogenic and hormonal stimulation in mammalian cells (Cheung *et al*., 2000; Lo *et al*., 2000; Clayton *et al*., 2000). In the phosphorylated-acetylated state, the modified H3 tail marks transcriptional activation.

Conversely, aberrant Lys9 methylation antagonizes Ser10 phosphorylation, leading to mitotic chromosome dysfunction (Rea *et al*., 2000; Turner *et al*., 1992). Additionally, the catalytic activity of an enzyme could be compromised by modification of its substrate recognition site, for example isomerization of H3 Pro38 affects methylation of H3 Lys36 by Set2 (Nelson *et al*., 2006).

Work over the past years provided an example of a modification on one histone tail governing another modification on a different tail *in trans*. Two different groups reported that ubiquitination of histone H2B is required for Set1-dependent methylation of H3 Lys4 in budding yeast (Sun and Allis, 2002; Dover *et al*., 2002). Deletion of RAD6, whose gene product is responsible for ubiquitination of histone H2B at Lys123, abolished H3 Lys4 methylation (Dover *et al*., 2002). Similarly, the H2B K123R mutation blocked H3 Lys4 methylation and impaired telomeric silencing. By contrast, Lys4 mutations did not cause the loss of H2B ubiquitination, suggesting that H3 Lys4 methylation does not govern H2B Lys123 ubiquitination (Lizuka and Smith 2003).

1.6. ATP - Dependent Chromatin Remodelers

The H4 domain consisting of amino acid residues 16–29, which take part in gene silencing, was proposed to form an α-helix that was required to form a repressive chromatin structure (Johnson *et al*., 1992). This induced α-helix of the N- termini of histones was suggested to interact directly either with a specific protein such as Sir3 or with the DNA molecule itself (Ebralidse *et al*., 1988). Acetylation of lysine residues in the N termini of the core histones has long been associated with transcriptionally active chromatin. The one view adopted by the chromatin community has been that the highly charged tails interacted strongly with DNA

when not acetylated, whilst acetylation liberated them from this interaction, and thus exposed the DNA molecule to transcription factors. A different view is that it is not the DNA molecule that becomes more accessible with acetylation of the N-terminal tails, but the N-terminal tails themselves that become accessible to other types of modifications and silencing regulators (Varga-Weisz *et al*., 1997). Nonetheless, both these views seem to suggest that acetylation exposed the histone molecule to non-histone proteins that may alter chromatin structure and thus reprogram DNA functionality. Therefore, acetylation plays an early role by relaxing higher order chromatin structure, thereby providing access to transcription factors and the large multi-protein nucleosome ATP-dependent remodelling complexes such as SWI/SNF (Varga-Weisz *et al*., 1997).

Remodelling enzymes that are involved in nucleosome structure alterations use the energy supplied by ATP hydrolysis to disrupt nucleosome structure. ATP is required as a positive cofactor for chromatin assembly, most likely because of its participation in phosphoryl-transfer reactions. Cdc9p, the ATP-dependent DNA ligase I of yeast (Johnston and Nasmyth, 1978; Kornberg and Baker, 1992), plays a role in template repair during assembly. Some remodelling factors have been shown to disrupt nucleosomes in a way that leads to histone octamer transfer to a separate segment of DNA (Lorch *et al*., 1999; Phelan *et al*., 2000). In all cases the movement of nucleosomes may either increase or reduce the accessibility of a site for DNA binding proteins such as transcription factors. All known classes of chromatin remodelling ATPases are recruited to specific sites such as promoters by direct interaction with sequence specific DNA binding proteins, such as transcription factors. Additionally, the ATP-dependent chromatin remodelling factors cooperate with histone modifying enzymes such as histone acetyltransferases (HATs) and deacetylases (HDACs) in the remodelling of gene promoters. HATs add acetyl groups to lysines at the amino termini of the core histones at such loci, a reaction usually associated with activation of gene expression (Brown *et al*., 2000; Howe *et al*., 1999; Imhof and Wolffe 1998).

Many chromatin remodelling factors have domains in one or more of their subunits that may be involved in recognizing modified histones. One such domain is the bromodomain, which recognises acetylated lysine in different sequence contexts, and is found in many chromatin remodelling factors, including the Swi2 ATPase of the SWI/SNF complex, the Sth1 ATPase of the RSC complex, and ACF1, a protein that interacts with the ISWI ATPase. This domain was also studied in several HATs, where it interacted specifically with acetylated histone tails (Dhalluin *et al*., 1999; Jacobson *et al*., 2000; Ornaghi *et al*., 1999). Therefore, it may serve in the communication between histone acetylation and the chromatin remodelling process in general.

1.7. Histone Core Domain Modifications

The use of mass spectrometry to scrutinize histone post-translational modifications (PTMs) identified H3 lysine 79 methylation and numerous other modifications in the core (histone fold) domains (Cocklin and Wang, 2003; Zhang *et al*., 2002). Mapping of the positions of these core modifications onto the nucleosome crystal structure showed that these modifications fell into groups that could be organized into three distinct classes: (i) the solute accessible face, (ii) the nucleosome lateral surface and (iii) the histone–histone contact sites (Freitas *et al*., 2004; Cosgrove *et al*., 2004). It is likely that modifications in these classes will have unique effects on chromatin structure and act through mechanisms that are distinct from those observed with tail domain modifications. The locations and the evolutionary conservation of the residues involved in these modifications predict that they may be of great physiological relevance. The limited data available concerning these modifications support this idea and suggest that histone core domain modifications may turn out to play as

significant a role as modifications of the histone tails. The different classes of core domain modifications are discussed below.

1.7.1. Solute Accessible Face

Similar to the situation observed with histone tail modifications, modifications located on the solute accessible face of the nucleosome have the ability to alter higher-order chromatin structure and chromatin–protein interactions (Mersfelder and Parthun, 2006). Histone lateral surface modifications are uniquely capable of affecting histone-DNA interaction, and modifications on the histone–histone interface have the exclusive ability to disrupt intra-nucleosomal, interactions thereby altering nucleosome stability. Mutations that alter sites of histone tail modifications have been shown to affect processes such as transcription, heterochromatic silencing and DNA damage repair; however, the effects in many cases were minor (Ma *et al*., 1998). Single amino acid substitutions of modifiable residues within the histone core have been shown to dramatically affect transcription, DNA damage repair, chromatin structure, chromatin assembly and heterochromatic gene silencing (van Leeuwen *et al*., 2002; Ng *et al*., 2002; Masumoto *et al*., 2005). Specific regions of the nucleosome surface are critical for the assembly of a silent chromatin structure in yeast, and contacts between surface residues of histones H2A and H2B may mediate the inter-nucleosome interactions involved in the formation of higher order chromatin structures (Park and Szostak, 1990; Schalch *et al*., 2005). Therefore, modifications to this surface may function through a number of mechanisms to regulate chromatin structure. First, they may function similarly to the N-terminal tail modifications by controlling the ability of non-histone proteins to bind to the nucleosome. Additionally, modifications to the nucleosome face may have

more direct structural effects by influencing nucleosome–nucleosome interactions that are thought to occur during the formation of the 30 nm chromatin fibre.

Histone H3 Lys79 methylation is the most well-characterized modification of the nucleosome face. This modification was observed in a number of organisms including yeast, calf thymus, human and chicken (van Leeuwen *et al*., 2002). This evolutionary conservation in such a wide variety of eukaryotes is a strong indication that it played a fundamental role in the regulation of chromatin structure (Mersfelder and Parthun, 2006).

1.7.2. Histone Lateral Surface

Several of the newly identified core modifications were mapped to residues that are involved in direct contacts with the DNA molecule, while others were positioned in close proximity to the DNA. The position of modifications on the lateral surface of the nucleosome immediately suggested that their primary function would be through the regulation of histone–DNA interactions (Freitas *et al*., 2004). A chromatin remodelling activity (either an ATP-dependent chromatin remodeler or nucleosome assembly/disassembly activity) acts on a nucleosome to alter histone–DNA contacts such that sites of modification on the lateral surface are exposed. The exposed sites can then be acted on by histone modifying activities to either add or remove post-translational modifications which, in turn, lead to nucleosomes with altered mobility, similar to a spool slipping more easily along a rope wound around it. This altered mobility can then lead to changes in the accessibility of specific sequences of DNA or changes in higher order chromatin structure. A lysine within the core domain of H3 (K56) has recently been found to be acetylated (Xu *et al*., 2005). The lysine 56 residue is facing toward

the major groove of the DNA within the nucleosome, so it is in a particularly good position to affect histone-DNA interactions when acetylated.

1.7.3. Histone-Histone Interfaces

At a very basic level, chromatin structure is dependent upon specific histone–histone interactions that lead to the formation of the histone octamer. These histone–histone interactions include those that mediate the formation of the H3/H4 and H2A/H2B histone fold pairs, those that allow the formation of the H3/H4 tetramer, and those between tetramers and H2A/H2B dimers that result in formation of the histone octamer. In this model, the modification of residues at points of histone–histone contact would influence chromatin structure by directly impacting the structure of the histone octamer. The best example of a PTM that functions through structural effects on the histone octamer is the acetylation of histone H4 lysine 91 which was first identified by mass spectrometric analysis of bovine histones (Brown *et al*., 2000; Zhang and Freitas, 2004). Lysine 91 is in the region of histone H4 that interacts with histone H2B and helps to stabilize the tetramer–dimer interaction necessary for the formation of the histone octamer (Santisteban *et al*., 1997). This PTM seems highly conserved, because it was also identified in yeast (Ye *et al*., 2005). The association of histone H4 acetylated on lysine 91 with proteins involved in histone deposition suggested that this modification occurred prior to chromatin assembly (Ye *et al*., 2005).

1.8. Role of Core Histone Tails in Chromatin Compaction

Studies conducted to date have shown that the histone N-terminal tail regions were of critical importance to the folding of nucleosome arrays and that the H3-H4 tetramer tails play a more important role than the H2A–H2B dimer tails (Krajewski and Ausió, 1996; Dorigo *et al*., 2003; Kan *et al*., 2007).

1.8.1. Position of Tails During Compaction

It was found that the tails played a crucial role in the electrostatic nucleosome-nucleosome and nucleosome-linker DNA interaction within a chromatin fibre, stabilizing the fibre at physiological ionic strength (Mühlbacher *et al*., 2006). It was suggested by Arya and Schlik that the electrostatic interactions in compact chromatin could only be achieved if the strong DNA-DNA repulsion as well as the entropic penalty associated with folding were relieved (Arya and Schlik, 2006). H4 histone tails mediate inter-nucleosomal interactions, especially in condensed chromatin folded into a 30 nm fibre in the presence of linker histone H1. The requirement for the histone tails to condense chromatin decreases in the order H4 > H3 > H2A > H2B. The H2A and the H4 tails extend in a direction normal to the nucleosomal plane because of their origin on the flat face of the nucleosome core (see Figure 2).

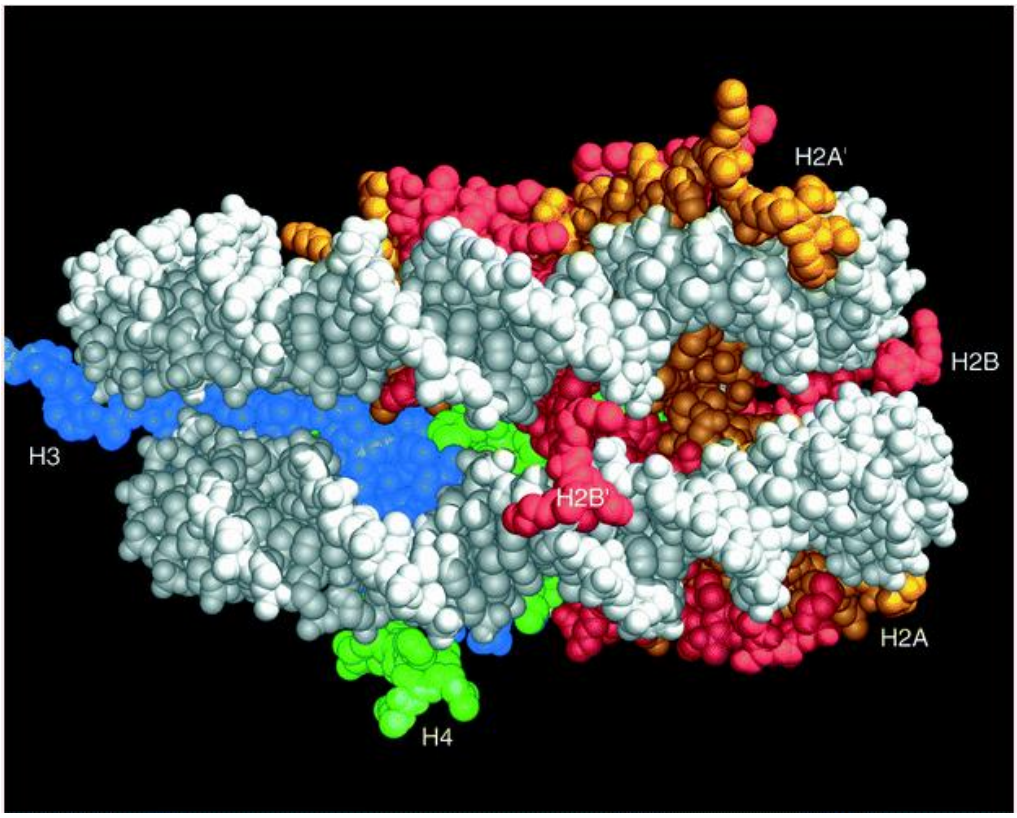

Figure 2. Position of histone N-terminal tails in the nucleosome. The nucleosome is shown with the pseudo two-fold axis of symmetry approximately perpendicular to the plane of the page. Where the tails from both copies of a histone in the octamer are visible, the tails are distinguished by a prime designation.The H2B (red) and H3 (blue) N-terminal tails pass though channels in the DNA superhelix (white). The other histones, H2A (yellow) and H4 (green) are indicated. (Adapted from Luger *et al*., 1997).

The longer H4 tails reaches further outwards compared to the H2A tails. Even though the N-termini of the H2A histones also originate on the flat portion of the nucleosome core, they cannot mediate inter-nucleosomal interactions to the same extent as the H4 tails because of their slightly shorter length and distant location from the linker DNAs (Arya and Schlick, 2006), where the latter is located on the inside of the 30nm fibre. On the other hand, the H2B and H3 tails, which originate from the curved side of the nucleosome core between the

supercoil gyres, spread predominantly along the nucleosomal plane. The H3 tails, in particular, tend to remain close to the position where the linker DNA enters and exits the nucleosome.

The histone H4 residue 16–25 region, which includes the acetylation site at lysine 16, makes multiple interactions with acidic side chains of H2A and H2B from an adjacent nucleosome in the crystal (Luger *et al*., 1997). The region of the H4 tail, which mediates compaction, is located in the stretch of amino acids 14–19 (Dorigo *et al*., 2003). It was also reported that a similar interaction could theoretically occur between adjacent nucleosomes in the solenoidal model of the 30 nm fibre (Finch and Klug, 1976). Acetylation may therefore be involved in disruption of the 30 nm higher-order chromatin structure, as opposed to disruption of the nucleosome structure itself (Dutnall and Ramakrishnan, 1997). The affinity of the cross-bridge formed by the H4 tail to the open face of the adjacent nucleosome in the 30 nm fibre is expected to be reduced by successive acetylation of the H4 lysines 5, 8, 12 and 16.

Core histones have also been shown to interact with histone H1 (van Holde and Zlatanova, 1996), and it is not unreasonable to suggest that these interactions involve mainly the protruding tails of the core histones. If the core histone tails interacted with both the linker DNA and the linker histones, one might expect these interactions to affect fibre structure. Indeed, numerous physical studies of partially trypsinised chromatin from which the core histone tails had been removed have reported such a connection (Allan *et al*., 1982; Chatterjee and Walker, 1973; Saccone *et al*., 1983).

1.8.2. Tail Modifications and Mechanisms that may Influence Chromatin Compaction

The influence of the core histone tails on the compaction and dynamics of the chromatin fibre is undoubtedly multi-faceted. Firstly, they may play a structural role in the compaction and the higher-order structure of chromatin. Secondly, the covalent modifications of core histone tails may be marked for signalling cascades. Thirdly, they may facilitate exclusion of proteins from the DNA molecule. Fourthly, the tails may also link separate fibres and form contacts with additional structures such as the nuclear scaffold or nucleolar framework in the nucleus. It has been hinted that the H4 tail was the most important for chromatin fibre condensation in the absence of other factors, whereas the tails of H2A, H2B and H3 most likely contributed to the other processes mentioned above (Dorigo *et al*., 2003).

The positively charged histone tails provide the necessary driving force for folding by mediating favourable inter-nucleosomal interactions and screening DNA-DNA repulsion (Arya and Schlick, 2006). The role of acetylation in releasing DNA bound in chromatin is more likely to be destabilization of the chromatin higher order structures than of the nucleosome itself (Luger *et al*., 1997).

Post-translational modifications of the histone tails are intimately associated with regulating chromatin structure: phosphorylation of histone H3 is linked to proper chromosome condensation and dynamics during mitosis, while multiple H2B, H3 and H4 tail acetylation groups destabilize the chromatin fibre and are sufficient to decondense chromatin fibres *in vitro*. Qualitative analysis demonstrated the potential for cell cycle dependent changes in both phosphorylation and acetylation of histones. It was also demonstrated that some modifications (PhosS10, PhosS28, AcK14, AcK9/PhosS10 and PhosS10/AcK14) increased as cells entered mitosis, while acetylation of Lys9 were lost. Because the abundance of

phosphorylation of Ser10 increased dramatically during mitosis, it is often referred to as a mitosis-specific marker (McManus and Hendzel, 2006). Although the dynamics of specific histone acetylation events are unknown for the whole genome, evidence suggested that many residues may rapidly become deacetylated upon entry into mitosis (Kruhlak *et al*., 2001). The mitosis-specific phosphorylation of histone tails clearly underlines the importance of tails and tail modifications in chromatin condensation and hence chromosome kinetics.

1.9. Problem Statement and Aim

Informative studies were undertaken to understand the role of histone tails in the higher order structure of chromatin *in vitro* using reconstituted nucleosome arrays, but little work has been published reporting on the interplay between histone tail modifications and chromatin structure in a living cell.

Genome-wide protein binding and compaction studies have illustrated that the yeast linker histone swiftly dissociated from chromatin when the cell exited stationary (G_0) phase, and that this occurred concomitantly with the genome-wide decondensation of chromatin (Schäfer *et al*., 2008). In addition, general induction of many genes occurred during stationary phase exit. The transition from stationary to exponential phase in *Saccharomyces cerevisiae* is therefore an ideal cellular transition during which to study the interplay between histone modifications, chromatin compaction, and transcriptional reprogramming of the genome.

In this project we investigated the reversible modifications that occurred on the N-terminal tails of histones H2A, H2B, H3 and H4 during exit of stationary phase in the model organism

S. cerevisiae, as part of a programme to understand the role of these modifications in the regulation of DNA function in a living cell.

1.10. Reference List

J. Allan, N. Harborne, D. C. Rau, and H. Gould. Participation of core histone "tails" in the stabilization of the chromatin solenoid. *J.Cell Biol.* 93 (2):285-297, 1982.

A. T. Annunziato, L. L. Frado, R. L. Seale, and C. L. Woodcock. Treatment with sodium butyrate inhibits the complete condensation of interphase chromatin. *Chromosoma* 96 (2):132-138, 1988.

G. Arents, R. W. Burlingame, B. C. Wang, W. E. Love, and E. N. Moudrianakis. The nucleosomal core histone octamer at 3.1 Å resolution: a tripartite protein assembly and a left-handed superhelix. *Proc.Natl.Acad.Sci.U.S.A* 88 (22):10148-10152, 1991.

G. Arya and T. Schlick. Role of histone tails in chromatin folding revealed by a mesoscopic oligonucleosome model. *Proc. Natl. Acad. Sci.U.S.A* 103 (44):16236-16241, 2006.

A. S. Belmont and K. Bruce. Visualization of G1 chromosomes: a folded, twisted, supercoiled chromonema model of interphase chromatid structure. *J.Cell Biol.* 127 (2):287-302, 1994.

T. Bonaldi, A. Imhof, and J. T. Regula. A combination of different mass spectroscopic techniques for the analysis of dynamic changes of histone modifications. *Proteomics* 4 (5):1382-1396, 2004.

D. Bonenfant, M. Coulot, H. Towbin, P. Schindler, and J. van Oostrum. Characterization of histone H2A and H2B variants and their post-translational modifications by mass spectrometry. *Mol.Cell Proteomics* 5 (3):541-552, 2006.

E. M. Bradbury, R. J. Inglis, H. R. Matthews, and N. Sarner. Phosphorylation of very-lysine-rich histone in *Physarum polycephalum*. Correlation with chromosome condensation. *Eur.J.Biochem.* 33 (1):131-139, 1973.

S. D. Briggs, M. Bryk, B. D. Strahl, W. L. Cheung, J. K. Davie, S. Y. Dent, F. Winston, and C. D. Allis. Histone H3 lysine 4 methylation is mediated by Set1 and required for cell growth and rDNA silencing in *Saccharomyces cerevisiae*. *Genes Dev.* 15 (24):3286-3295, 2001.

C. E. Brown, T. Lechner, L. Howe, and J. L. Workman. The many HATs of transcription coactivators. *Trends Biochem.Sci.* 25 (1):15-19, 2000.

J. E. Brownell, J. Zhou, T. Ranalli, R. Kobayashi, D. G. Edmondson, S. Y. Roth, and C. D. Allis. *Tetrahymena histone* acetyltransferase A: a homolog to yeast Gcn5p linking histone acetylation to gene activation. *Cell* 84 (6):843-851, 1996.

M. Bryk, S. D. Briggs, B. D. Strahl, M. J. Curcio, C. D. Allis, and F. Winston. Evidence that Set1, a factor required for methylation of histone H3, regulates rDNA silencing in *S. cerevisiae* by a Sir2-independent mechanism. *Curr.Biol.* 12 (2):165-170, 2002.

C. Caron, C. Boyault, and S. Khochbin. Regulatory cross-talk between lysine acetylation and ubiquitination: role in the control of protein stability. *Bioessays* 27 (4):408-415, 2005.

S. Chatterjee and I. O. Walker. The modification of deoxyribonucleohistone by trypsin and chymotrypsin. *Eur.J.Biochem.* 34 (3):519-526, 1973.

P. Cheung, C. D. Allis, and P. Sassone-Corsi. Signaling to chromatin through histone modifications. *Cell* 103 (2):263-271, 2000.

P. Cheung, C. D. Allis, and P. Sassone-Corsi. Signaling to chromatin through histone modifications. *Cell* 103 (2):263-271, 2000.

P. Cheung, C. D. Allis, and P. Sassone-Corsi. Signaling to chromatin through histone modifications. *Cell* 103 (2):263-271, 2000.

A. L. Clayton, S. Rose, M. J. Barratt, and L. C. Mahadevan. Phosphoacetylation of histone H3 on c-fos- and c-jun-associated nucleosomes upon gene activation. *EMBO J.* 19 (14):3714-3726, 2000.

A. L. Clayton, C. A. Hazzalin, and L. C. Mahadevan. Enhanced histone acetylation and transcription: a dynamic perspective. *Mol.Cell* 23 (3):289-296, 2006.

R. R. Cocklin and M. Wang. Identification of methylation and acetylation sites on mouse histone H3 using matrix-assisted laser desorption/ionization time-of-flight and nanoelectrospray ionization tandem mass spectrometry. *J.Protein Chem.* 22 (4):327-334, 2003.

M. S. Cosgrove, J. D. Boeke, and C. Wolberger. Regulated nucleosome mobility and the histone code. *Nat.Struct.Mol.Biol.* 11 (11):1037-1043, 2004.

C. A. Davey, D. F. Sargent, K. Luger, A. W. Maeder, and T. J. Richmond. Solvent mediated interactions in the structure of the nucleosome core particle at 1.9 Å resolution. *J.Mol.Biol.* 319 (5):1097-1113, 2002.

J. G. de Nobel, F. M. Klis, J. Priem, T. Munnik, and Ende H. van den. The glucanase-soluble mannoproteins limit cell wall porosity in *Saccharomyces cerevisiae*. *Yeast* 6 (6):491-499, 1990.

C. Dhalluin, J. E. Carlson, L. Zeng, C. He, A. K. Aggarwal, and M. M. Zhou. Structure and ligand of a histone acetyltransferase bromodomain. *Nature* 399 (6735):491-496, 1999.

B. Dorigo, T. Schalch, K. Bystricky, and T. J. Richmond. Chromatin fiber folding: requirement for the histone H4 N-terminal tail. *J.Mol.Biol.* 327 (1):85-96, 2003.

J. Dover, J. Schneider, M. A. Tawiah-Boateng, A. Wood, K. Dean, M. Johnston, and A. Shilatifard. Methylation of histone H3 by COMPASS requires ubiquitination of histone H2B by Rad6. *J.Biol.Chem.* 277 (32):28368-28371, 2002.

J. Dover, J. Schneider, M. A. Tawiah-Boateng, A. Wood, K. Dean, M. Johnston, and A. Shilatifard. Methylation of histone H3 by COMPASS requires ubiquitination of histone H2B by Rad6. *J.Biol.Chem.* 277 (32):28368-28371, 2002.

R. N. Dutnall and V. Ramakrishnan. Twists and turns of the nucleosome: tails without ends. *Structure.* 5 (10):1255-1259, 1997.

K. K. Ebralidse, S. A. Grachev, and A. D. Mirzabekov. A highly basic histone H4 domain bound to the sharply bent region of nucleosomal DNA. *Nature* 331 (6154):365-367, 1988.

J. T. Finch and A. Klug. Solenoidal model for superstructure in chromatin. *Proc.Natl.Acad.Sci.U.S.A* 73 (6):1897-1901, 1976.

W. Fischle, Y. Wang, S. A. Jacobs, Y. Kim, C. D. Allis, and S. Khorasanizadeh. Molecular basis for the discrimination of repressive methyl-lysine marks in histone H3 by Polycomb and HP1 chromodomains. *Genes Dev.* 17 (15):1870-1881, 2003.

M. A. Freitas, A. R. Sklenar, and M. R. Parthun. Application of mass spectrometry to the identification and quantification of histone post-translational modifications. *J.Cell Biochem.* 92 (4):691-700, 2004.

B. A. Garcia, J. Shabanowitz, and D. F. Hunt. Characterization of histones and their post-translational modifications by mass spectrometry. *Curr.Opin.Chem.Biol.* 11 (1):66-73, 2007.

P. A. Grant, D. Schieltz, M. G. Pray-Grant, D. J. Steger, J. C. Reese, J. R. Yates, III, and J. L. Workman. A subset of TAF(II)s are integral components of the SAGA complex required for nucleosome acetylation and transcriptional stimulation. *Cell* 94 (1):45-53, 1998.

J. V. Gray, G. A. Petsko, G. C. Johnston, D. Ringe, R. A. Singer, and M. Werner-Washburne. "Sleeping beauty": quiescence in *Saccharomyces cerevisiae*. *Microbiol.Mol.Biol.Rev.* 68 (2):187-206, 2004.

L. R. Gurley, R. A. Walters, and R. A. Tobey. Cell cycle-specific changes in histone phosphorylation associated with cell proliferation and chromosome condensation. *J.Cell Biol.* 60 (2):356-364, 1974.

J. C. Hansen, C. Tse, and A. P. Wolffe. Structure and function of the core histone N-termini: more than meets the eye. *Biochemistry* 37 (51):17637-17641, 1998.

P. O. Hassa, S. S. Haenni, M. Elser, and M. O. Hottiger. Nuclear ADP-ribosylation reactions in mammalian cells: where are we today and where are we going? *Microbiol.Mol.Biol.Rev.* 70 (3):789-829, 2006.

T. R. Hebbes, A. W. Thorne, and C. Crane-Robinson. A direct link between core histone acetylation and transcriptionally active chromatin. *EMBO J.* 7 (5):1395-1402, 1988.

T. R. Hebbes, A. W. Thorne, A. L. Clayton, and C. Crane-Robinson. Histone acetylation and globin gene switching. *Nucleic Acids Res.* 20 (5):1017-1022, 1992.

B. Hendrich and W. Bickmore. Human diseases with underlying defects in chromatin structure and modification. *Hum.Mol.Genet.* 10 (20):2233-2242, 2001.

M. J. Hendzel and J. R. Davie. Dynamically acetylated histones of chicken erythrocytes are selectively methylated. *Biochem.J.* 273 (Pt 3):753-758, 1991.

P. J. Horn and C. L. Peterson. Molecular biology. Chromatin higher order folding--wrapping up transcription. *Science* 297 (5588):1824-1827, 2002.

L. Howe, C. E. Brown, T. Lechner, and J. L. Workman. Histone acetyltransferase complexes and their link to transcription. *Crit Rev.Eukaryot.Gene Expr.* 9 (3-4):231-243, 1999.

J. Y. Hsu, Z. W. Sun, X. Li, M. Reuben, K. Tatchell, D. K. Bishop, J. M. Grushcow, C. J. Brame, J. A. Caldwell, D. F. Hunt, R. Lin, M. M. Smith, and C. D. Allis. Mitotic phosphorylation of histone H3 is governed by Ipl1/aurora kinase and Glc7/PP1 phosphatase in budding yeast and nematodes. *Cell* 102 (3):279-291, 2000.

M. Iizuka and M. M. Smith. Functional consequences of histone modifications. *Curr.Opin.Genet.Dev.* 13 (2):154-160, 2003.

S. Imai, C. M. Armstrong, M. Kaeberlein, and L. Guarente. Transcriptional silencing and longevity protein Sir2 is an NAD-dependent histone deacetylase. *Nature* 403 (6771):795-800, 2000.

A. Imhof and A. P. Wolffe. Transcription: gene control by targeted histone acetylation. *Curr.Biol.* 8 (12):R422-R424, 1998.

R. H. Jacobson, A. G. Ladurner, D. S. King, and R. Tjian. Structure and function of a human TAFII250 double bromodomain module. *Science* 288 (5470):1422-1425, 2000.

T. Jenuwein and C. D. Allis. Translating the histone code. *Science* 293 (5532):1074-1080, 2001.

C. A. Johnson, L. P. O'Neill, A. Mitchell, and B. M. Turner. Distinctive patterns of histone H4 acetylation are associated with defined sequence elements within both heterochromatic and euchromatic regions of the human genome. *Nucleic Acids Res.* 26 (4):994-1001, 1998.

L. M. Johnson, G. Fisher-Adams, and M. Grunstein. Identification of a non-basic domain in the histone H4 N-terminus required for repression of the yeast silent mating loci. *EMBO J.* 11 (6):2201-2209, 1992.

L. H. Johnston and K. A. Nasmyth. Saccharomyces cerevisiae cell cycle mutant cdc9 is defective in DNA ligase. *Nature* 274 (5674):891-893, 1978.

P. Y. Kan, X. Lu, J. C. Hansen, and J. J. Hayes. The H3 tail domain participates in multiple interactions during folding and self-association of nucleosome arrays. *Mol.Cell Biol.* 27 (6):2084-2091, 2007.

Y. Katan-Khaykovich and K. Struhl. Dynamics of global histone acetylation and deacetylation *in vivo*: rapid restoration of normal histone acetylation status upon removal of activators and repressors. *Genes Dev.* 16 (6):743-752, 2002.

S. Khorasanizadeh. The nucleosome: from genomic organization to genomic regulation. *Cell* 116 (2):259-272, 2004.

R. D. Kornberg. Chromatin structure: a repeating unit of histones and DNA. *Science* 184 (139):868-871, 1974.

T. Kouzarides. Histone methylation in transcriptional control. *Curr.Opin.Genet.Dev.* 12 (2):198-209, 2002.

T. Kouzarides. Chromatin modifications and their function. *Cell* 128 (4):693-705, 2007.

W. A. Krajewski and J. Ausio. Modulation of the higher-order folding of chromatin by deletion of histone H3 and H4 terminal domains. *Biochem.J.* 316 (Pt 2):395-400, 1996.

W. L. Kraus and J. T. Lis. PARP goes transcription. *Cell* 113 (6):677-683, 2003.

M. J. Kruhlak, M. J. Hendzel, W. Fischle, N. R. Bertos, S. Hameed, X. J. Yang, E. Verdin, and D. P. Bazett-Jones. Regulation of global acetylation in mitosis through loss of histone

acetyltransferases and deacetylases from chromatin. *J.Biol.Chem.* 276 (41):38307-38319, 2001.

J. Kwon, K. B. Morshead, J. R. Guyon, R. E. Kingston, and M. A. Oettinger. Histone acetylation and hSWI/SNF remodeling act in concert to stimulate V(D)J cleavage of nucleosomal DNA. *Mol.Cell* 6 (5):1037-1048, 2000.

M. Lachner and T. Jenuwein. The many faces of histone lysine methylation. *Curr.Opin.Cell Biol.* 14 (3):286-298, 2002.

R. W. Lennox and L. H. Cohen. Analysis of histone subtypes and their modified forms by polyacrylamide gel electrophoresis. *Methods Enzymol.* 170:532-549, 1989.

W. S. Lo, R. C. Trievel, J. R. Rojas, L. Duggan, J. Y. Hsu, C. D. Allis, R. Marmorstein, and S. L. Berger. Phosphorylation of serine 10 in histone H3 is functionally linked *in vitro* and *in vivo* to Gcn5-mediated acetylation at lysine 14. *Mol.Cell* 5 (6):917-926, 2000.

Y. Lorch, M. Zhang, and R. D. Kornberg. Histone octamer transfer by a chromatin-remodeling complex. *Cell* 96 (3):389-392, 1999.

K. Luger, A. W. Mader, R. K. Richmond, D. F. Sargent, and T. J. Richmond. Crystal structure of the nucleosome core particle at 2.8 Å resolution. *Nature* 389 (6648):251-260, 1997.

K. Luger and T. J. Richmond. DNA binding within the nucleosome core. *Curr.Opin.Struct.Biol.* 8 (1):33-40, 1998.

X. J. Ma, J. Wu, B. A. Altheim, M. C. Schultz, and M. Grunstein. Deposition-related sites K5/K12 in histone H4 are not required for nucleosome deposition in yeast. *Proc.Natl.Acad.Sci.U.S.A* 95 (12):6693-6698, 1998.

R. Marmorstein. Structure of histone acetyltransferases. *J.Mol.Biol.* 311 (3):433-444, 2001.

M. J. Martinez, S. Roy, A. B. Archuletta, P. D. Wentzell, S. S. Anna-Arriola, A. L. Rodriguez, A. D. Aragon, G. A. Quinones, C. Allen, and M. Werner-Washburne. Genomic analysis of stationary-phase and exit in *Saccharomyces cerevisiae*: gene expression and identification of novel essential genes. *Mol.Biol.Cell* 15 (12):5295-5305, 2004.

H. Masumoto, D. Hawke, R. Kobayashi, and A. Verreault. A role for cell-cycle-regulated histone H3 lysine 56 acetylation in the DNA damage response. *Nature* 436 (7048):294-298, 2005.

K. J. McManus and M. J. Hendzel. The relationship between histone H3 phosphorylation and acetylation throughout the mammalian cell cycle. *Biochem.Cell Biol.* 84 (4):640-657, 2006.

E. L. Mersfelder and M. R. Parthun. The tale beyond the tail: histone core domain modifications and the regulation of chromatin structure. *Nucleic Acids Res.* 34 (9):2653-2662, 2006.

N. Minsky and M. Oren. The RING domain of Mdm2 mediates histone ubiquitylation and transcriptional repression. *Mol.Cell* 16 (4):631-639, 2004.

F. Muhlbacher, H. Schiessel, and C. Holm. Tail-induced attraction between nucleosome core particles. *Phys.Rev.E.Stat.Nonlin.Soft.Matter Phys.* 74 (3 Pt 1):031919, 2006.

C. J. Nelson, H. Santos-Rosa, and T. Kouzarides. Proline isomerization of histone H3 regulates lysine methylation and gene expression. *Cell* 126 (5):905-916, 2006.

H. H. Ng, Q. Feng, H. Wang, H. Erdjument-Bromage, P. Tempst, Y. Zhang, and K. Struhl. Lysine methylation within the globular domain of histone H3 by Dot1 is important for telomeric silencing and Sir protein association. *Genes Dev.* 16 (12):1518-1527, 2002.

S. J. Nowak and V. G. Corces. Phosphorylation of histone H3: a balancing act between chromosome condensation and transcriptional activation. *Trends Genet.* 20 (4):214-220, 2004.

P. Nurse. A long twentieth century of the cell cycle and beyond. *Cell* 100 (1):71-78, 2000.

P. Ornaghi, P. Ballario, A. M. Lena, A. Gonzalez, and P. Filetici. The bromodomain of Gcn5p interacts *in vitro* with specific residues in the N terminus of histone H4. *J.Mol.Biol.* 287 (1):1-7, 1999.

E. C. Park and J. W. Szostak. Point mutations in the yeast histone H4 gene prevent silencing of the silent mating type locus HML. *Mol.Cell Biol.* 10 (9):4932-4934, 1990.

M. J. Pazin and J. T. Kadonaga. What's up and down with histone deacetylation and transcription? *Cell* 89 (3):325-328, 1997.

M. L. Phelan, G. R. Schnitzler, and R. E. Kingston. Octamer transfer and creation of stably remodeled nucleosomes by human SWI-SNF and its isolated ATPases. *Mol.Cell Biol.* 20 (17):6380-6389, 2000.

S. Rea, F. Eisenhaber, D. O'Carroll, B. D. Strahl, Z. W. Sun, M. Schmid, S. Opravil, K. Mechtler, C. P. Ponting, C. D. Allis, and T. Jenuwein. Regulation of chromatin structure by site-specific histone H3 methyltransferases. *Nature* 406 (6796):593-599, 2000.

J. P. Rheeder and W. F. Marasas. Fusarium species from plant debris associated with soils from maize production areas in the Transkei region of South Africa. *Mycopathologia* 143 (2):113-119, 1998.

J. C. Rice, S. D. Briggs, B. Ueberheide, C. M. Barber, J. Shabanowitz, D. F. Hunt, Y. Shinkai, and C. D. Allis. Histone methyltransferases direct different degrees of methylation to define distinct chromatin domains. *Mol.Cell* 12 (6):1591-1598, 2003.

G. T. Saccone, J. D. Skinner, and L. A. Burgoyne. Resistance of chromatin superstructure to tryptic digestion modulated by conjugated polyacrylamide. *FEBS Lett.* 157 (1):111-114, 1983.

M. S. Santisteban, G. Arents, E. N. Moudrianakis, and M. M. Smith. Histone octamer function *in vivo*: mutations in the dimer-tetramer interfaces disrupt both gene activation and repression. *EMBO J.* 16 (9):2493-2506, 1997.

G. Schäfer, C. R. McEvoy, and H. G. Patterton. The *Saccharomyces cerevisiae* linker histone Hho1p is essential for chromatin compaction in stationary phase and is displaced by transcription. *Proc.Natl.Acad.Sci.U.S.A* 105 (39):14838-14843, 2008.

T. Schalch, S. Duda, D. F. Sargent, and T. J. Richmond. X-ray structure of a tetranucleosome and its implications for the chromatin fibre. *Nature* 436 (7047):138-141, 2005.

D. Schubeler, D. Scalzo, C. Kooperberg, B. van Steensel, J. Delrow, and M. Groudine. Genome-wide DNA replication profile for *Drosophila melanogaster*: a link between transcription and replication timing. *Nat.Genet.* 32 (3):438-442, 2002.

Y. Shiio and R. N. Eisenman. Histone sumoylation is associated with transcriptional repression. *Proc.Natl.Acad.Sci.U.S.A* 100 (23):13225-13230, 2003.

M. Shogren-Knaak, H. Ishii, J. M. Sun, M. J. Pazin, J. R. Davie, and C. L. Peterson. Histone H4-K16 acetylation controls chromatin structure and protein interactions. *Science* 311 (5762):844-847, 2006.

M. R. Starich, K. Sandman, J. N. Reeve, and M. F. Summers. NMR structure of HMfB from the hyperthermophile, *Methanothermus fervidus*, confirms that this archaeal protein is a histone. *J.Mol.Biol.* 255 (1):187-203, 1996.

B. D. Strahl, R. Ohba, R. G. Cook, and C. D. Allis. Methylation of histone H3 at lysine 4 is highly conserved and correlates with transcriptionally active nuclei in *Tetrahymena*. *Proc.Natl.Acad.Sci.U.S.A* 96 (26):14967-14972, 1999.

B. D. Strahl and C. D. Allis. The language of covalent histone modifications. *Nature* 403 (6765):41-45, 2000.

K. Struhl. Histone acetylation and transcriptional regulatory mechanisms. *Genes Dev.* 12 (5):599-606, 1998.

N. Suka, Y. Suka, A. A. Carmen, J. Wu, and M. Grunstein. Highly specific antibodies determine histone acetylation site usage in yeast heterochromatin and euchromatin. *Mol.Cell* 8 (2):473-479, 2001.

Z. W. Sun and C. D. Allis. Ubiquitination of histone H2B regulates H3 methylation and gene silencing in yeast. *Nature* 418 (6893):104-108, 2002.

S. Thomson, A. L. Clayton, C. A. Hazzalin, S. Rose, M. J. Barratt, and L. C. Mahadevan. The nucleosomal response associated with immediate-early gene induction is mediated via alternative MAP kinase cascades: MSK1 as a potential histone H3/HMG-14 kinase. *EMBO J.* 18 (17):4779-4793, 1999.

B. M. Turner, A. J. Birley, and J. Lavender. Histone H4 isoforms acetylated at specific lysine residues define individual chromosomes and chromatin domains in *Drosophila polytene* nuclei. *Cell* 69 (2):375-384, 1992.

B. M. Turner. Histone acetylation and an epigenetic code. *Bioessays* 22 (9):836-845, 2000.

K. van Holde and J. Zlatanova. What determines the folding of the chromatin fiber? *Proc.Natl.Acad.Sci.U.S.A* 93 (20):10548-10555, 1996.

F. van Leeuwen, P. R. Gafken, and D. E. Gottschling. Dot1p modulates silencing in yeast by methylation of the nucleosome core. *Cell* 109 (6):745-756, 2002.

P. D. Varga-Weisz, M. Wilm, E. Bonte, K. Dumas, M. Mann, and P. B. Becker. Chromatin-remodelling factor CHRAC contains the ATPases ISWI and topoisomerase II. *Nature* 388 (6642):598-602, 1997.

A. R. Venkitaraman. Modifying chromatin architecture during the response to DNA breakage. *Crit Rev.Biochem.Mol.Biol.* 45 (1):2-13, 2010.

P. A. Wade and A. P. Wolffe. Histone acetyltransferases in control. *Curr.Biol.* 7 (2):R82-R84, 1997.

H. Wang, R. Cao, L. Xia, H. Erdjument-Bromage, C. Borchers, P. Tempst, and Y. Zhang. Purification and functional characterization of a histone H3-lysine 4-specific methyltransferase. *Mol.Cell* 8 (6):1207-1217, 2001.

J. H. Waterborg and T. Kapros. Kinetic analysis of histone acetylation turnover and Trichostatin A induced hyper- and hypoacetylation in alfalfa. *Biochem.Cell Biol.* 80 (3):279-293, 2002.

S. A. Wolfe and S. R. Grimes. Histone H1t: a tissue-specific model used to study transcriptional control and nuclear function during cellular differentiation. *J.Cell Biochem.* 53 (2):156-160, 1993.

A. P. Wolffe. New insights into chromatin function in transcriptional control. *FASEB J.* 6 (15):3354-3361, 1992.

X. Xie, T. Kokubo, S. L. Cohen, U. A. Mirza, A. Hoffmann, B. T. Chait, R. G. Roeder, Y. Nakatani, and S. K. Burley. Structural similarity between TAFs and the heterotetrameric core of the histone octamer. *Nature* 380 (6572):316-322, 1996.

F. Xu, K. Zhang, and M. Grunstein. Acetylation in histone H3 globular domain regulates gene expression in yeast. *Cell* 121 (3):375-385, 2005.

J. Ye, X. Ai, E. E. Eugeni, L. Zhang, L. R. Carpenter, M. A. Jelinek, M. A. Freitas, and M. R. Parthun. Histone H4 lysine 91 acetylation a core domain modification associated with chromatin assembly. *Mol.Cell* 18 (1):123-130, 2005.

K. Zhang, H. Tang, L. Huang, J. W. Blankenship, P. R. Jones, F. Xiang, P. M. Yau, and A. L. Burlingame. Identification of acetylation and methylation sites of histone H3 from chicken erythrocytes by high-accuracy matrix-assisted laser desorption ionization-time-of-flight, matrix-assisted laser desorption ionization-postsource decay, and nanoelectrospray ionization tandem mass spectrometry. *Anal.Biochem.* 306 (2):259-269, 2002.

L Zhang and M. A. Freitas. Comparison of peptide mass mapping and electron capture dissociation as assays for histone posttranslational modifications. *International Journal of Mass Spectrometry* 234 (1-3):213-225, 2004.

L. Zhang, E. E. Eugeni, M. R. Parthun, and M. A. Freitas. Identification of novel histone post-translational modifications by peptide mass fingerprinting. *Chromosoma* 112 (2):77-86, 2003.

Y. Zhang and D. Reinberg. Transcription regulation by histone methylation: interplay between different covalent modifications of the core histone tails. *Genes Dev.* 15 (18):2343-2360, 2001.

A. Zweidler. Resolution of histones by polyacrylamide gel electrophoresis in presence of nonionic detergents. *Methods Cell Biol.* 17:223-233, 1978.

CHAPTER 2

Rapid Isolation of Histones

2.1. Introduction

The surface of the nucleosome is decorated with multiple covalent modifications. The presence of these modifications dictates the higher order structure of chromatin. The rapid discovery of histone post-translational modifications and their implicated roles in regulating chromatin structure has lead to a demand to devise more rapid, effective methods in isolation of histones. This is important to ensure that the isolated histone faithfully reflects its native modification state, and that this state is not altered during the isolation procedure due to the action of active modification enzymes.

There are currently a number of published methods for the isolation of histones from baker's yeast (*Saccharomyces cerevisiae*). The two most widely used methods involve the preparation of nuclei following Zymolyase digestion, and the homogenisation of cells with glass beads. However, both these methods have periods during which histone modifications can occur, masking the true *in vivo* state of the histone. In the Zymolyase method, for example: the enzyme incubation time at 30ºC to produce spheroplasts is extensive, and will allow continued activity of nuclear enzymes. In the glass bead method the average yield of histones is very low, and with more vigorous agitation such as using a "Bead Beater" protein denaturation occurs (Roberts, 1999).

In this study we aimed to develop a protocol that would arrest any metabolic activity inside the living cell and hence avoid any histone modifications that might occur during histone isolation. In addition, the method should also allow reproducible yield of histones from stationary phase, a growth phase of *S. cerevisiae* where the cell wall is thick and isolation of cellular content is difficult (De Nobel *et al*., 1990). To address these considerations we used a rapid freeze-thawing step with liquid nitrogen and ice-cold purification buffers in subsequent purification steps. This method causes cells to swell and ultimately break during the freezing process and then contract during thawing. We anticipated that by keeping cells frozen during lysis, proteolysis and changes in protein modification status should be minimized.

2.2. Materials and Methods

2.2.1. Yeast Strains and Growth Media

W303-1A { MATa, *leu2-3, 112 trp1-1, can1-100, ura3-1, ade2-1, his3-11,15*}; JDY 43 {MATa, *leu2-3, leu2-112, his 4-580, ura3-52, tpl-289,* genomic C-terminally Myc-tagged *HHO1*} and BY 4742 { MATα, *his3Δ1, leu2Δ0, lys2Δ0, ura3Δ0* }. All chemicals were of biochemical analysis or of molecular biology purity.

2.2.2. Histone Purification by the Rapid Method

S. cerevisiae cultures of 1L or 2L volumes, as indicated of strain W303-1A or other strains, were cultured in YPD medium for approximately 16 hours at 30ºC to a density of approximately 10^7 cells/ml, for late exponential phase cells. Cells were harvested by centrifugation at 2449 x g_{av} for 5min at 4°C in a GA6 rotor (Beckman), washed with sterile water, and immediately frozen at -60°C. When needed, cells were resuspended in a

minimum volume of cold (4°C) Nuclei Isolation Buffer (NIB) [10% (v/v) glycerol, 0.25M sucrose, 60mM KCl, 15mM NaCl, 15mM $MgCl_2$, 1mM $CaCl_2$, 15mM MES (pH 6.6), 1mM phenylmethylsulfonyl fluoride (PMSF), 0.8% (v/v) Triton X-100, 0.5μg/ml leupeptin, 0.7μg/ml pepstatin]. The resuspended cells were then flash frozen in liquid nitrogen and thawed at room temperature. The lysed cells were washed three times with 50ml cold NIB and held on ice for 10min between wash steps. Cell debris was pelleted by centrifugation at 2449 x g_{av} for 5min at 4ºC for the first wash, and at 1482 x g_{av} for the remaining two. The membranous proteins were removed from the cell pellet by washing twice with cold A buffer that contained a detergent [10mM Tris-HCl pH8.0, 0.5% (v/v) NP-40, 75mM NaCl, 30mM sodium butyrate, 1mM PMSF, 0.5μg/ml leupeptin and 0.7μg/ml pepstatin], held on ice for 5min and spun at 1482 x g_{av} for 5min at 4°C. The weakly binding proteins were removed from the cell pellet by washing twice with B buffer that contained a high salt concentration (10mM Tris-HCl pH8.0, 0.4M NaCl, 30mM sodium butyrate, 1mM PMSF, 0.5μg/ml leupeptin, 0.7μg/ml pepstatin), held on ice for 5min only for the first wash and immediately centrifuged for the last wash. The histones were extracted by resuspending the pellet in 10ml of cold 0.4N H_2S0_4 and incubating on ice for 30 min with mild shaking. Cell debris was removed from the solution by centrifugation for 30 min at 17418 x g_{av} at 4°C in a J25.50 rotor (Beckman). The supernatant, which contained the extracted histones, was precipitated by adding trichloroacetic acid (TCA) to a final concentration of 20% (w/v). The supernatant was incubated at 4°C overnight and the histones were collected by centrifugation for 30min at 17418 x g_{av} at 4°C in a J25.50 rotor (Beckman). The histone pellet was washed with cold (-20ºC) acetone twice, spun at 12096 x g_{av} for 5min and air dried. The histone was dissolved in 200μl of 10mM Tris-HCl pH8.0.

2.2.3. Isolation of Histones by the Conventional Zymolyase Method

S. cerevisiae cultures (1L or 2L volumes, as indicated) of strain W303-1A, were grown in YPD medium for approximately 16 hours to a density of approximately 10^7 cells/ml at 30°C

for late exponential phase cells. Cells were harvested by centrifugation at 2449 x g_{av} for 5min at 4°C in a GA6 rotor (Beckman), and washed once with sterile water. Histones were extracted as described in (Edmondson *et al*., 1996). In short, the yeast cell wall was disrupted by resuspending the cell pellets in 10mM dithriothreitol (DTT)/0.1mM Tris-HCl pH 9.4, incubated at 30°C for 15min with gently shaking, and then centrifuged as above. The cell pellets were washed in Buffer 2 (1.2M sorbitol, 20mM Hepes pH7.4, 1mM PMSF, 0.5μg/ml leupeptin, 0.7μg/ml pepstatin), and resuspended in 1ml of the same buffer adjusted to 6mg/ml Zymolyase (Seikagaku). Cells were spheroplasted at 30°C for 60min. The spheroplast preparation was washed in Buffer 3 (1.2M sorbitol, 20mM Pipes, 1mM NaCl, 1mM PMSF, 0.5g/ml leupeptin, 0.7μg/ml pepstatin) and centrifuged at 1482 x g_{av} for 5min at 4°C. Yeast nuclei were prepared as described above for the rapid method, except that 10% (v/v) glycerol was omitted from the NIB. The histones were acid-extracted; TCA-precipitated and resuspended in 200μl of 10mM Tris-HCl pH8.0 as detailed above in histone purification by rapid method.

2.2.4. Sodium Dodecylsulfate Polyacrylamide Gel Electrophoresis (SDS-PAGE)

The crude histone extract was electrophoresed in 8cm long 15% and 18% (w/v total acrylamide) (19:1 acrylamide:bis-acrylamide) SDS-PAGE gels using 1mm plate spacers. Gels were routinely electrophoresed at 16mA at room temperature, and protein visualised by staining with Coomassie Blue G-250 as detailed in Current Protocols in Molecular Biology.

2.2.5. Separation of core Histones by Reverse Phase High-Performance Liquid Chromatography on C_{18} (RP-HPLC) Columns.

HPLC grade acetonitrile, Trifluoroactetic acid (TFA) and milli Q water was used. All RP-HPLC experiments were performed on Shimadzu HPLC gradient system. The eluted

histones were detected by their UV absorption at 210nm. Histone separations were performed on a Phenomenex C_{18} Jupiter column (4.6mm x 250mm) packed with 15µm spherical particles with 300Å poresize. Solvent A (5% acetonitrile, 0.1% TFA) and Solvent B (95% acetonitrile, 0.1% TFA). The concentration of Solvent B was increased in the following order at a flow rate of 1ml/min: from 25-40%B for 20min, 40-50%B in 30min, 55-60%B, held at 60%B for 10min. The injection volume was 20µl of the sample.

2.2.6. SDS Polyacrylamide Gel Electrophoresis of Chromatographic Fractions

On the basis of UV absorption at 210nm, each eluted peak was freeze-dried and electrophoresed in 8cm long 18% SDS Polyacrylamide gel. The gel was stained with Coomassie blue G-250.

2.3. Results

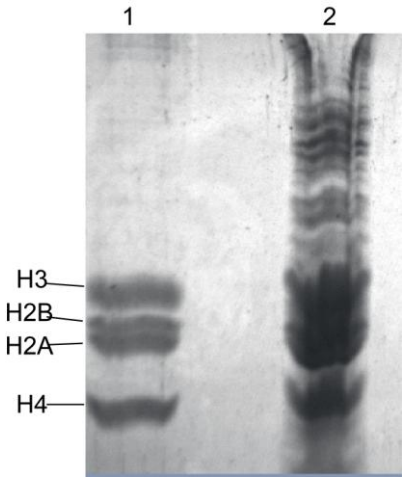

Figure 2.1. Purification of total yeast histone by the long conventional Zymolyase method. Chicken core histone standard (lane 1), and Zymolyase-extracted total yeast histones (lane 2) were analysed on a 15% SDS-PAGE gel. The gel was visualised with Coomassie Blue G250 stain.

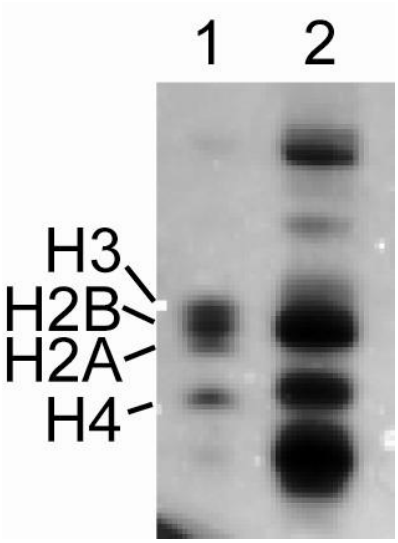

Figure 2.2. Rapid histone purification from yeast cells. Migration of chicken core histone standard (lane 1), and total histone extract for *S. cerevisiae* late exponential phase cells (lane 2) on a 15% SDS-PAGE gel. This gel was stained with Coomassie Blue G250.

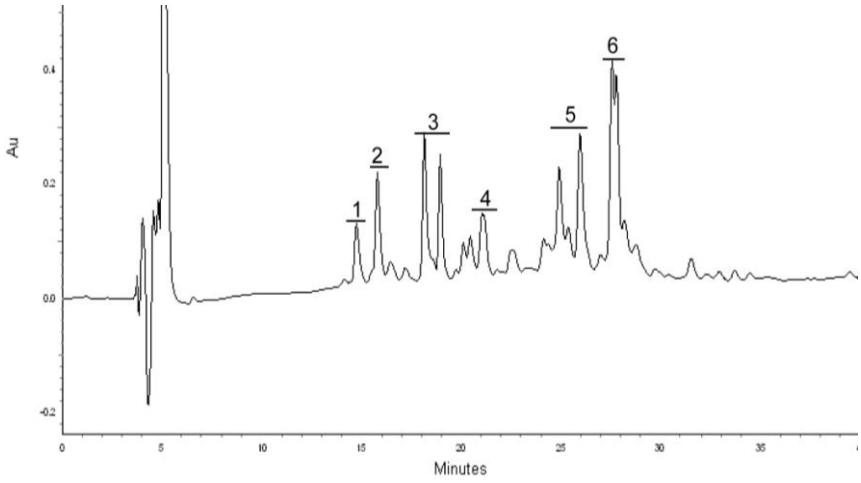

Figure 2.3(a). Separation of yeast histones purified by the rapid method using RP-HPLC. The yeast histone extract was eluted on a C_{18} column at a flow rate of 1ml/min. The numbered fractions (1-6) were freeze-dried and subjected to 18% SDS-PAGE gels analysis as shown in fig. 2.3(b).

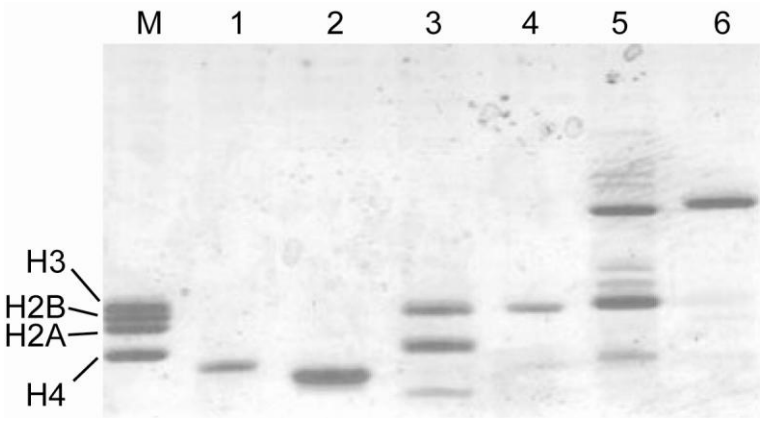

Figure 2.3(b). Demonstrates 18% SDS-PAGE of fractions (1-6) from the separation described in fig. 2.3(a). The yeast core histone fractions were identified by comparison with chicken core histone standard (lane M). The gel was visualised with Coomassie Blue G250 stain.

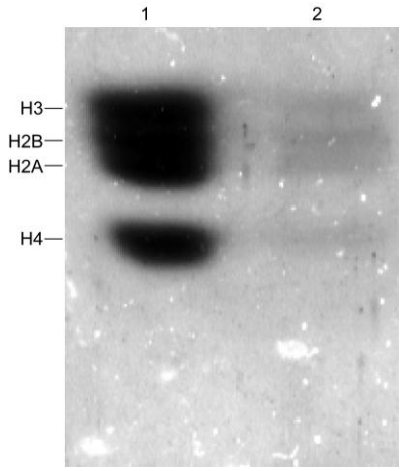

Figure 2.4. SDS-PAGE of "mock isolation" of chicken core histone standard. Lane 1- represent 12µg of chicken core histone standard and lane 2 - represent final extract of chicken core histone standard from "mock isolation". The gel was visualised by Coomassie Blue G250.

As a first step, histones were isolated by conventional Zymolyase method to serve as standard with which to compare histone yield and integrity of the rapid methods. The result of the conventional isolation method is shown in Figure 2.1. Histones were isolated by the rapid method. The result of the isolation is shown in Figure 2.2. Looking at this Figure the presence of the yeast core histones are clearly evident when compared to the standard chicken histones (compare lane 2 to lane 1 in Fig. 2.2). The histones H2A, H2B and H3 were not well-resolved in the gel shown. The histones H2A, H2B and H3 were further fractionated by RP-HPLC using a C_{18} analytical column. The core histones were eluted using an acetonitrile multi-step gradient. Figure 2.3(a) shows the RP-HPLC profile of the eluted histones, and figure 2.3(b) illustrates a 18% SDS-PAGE gel of the eluted peaks. Figure 2.3(b) shows chicken core histone standard (lane M), and the collected fractions (lane 1-6).

We were concerned by the large protein band that migrated faster than histone H4 (lane 2 of Fig. 2.2), and considered the possibility that this may be a degradation product of one of the core histones. To test this possibility we performed a "mock isolation", where the standard chicken histones were subjected to the full rapid histone isolation procedure. The result of this experiment is shown in Figure 2.4. As can be seen in this figure, no evidence of any histone degradation was evident. We therefore concluded that the band observed with the rapid isolation of histones from yeast was not due to histone degradation, but represented another non-histone protein enriched in the procedure. Also, no degradation of histones was evident in the Zymolyase isolated histones (see Fig. 2.1) in the presence of the leupeptin and pepstatic protease inhibitors, and we therefore expected that the inhibitors would similarly protect the core histones from protease-mediated degradation during the rapid isolation procedure. We do note, however, that the difference between the techniques may have exposed the histones in the rapid isolation procedure to different proteases compared to the Zymolyase method.

2.4. Discussion and Conclusions

Rapid acid extraction from crude cells typically results in tremendous enrichment of histone proteins. Histones are quite abundant proteins, usually present in cells in equal mass with the DNA (Oliver *et al*., 1974). Generally, in the continuing identification of histone tail modifications there exists a wide gap between the preparation time and the histone purity. The currently intensively studied methods allow times for remodeling of histone to occur by a numerous multi-subunit enzymes such as kinases, histone methyltransferases (HMTases), protein R methyltransferase (PMRT) and histone acetyltransferases (HATs) (McManus and Hendzel, 2006). The method that we detailed here can be used to get a “snap-shot” representation of *in vivo* profile of the histone molecules, before nucleic enzymes can modify the histone proteins. In this method it takes under 90min to isolate nuclei with all steps carried out at 4°C, as compared to 175min required to isolate nuclei by the conventional Zymolyase method. The 175min includes 75 min that is carried out at 30°C, this is sufficient time to allow enzymes to modify yeast histones inside the cells.

Investigation by following this method should be able to routinely isolate purified histones for a myriad of follow-up experiments, including immunoblotting, identification of acetylation patterns by TAU gels and mass spectrometry.

2.5. Reference List

F. M. Ausubel, R. Brent, R. E. Kingston, D. D. Moore, J. G. Seidman, J. A. Smith, K. Struhl. *Current Protocols in Molecular Biology,* John Wiley & Sons, 2003.

J. G. de Nobel, F. M. Klis, J. Priem, T. Munnik, and Ende H. van den. The glucanase-soluble mannoproteins limit cell wall porosity in *Saccharomyces cerevisiae*. *Yeast* 6 (6):491-499, 1990.

D. G. Edmondson, M. M. Smith, and S. Y. Roth. Repression domain of the yeast global repressor Tup1 interacts directly with histones H3 and H4. *Genes Dev.* 10 (10):1247-1259, 1996.

K. J. McManus and M. J. Hendzel. The relationship between histone H3 phosphorylation and acetylation throughout the mammalian cell cycle. *Biochem.Cell Biol.* 84 (4):640-657, 2006.

D. Oliver, D. Granner, and R. Chalkley. Identification of a distinction between cytoplasmic histone synthesis and subsequent histone deposition within the nucleus. *Biochemistry* 13 (4):746-749, 1974.

S. M. Roberts. Biocatalysts for fine chemicals synthesis. *Wiley, New York*, 1999

CHAPTER 3

Analysis of Histone Acetylation State by Triton-acid-urea (TAU) Gel Electrophoresis.

3.1. Introduction

It was previously shown in the Patterton group that yeast linker histone Hho1p rapidly dissociated from chromatin during exit of stationary phase and re-initiation of the cell cycle (Schäfer *et al*., 2008). General up-regulation of certain genes occur during the stationary phase exit followed by a positive control of genes normally activated during the exponential phase. Stationary phase exit, promisingly, is the reference phase in which to study the preliminary events and sequence of events preceding chromatin decondensation and subsequent gene expression.

The main regulatory mechanism of chromatin structure is the covalent modification of the core histone N-terminal tails (Annunziato *et al*., 1988; Kouzarides, 2007). One particular modification, histone acetylation, was shown to correlate with transcriptional regulation, making chromatin accessible to the transcription-activating machinery and resulting in gene expression (Struhl, 1998). Continued research in this area has advanced our understanding of how histone acetylation patterns, linked with gene expression, may provide dynamic recognition sites for transcription factors. The association of bromodomains of the HAT complexes with histone acetylation sites recruits transcription-initiation complexes. The higher-order structure of chromatin plays a pivotal role in mediating gene activity by constraining the accessibility of sequence-specific binding proteins to DNA. The association

between histone acetylation and transcriptionally active chromatin was reported many years ago (Hebbes *et al*., 1988).

Triton-acetic acid-urea (TAU) gels, unlike sodium dodecylsulfate polyacrylamide gel electrophoresis (SDS-PAGE) gels, can separate the subtypes of histone H2A, H2B, H4 and H3, acetylated to different levels, based on charge as well as mass (Waterborg, 2002). It was found that the core histones (but not linker histones) bind triton-X100, a non-ionic detergent (Zweidler, 1978). The differential binding of triton-X100 by the core histones is based upon the hydrophobicity of the protein. The overall mass of the protein is increased due to binding of Triton, however, the charge remain unchanged. Urea is used to denature proteins and, in the presence of acetic acid, histones become positively charged and migrate towards the negative electrode (Lennox and Cohen, 1989). Acetylation abolished the positive charge of the ε-amino group of a lysine side-chain. Thus, acetylation reduces the positive charge of the basic core histones at low pH, decreasing the electrophoretic mobility towards the cathode in a TAU gel. This method therefore allows the separation of histones and some histone subtypes that have been acetylated to different degrees.

3.2. Materials and Methods

3.2.1. Isolation of histones from stationary phase yeast cells

Cultures (1L or 2L) of yeast strain W303-1A, were maintained in YPD medium to a density of approximately 10^8 cells/ml for 6 days at 30°C to ensure that the culture had entered proper G_0 growth phase (Gray *et al*., 2004). Cells were harvested by centrifugation at 2449 $\times g_{av}$ for 5min at 4°C in a GA6 rotor (Beckman), washed twice with sterile water and were immediately frozen at -60°C. Where cells were required that had exited stationary phase,

and re-entered the cell-cycle, stationary phase yeast cells were re-inoculated into 1L of YPD medium and incubated at 30°C. At time 0, 15min and 60min cells were harvested as mentioned above. Histones were extracted from stationary phase and stationary phase exit cells at the indicated times by the rapid method (see fig. 3.4).

3.2.2. Separation of core histones by Reverse Phase High-Performance Liquid Chromatography (RP -HPLC) on C18 columns.

HPLC grade acetonitrile (Sigma), trifluoroacetic acid (TFA; Sigma) and high quality water (milli-Q, Millipore) was used. All RP-HPLC experiments were performed on an HPLC gradient system (Shimadzu, Prominence). The eluted histones were detected by their UV absorption at 210nm. Histone separations were performed on a C18 Jupiter column (4.6mm x 250mm) (Phenomenex) packed with 15μm spherical particles with 300Å pore-size. Solvent A was 5% (v/v) acetonitrile, 0.1% (v/v) TFA and solvent B was 95% (v/v) acetonitrile, 0.1% (v/v) TFA. The concentration of Solvent B was adjusted according to the following profile: 25-40% B over 20min, 40-50% B over 30min, 55-60% B 10min, held at 60% B for 10min, and 60-0% B over 10min. A flow rate of 1ml/min was used, and a sample volume of 20μl was injected. The HPLC eluate was fractionated according to peak positions indicated in the text, the sample was freeze-dried, and the protein composition subsequently analysed on an 18% SDS-PAGE gel.

3.2.3. Separation of Core Histone Isoforms by TAU Gel Electrophoresis

Isolated histones were electrophoresed on 16cm long 15% [total acrylamide, w/v; 19:1 (w/w) acrylamide : bis-acrylamide] TAU gels using 350μm plate spacers as modified from (Lennox and Cohen, 1989). The running gel contained 10% (v/v) triton X-100, 6.0 M urea and 5% (v/v) acetic acid, and was filtered through a 0.25 μm filter and degassed against water

vacuum prior to polymerization. The stacking gel contained 4% (w/v) total acrylamide [19:1 (w/w) acrylamide:bisacrylamide], 10% (v/v) triton X-100, 6.0 M urea and 5% (v/v) acetic acid, and was overlaid with 300μl overlay solution [0.02% (v/v) pyronine Y, 6.0 M urea, 5% (v/v) acetic acid], pre-electrophoresed overnight at 180V at 4ºC, using 5% (v/v) acetic acid as running buffer. All the electrophoresis runs were in a reverse direction. The flow of electrons was from the cathode to the anode. The overlay solution was rinsed off with 5% (v/v) acetic acid, and 150μl of scavenging solution [0.02% (v/v) pyronine Y, 2.5 M cysteamine-HCl, 6.0 M urea, 5% (v/v) acetic acid) was loaded and the gel subjected to electrophoresis at 150V for 20min. This step removed the free radicals that can modify proteins and alter their migration. In order to block non-specific interactions between the gel matrix and the histones, 150μl of protamine solution [0.02% (v/v) pyronine Y, 25 mg/ml protamine sulphate, 6.0 M Urea, 5% (v/v) acetic acid] was loaded onto the stacking gel at 200 V overnight. A comb was placed on top of the stacking gel to create wells. The protamine solution was used as a sample buffer. A maximum of 6μl of protein (30μg) was loaded. The gel was electrophoresed at 200V for approximately 16h, allowing the fast migrating proteins to transverse approximately three-quarters of the gel. The TAU gels were stained with Coomassie blue G-250 as detailed in Current Protocols in Molecular Biology (Ausubel *et al*., 2003). The stained gels were scanned on a Molecular Imager laser scanner (Bio-Rad) and the densitometric analysis of the image to quantitate acetylation levels was performed with Quantity One quantification analysis software v 4.5.2 (Bio-Rad). Data in the text are expressed as the average plus/minus the standard deviation at 3σ from three independent samples and gels.

3.3. Results

TAU gels have often been used to investigate the level of acetylation of core histones isolated from different tissues or organisms. We were interested in applying this technique to investigate possible differences in the level of acetylation of the core histones isolated from yeast cells in stationary phase (6 day old culture) or from cultures at various time points during stationary phase exit. In order to accurately identify the various levels of possible acetylation of histones, we decided to first isolate the four core histones by conventional Zymolyase isolation technique, purify each histone by RP-HPLC, and electrophorese each purified histone sample in separate lanes of a TAU gel to allow unambiguous identification of each of the core histones in subsequent experiments.

The core histones were isolated from an exponential culture of *S. cerevisiae* strain W303-1A and purified by RP-HPLC using a step-gradient of acetonitrile and TFA. This isolation was prepared in the absence of the histone de-acetyltransferase (HDAC) inhibitor, sodium butyrate, and it is therefore likely that a significant proportion of acetyl moieties were removed from lysine residues during the isolation procedure. The HPLC elution profile, was recorded at 210nm to maximize detection of the histones that are low in aromatic amino acids, and is shown in Figure 3.1.

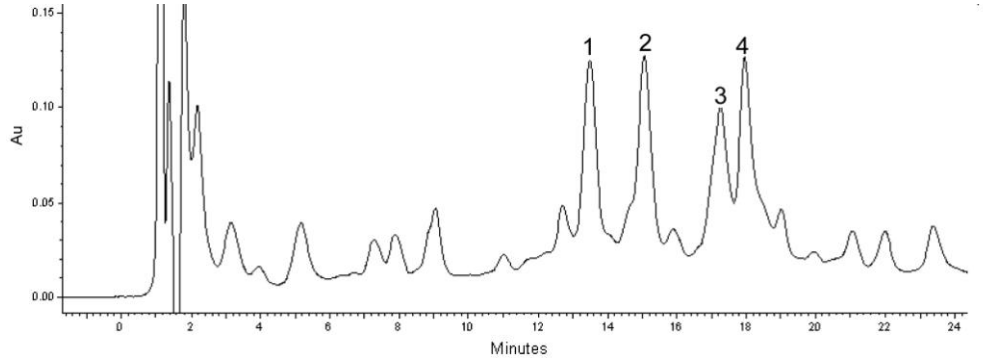

Figure 3.1. Elution profile of core histones. Core histones were isolated using the Zymolyase method in the absence of the de-acetylase inhibitor, sodium butyrate, and purified by RP-HPLC using a multi-step acetonitrile/TFA gradient. Peaks 1-4, indicated, were collected for further SDS-PAGE analysis.

Referring to this figure, a number of peaks were observed, with four prominent peaks at elution times between 13 and 18 min. These four prominent peaks were collected, the organic solvent evaporated, the samples freeze-dried, and the protein content of each of the four peaks analyzed by SDS-PAGE. The Coomassie stain of the gel is shown in Figure 3.2.

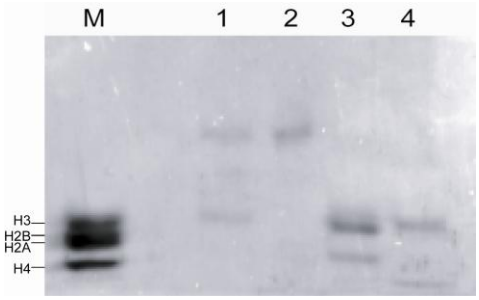

Figure 3.2. Electrophoretic separation of collected peaks. The proteins recovered in peaks 1-4 (lanes 1-4) in the RP-HPLC eluate of the isolated core histones were separated by SDS-PAGE gel. A Coomassie stain of the gel is shown. Chicken core histones were used as size standard (lane M).

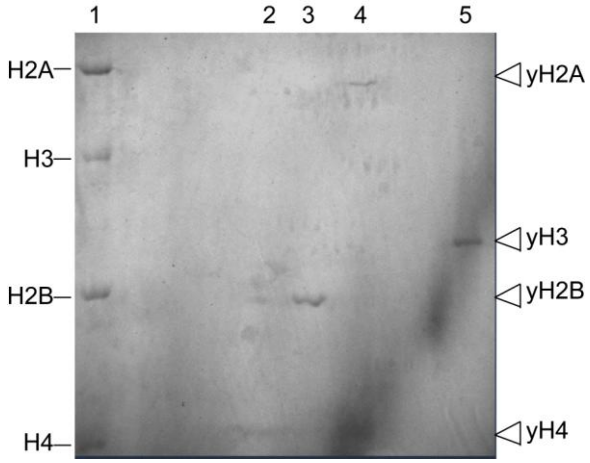

Figure 3.3. Calibration of the 15% TAU gel with RP-HPLC separated yeast histones as shown in figure 3.1. Lane 1 - chick core histone standard; lane 2 - yeast H4 and H2B; lane 3 - yeast H2B, a carry-over from lane 2; lane4 - yeast H2A and H4; lane 5 - yeast H3.

The identified yeast core histone fraction was then resolved in separate lanes of a 15% TAU gel. The result is shown in Figure 3.3. In Figure 3.3, lane 1 shows the migration pattern of standard chick core histones on a TAU PAGE gel, and is similar to that previously reported (Hebbes *et al*., 1992). However, according to our knowledge no group has reported a direct comparison of yeast and chicken histones electrophoresed on the same TAU gel. In Figure 3.3, lane 2 showed yeast H4 and H2B migrated similarly to chicken H4 and H2B. Lane 3 is a carry-over from lane 2, with yeast H2B being more prominent than yeast H4. In lane 4 yeast H2A migrates comparable to chicken H2A. The band in lane 5 corresponds to purified yeast histone H3, and electrophoreses quite differently on the TAU gel compared to chicken H3. With this knowledge on the electrophoretic behaviour of the pure yeast histones, we can accurately identify the individual histones in a mixture of histones resolved by TAU PAGE.

Histones H2A, H2B, H3 and H4 were isolated from stationary phase cultures, and at 15 min and 1 h time points after stationary phase exit following transfer of the culture to fresh growth medium, using the rapid histone isolation procedure. The pure histones were electrophoresed on 15% TAU gels to resolve the individual acetylation isoforms for each histone. The result is shown in Figure 3.4.

Referring to this figure, four different acetylation isoforms were seen for histone H4 (Fig. 3.4 A), and three, three and two for each of histones H3, H2B and H2A, respectively (Fig. 3.4 B-D). Yeast histone H4 has a total of 11 lysine residues, of which 4 appear in the N-terminal tail. All four of these lysine residues have previously been shown to be acetylated under different conditions. It is therefore clear that only a fraction of all H4 lysine residues that can be acetylated, were, in fact, acetylated in yeast. It should be noted that a single acetylation histone isoform resolved on the TAU gel contains the same total number of acetylated residues, but may be different combinations of acetylated lysine residues. Intriguingly, even though acetylated H3 and H4, in particular, are associated with transcriptional activity, and

stationary phase is a state of extensive transcriptional repression (Choder, 1991), acetylated isoforms were visible for all four core histones in stationary phase (see lanes 2 of Fig. 3.4 A-D). The non-acetylated isoform, however, was the dominant isoform for each histone at the three different time points (see lanes 2-4 of Fig. 3.4 A-D).

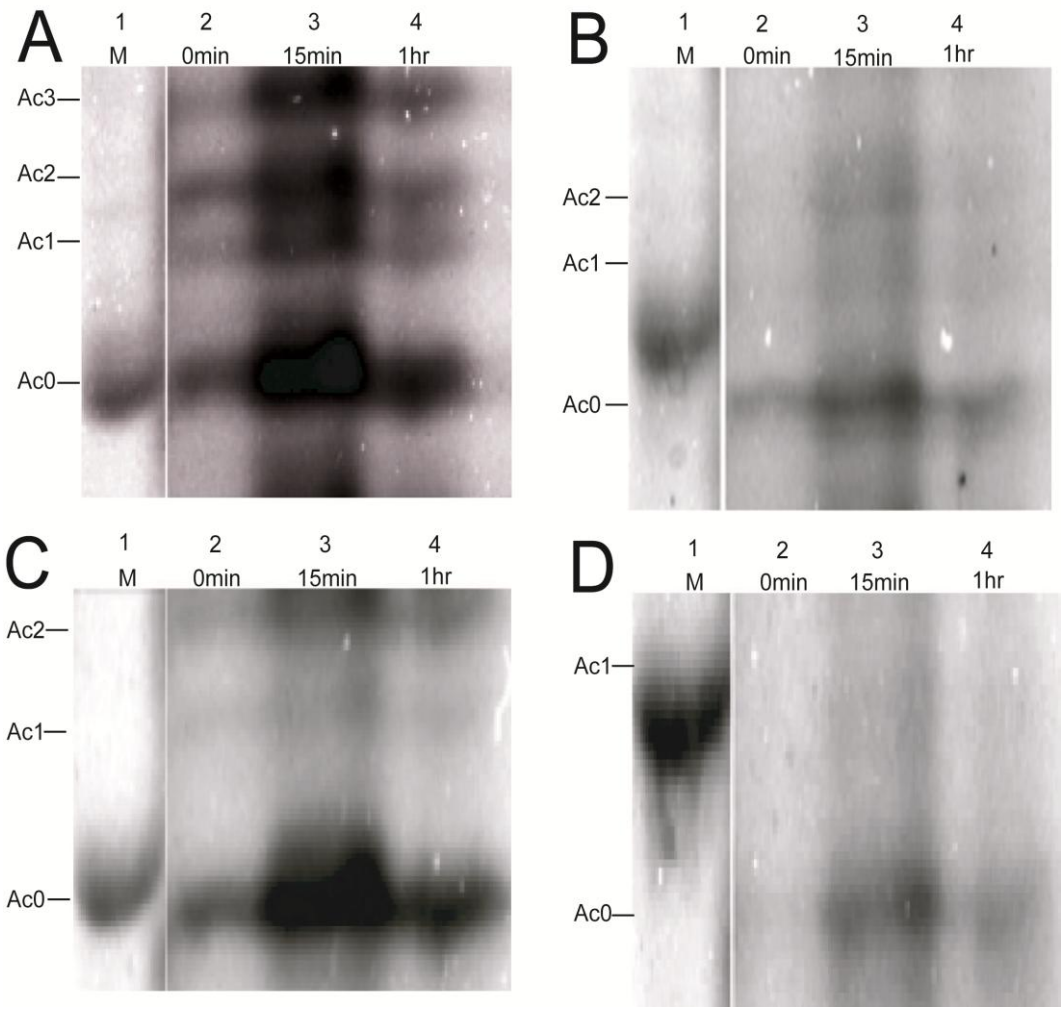

Figure 3.4. Acetylation isoforms of the core histones during stationary phase exit. Histones H4 (A), H3 (B), H2B (C) and H2A (D) were isolated from 6 day stationary phase yeast cultures (lanes 2), 15 min after stationary phase exit (lanes 3) and 1 h after stationary phase exit (lanes 4) and electrophoresed on a 15% TAU gel. A Coomassie stain of the gel is shown. A chicken histone standard, taken from another part of the same gel, is shown in lanes 1. The acetylation isoforms of the yeast histones are indicated to the left of each panel. A representative gel is shown.

In order to gain insight into quantitative differences in the level of acetylation of the four core histones during exit of stationary phase, the Coomassie stained TAU gels were scanned, and the intensity of each isoform band quantitated. To allow direct comparison between different time points, the total of all isoforms at each time point, resolved in one lane of a gel, was normalized to 100%. The results of three independent experiments for each of the four core histones are shown in Figures 3.5 to 3.8.

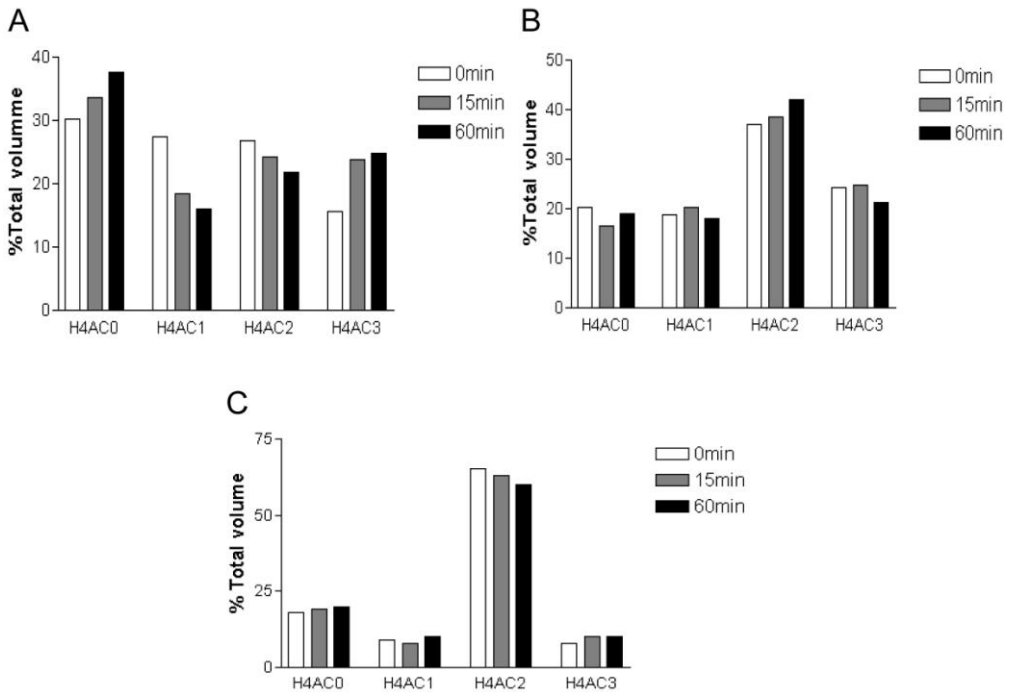

Figure 3.5. Quantitative analysis of the level of acetylation of histone H4 during stationary phase exit in yeast. Histone H4 was isolated by the rapid isolation procedure in the presence of a de-acetylase inhibitor from 6 day stationary phase cultures (white bars), and 15 min (gray bars) and 1 h (black bars) after stationary phase exit, resolved on a TAU gel, and the level of each acetylation isoform quantitated with in a scanned image of the Coomassie stained gel. The total level for all isoforms was normalized to 100% for each time point. The results of three independent experiments are shown (A-C).

Looking first at histone H4 (Fig. 3.5), it appears that the isoform representing intermediate levels of acetylation (mono- and di-acetylated forms) diminished during stationary phase exit, whereas the un-acetylated and tri-acetylated isoforms increased over the same time period (see Fig. 3.5 A). However, this same tendency was not reproducibly visible in independent experiments (compare panels A-C of Fig. 3.5).

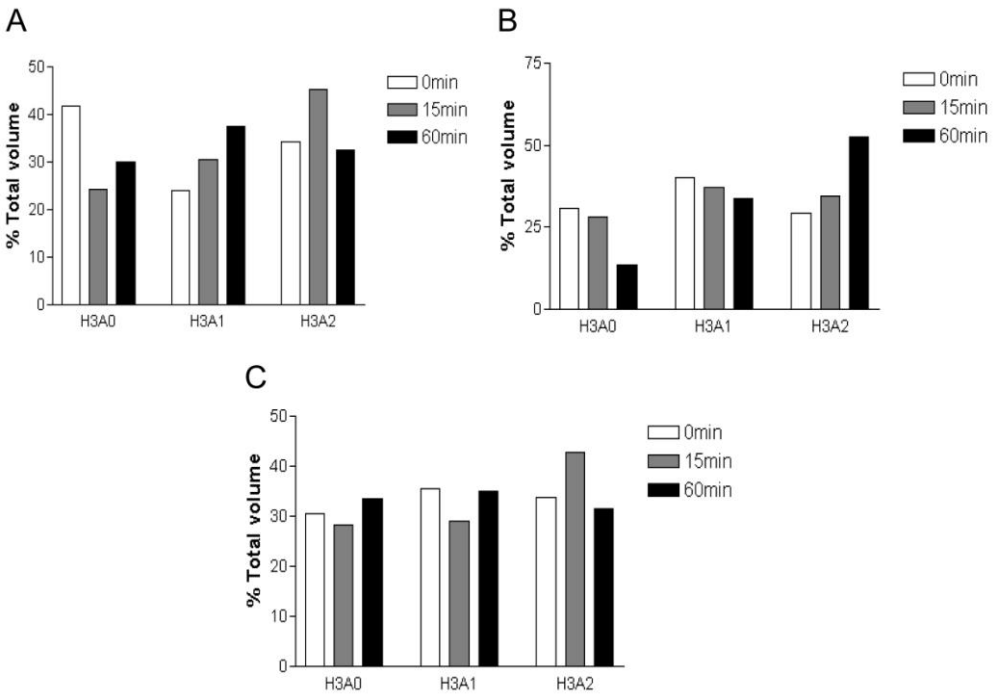

Figure 3.6. Quantitative analysis of the level of acetylation of histone H3 during stationary phase exit in yeast. The level of each acetylation isoform of histone H3 was determined in 6 day stationary phase cultures (white bars), and 15 min (gray bars) and 1 h (black bars) after stationary phase exit as described in Figure 3.5. The results of three independent experiments are shown (A-C).

Considering histone H3 next, there appears to be an increase in the level of acetylation during stationary phase exit (see Fig. 3.6 A-C). This tendency is, however, modest in triplicate experiments (compare panels A-C of Fig. 3.6).

Very little change in the level of each acetylation isoform is seen for both histones H2A and H2b during exit of stationary phase (see Figs. 3.7 and 3.8).

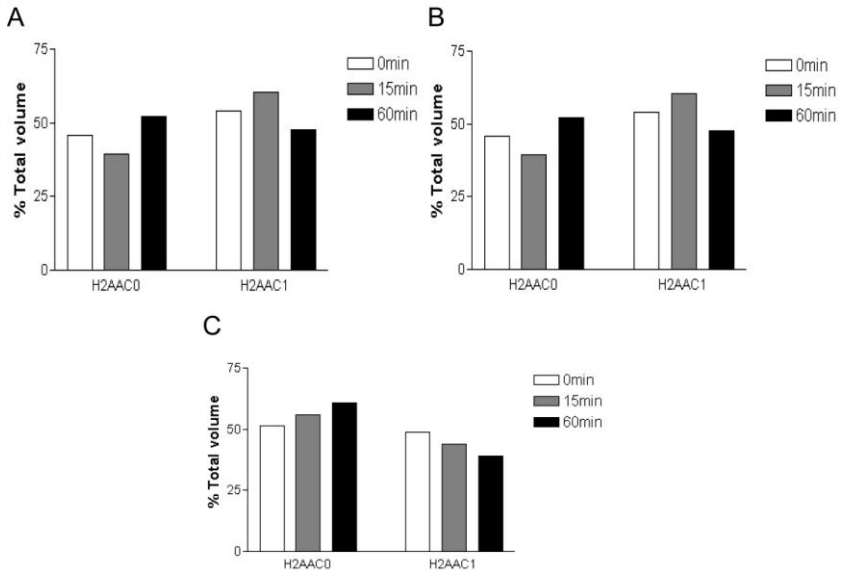

Figure 3.7. Quantitative analysis of the level of acetylation of histone H2A during stationary phase exit in yeast. The level of each acetylation isoform of histone H2A was determined in 6 day stationary phase cultures (white bars), and 15 min (gray bars) and 1 h (black bars) after stationary phase exit as described in Figure 3.5. The results of three independent experiments are shown (A-C).

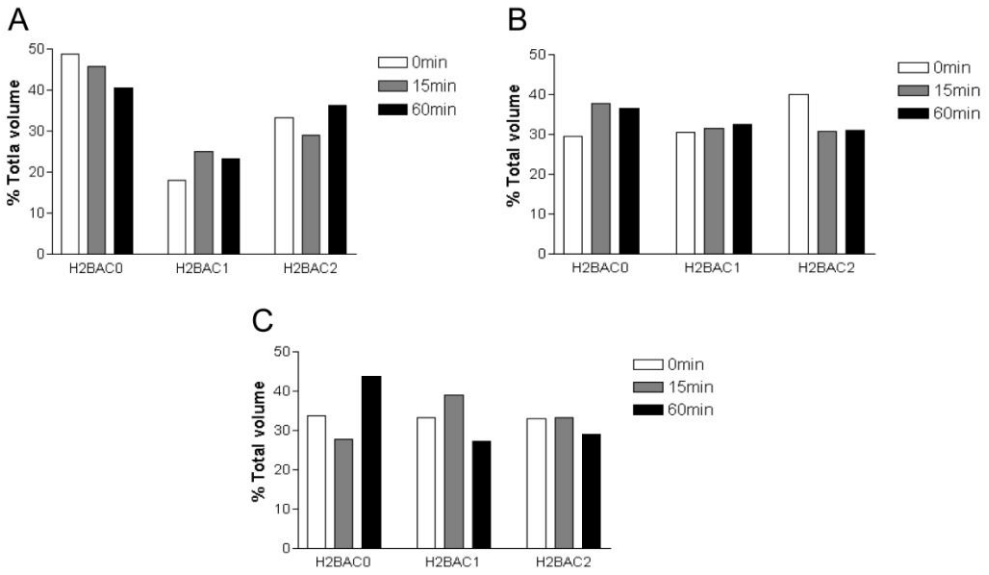

Figure 3.8. Quantitative analysis of the level of acetylation of histone H2B during stationary phase exit in yeast. The level of each acetylation isoform of histone H2B was determined in 6 day stationary phase cultures (white bars), and 15 min (gray bars) and 1 h (black bars) after stationary phase exit as described in Figure 3.5. The results of three independent experiments are shown (A-C).

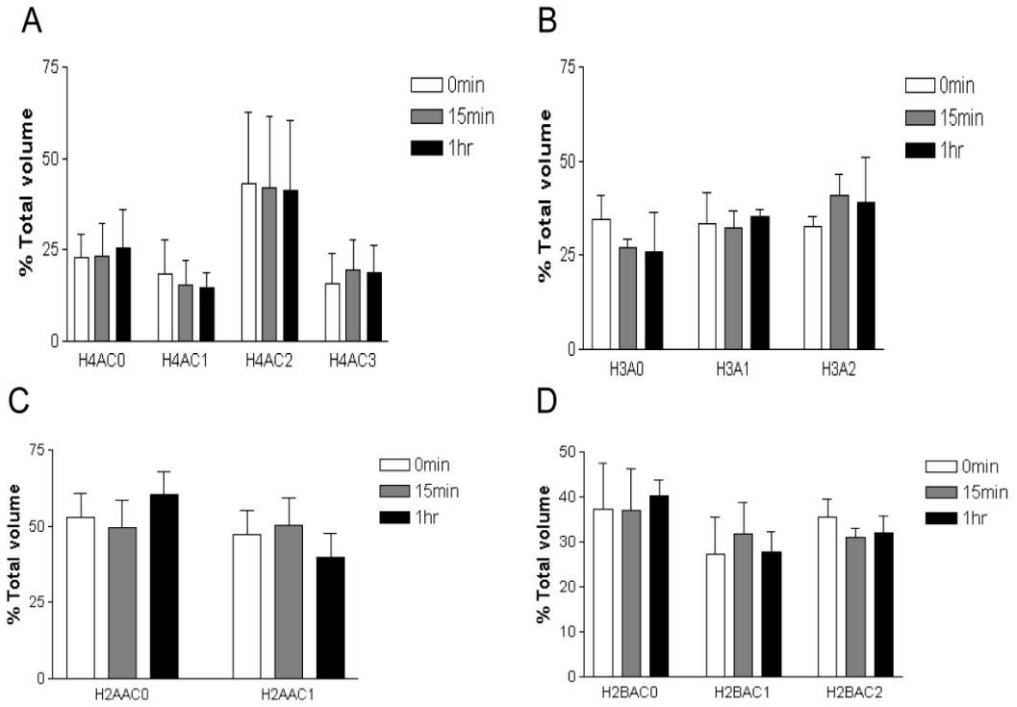

Figure 3.9. Quantitative analysis of the level of acetylation of core histones during exit of stationary phase in yeast. TAU gels were scanned in a laser imager, and the volume of each band, corresponding to different levels of lysine acetylation for each core histone, quantitated with image software. The histograms shows the average value from three independent gels for the three acetylation isoforms of H4 (A), two acetylation isoforms of H3 (B)the one acetylation isoform of H2A (C), and the two acetylation isoforms of H2B (D). In order to correct for total intensity differences between gel images, the total level of all isoforms for each histone was normalized to 100% for every individual TAU gel image prior to calculating the average. The different panels each show the average level of each isoform in a six day stationary phase culture (white), 15 min after initiation of stationary phase exit following re-feeding (gray), and 1 h after stationary phase exit (black).

In order to formalize the tendency observed in the separate triplicate experiments for each of the core histones, the average level for each isoform was calculated for each time point for the four core histones. The result is shown in Figure 3.9. Looking first at histone H4 (Fig. 3.9 A) it is seen that the di-acetylated isoform predominates. There was no statistically significant redistribution between the different acetylation isoforms of H4 during exit of stationary phase (one way Anova analysis; $p<0.05$). In the case of histone H3, a tendency towards higher levels of acetylation is again seen during exit of stationary phase (see Fig. 3.9 B). However, this tendency was not statistically significant (one way Anova analysis; $p<0.05$). The distribution of the different acetylation isoforms remained even during exit of stationary phase for both histones H2A and H2B (see Fig. 3.9 C and D).

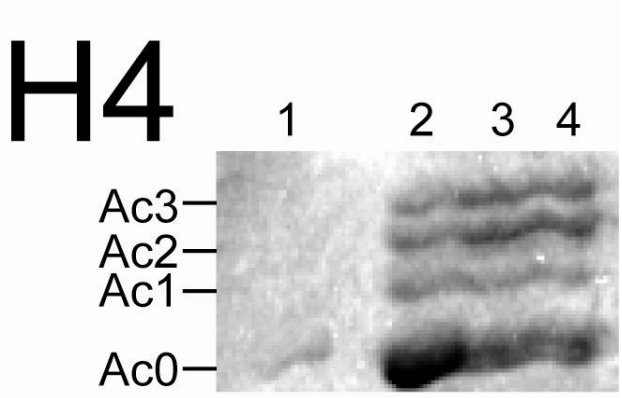

Figure 3.10. The level of histone H4 acetylation isoforms in three different yeast strains. Histone H4 was isolated by the rapid procedure in the presence of a de-acetylase inhibitor from exponentially growing *S. cerevisiae* strains BY4742 (lane 2), W303-1A (lane 3) and JDY43 (lane 4) and resolved on a TAU gel. A Coomassie stain of the gel is shown. A chicken histone standard is shown in lane 1. The different yeast histone acetylation isoforms are indicated to the left of the panel.

We were surprised by the fact that no statistically compelling difference in the level of acetylation of any of the histones could reproducibly be seen during exit of stationary phase. We therefore investigated the possibility that the isoform distributions that we observed were typifying of a specific yeast strain. Different strains of *Saccharomyces cerevisiae* have many genetic differences which can be observed in clear phenotypic differences. To address the possibility of a strain-specific effect, we isolated histone H4, which showed a clear distribution over 4 different acetylation isoforms, from yeast strains BY4742 W303-1A and JDY43, and resolved the isoforms on a TAU gel. The result is shown in Figure 3.10. It was found that the predominant isoform in each strain was the un-acetylated species, with the di-acetylated species the next most abundant (see Fig. 3.10). No difference in the distribution among the different acetylation isoforms was evident for the three strains (see Fig. 3.10) showing that the isoform distribution observed for each of the four core histones were likely not to be strain-specific.

3.4. Discussion and Conclusion

It is well-established that significant transcriptional re-programming takes place in *S. cerevisiae* during exit of stationary phase, with an extensive induction of gene expression. This increase in transcriptional activity, which requires access to the DNA molecule, occurs concomitant with the rapid dissociation of linker histone H1 from chromatin during re-initiation of the cell cycle (Schäfer *et al*., 2008), and the general decondensation of the 30 nm fiber during the transition from stationary to exponential phase. It is also well-established, making use of chromatin immuno-precipitation techniques, that transcriptionally active genes are associated with highly acetylated histones, particularly histones H3 and H4 (Hebbes *et al.*, 1988). It was therefore surprising to observe that the distribution of the acetylated forms remained fairly constant for H3 and H4 during the transition from stationary to exponential phase. The absence of an observed change in histone acetylation isoforms of H2A and H2B is less surprising, since these proteins have previously been shown to play a lesser role in chromatin compaction (Krajewski and Ausió, 1996).

This observation was not due to a large “free” pool of histones that diluted any change that occurred with this transition, since approximately 0.2% of the total cellular histone pool is incorporated into chromatin at any one time (Oliver *et al*., 1974). Also, histones were isolated using a rapid freezing method to limit any change in the acetylation pattern that may occur with prolonged exposure to de-acetylase enzymes.

In previous studies the level of acetylation of core histones associated with single specific genes were generally measured using anti-bodies directed at specific acetylation isoforms, polymerase chain reaction amplification of the gene of interest, followed by immuno-precipitation, a technique known as chromatin immuno-precipitation. This technique allowed quantitation of different acetylation isoforms associated with different regions of the genome.

However, since the anti-bodies directed at different acetylation isoforms had different affinities to their antigenic groups, it remained problematic to study redistributions between different isotypes for a given histone. Also, quantitation often relied on amplification of the DNA to measure the relative amount of a given isoform bound to the gene of interest, resulting in non-linear measurements that are typically described as "semi-quantitative". Nevertheless, the association of hyper-acetylated histones and actively transcribed genes is widely accepted in the literature. However, the level of acetylated histone is not evenly distributed along the full length of the gene, but appears concentrated in the promoter areas. This is understandable in light of the requirement for chromatin to become decondensed to allow general transcriptional activators to bind to the promoter-enclosed *cis* elements. However, the fractional change in the level of acetylation of histones associated with the entire gene may be small. Thus, our results showing a modest effect for total cellular histone may reflect the very focused patches in the genome where these changes occur, representing a tiny percentage of the total histone pool.

An additional consideration is that a given acetylation isoform may be constituted by several different patterns of acetylated lysines. For instance, histone H4 may be acetylated on lysines 5, 8, 12 and 16. In a tri-acetylated population, four different combinations of tri-acetylated lysines are possible. Thus, if there is any dynamic redistribution between the precise patterns of acetylation, which was shown to occur at different genes, this change would not be visible to the current TAU analysis. In addition, acetylation is one of several post-translational modifications that occurs in chromatin that involved in the regulation of DNA function. Modifications other than acetylation would not have been picked up in the TAU analysis.

We additionally decided to extend our study with mass spectrometry, where precise residues involved may be identified.

3.5. Reference List

A. T. Annunziato, L. L. Frado, R. L. Seale, and C. L. Woodcock. Treatment with sodium butyrate inhibits the complete condensation of interphase chromatin. *Chromosoma* 96 (2):132-138, 1988.

M. Choder. A general topoisomerase I-dependent transcriptional repression in the stationary phase in yeast. *Genes Dev.* 5 (12A):2315-2326, 1991.

J. V. Gray, G. A. Petsko, G. C. Johnston, D. Ringe, R. A. Singer, and M. Werner-Washburne. "Sleeping beauty": quiescence in *Saccharomyces cerevisiae*. *Microbiol.Mol.Biol.Rev.* 68 (2):187-206, 2004.

T. R. Hebbes, A. W. Thorne, and C. Crane-Robinson. A direct link between core histone acetylation and transcriptionally active chromatin. *EMBO J.* 7 (5):1395-1402, 1988.

T. R. Hebbes, A. W. Thorne, A. L. Clayton, and C. Crane-Robinson. Histone acetylation and globin gene switching. *Nucleic Acids Res.* 20 (5):1017-1022, 1992.

T. Kouzarides. Chromatin modifications and their function. *Cell* 128 (4):693-705, 2007.

W. A. Krajewski and J. Ausio. Modulation of the higher-order folding of chromatin by deletion of histone H3 and H4 terminal domains. *Biochem.J.* 316 (Pt 2):395-400, 1996.

R. W. Lennox and L. H. Cohen. Analysis of histone subtypes and their modified forms by polyacrylamide gel electrophoresis. *Methods Enzymol.* 170:532-549, 1989.

D. Oliver, D. Granner, and R. Chalkley. Identification of a distinction between cytoplasmic histone synthesis and subsequent histone deposition within the nucleus. *Biochemistry* 13 (4):746-749, 1974.

G. Schäfer, C. R. McEvoy, and H. G. Patterton. The *Saccharomyces cerevisiae* linker histone Hho1p is essential for chromatin compaction in stationary phase and is displaced by transcription. *Proc.Natl.Acad.Sci.U.S.A* 105 (39):14838-14843, 2008.

K. Struhl. Histone acetylation and transcriptional regulatory mechanisms. *Genes Dev.* 12 (5):599-606, 1998.

J. H. Waterborg and T. Kapros. Kinetic analysis of histone acetylation turnover and Trichostatin A induced hyper- and hypoacetylation in alfalfa. *Biochem.Cell Biol.* 80 (3):279-293, 2002.

A. Zweidler. Resolution of histones by polyacrylamide gel electrophoresis in presence of nonionic detergents. *Methods Cell Biol.* 17:223-233, 1978.

CHAPTER 4.

Mass Spectrometric Analysis of the Acetylation State of Core Histones of *Saccharomyces Cerevisiae* in Stationary and Exponential Phase.

4.1. Introduction

Various chemical modifications of the N-termini of core histones play an important role in the modulation of chromatin structure and regulate various DNA functions, including transcription, recombination, repair and replication (Kouzarides, 2007). In addition to the much studied histone acetylation, there are other modifications that have been identified by mass spectrometry (MS) including methylation, phosphorylation, ubiquitination and ADP ribosylation. Histone acetylation is believed to disrupt the ability of the N-terminal tail to form secondary structures that are involved in chromatin compaction as well as the binding of proteins that are involved in transcription (Hansen, 1998). In a more “open” chromatin state, H4 lysines 5, 8, and 12 are predominantly bound by the bromodomain of transcription activators. This strengthens the notion that acetylation enhances transcription (Johnson *et al*., 1998). In addition, a recent study has suggested a central role for acetylation of H4 at lysine 16 in the control of chromatin higher order structure, where the presence of acetylated H4 lysine 16 inhibited the formation of the 30 nm chromatin fibre as well as disrupting fibre-fibre interactions (Shogren-Knaak, 2006).

Previous studies have demonstrated that several lysine residues, including lysines 4, 9, 27, and 36 of H3 and lysine 20 of H4, were also sites of methylation (Strahl *et al*., 1999). Different histone methylation states are associated with different chromatin functions. It was

shown that H3 Lys4 methylation was linked to active genes, whereas H3 Lys9 methylation was linked to inactive genes (Lachner and Jenuwein, 2002).

It was found that the *S. cerevisiae* linker histone Hho1p rapidly dissociated from chromatin during exit of stationary phase (Schäfer *et al*., 2008). A general activation of numerous genes occurred during stationary phase exit, followed by subsequent regulated control of classes of genes in exponential phase. This extensive transcriptional "re-programming" of the genome with the transition of transcriptionally repressed and highly compacted chromatin in stationary phase to transcriptionally active and decondensed chromatin in exponential phase, provides a unique window in which to investigate covalent modifications of the core histones as a regulatory switch that controls this reprogramming event.

Protein micro-sequencing were traditionally used for the identification of post-translational modifications of the core histones (Vidali *et al*., 1968). However, it is a tedious technique that requires relatively large and highly purified samples. In addition, the presence of a blocked N-terminus on many histone complicated protein sequencing efforts. Anti-body based methods require prior knowledge of individual modifications in order to raise and/or select antibodies appropriate to recognize a given modification. Mass spectrometry (MS), on the other hand, does not require prior knowledge of the modification. To avoid the limitations of protein sequencing and antibody based methods, researchers have more recently been using MS for the characterization of histone post-translational modifications.

MS is an analysis technique that detects molecules or molecular fragments based on their mass-to-charge (*m/z*) ratio The use of MS has allowed the identification of numerous residues that are post-translationally modified in histones, many of which are located outside of the amino terminal tail (Kouzarides, 2007). Because of the high sensitivity, specificity and

the ability to locate the precise location of the modification sites, MS is the preferred method for the identification and analysis of post-translational modifications (PTMs) in histones.

Triton-acid-urea gels are used to assess the net acetylation state of a histone, but cannot detect any change in the specific residue(s) that is/are acetylated. It is also possible that modifications other than acetylation underlie the transition in functional state of the chromatin with the exit of stationary phase in yeast. We therefore decided to investigate the PTM patterns of histones in yeast by using MS. We made use of a nanoflow-HPLC system linked to a nano electro-spay interface (ESI) that delivered the sample to a hybrid triple quadrupole MS. The third quadrupole could also be set to act as a linear ion-trap. This increases the sensitivity of the instrument, and provides an ideal technique to detect PTMs that may be present at low levels in the samples.

4.2. Materials and Methods

4.2.1. In-Gel Digestion

Histones were purified by the Zymolyase method and resolved by SDS-PAGE electrophoresis as detailed previously. The enzymatic digestion of the histone bands in the polyacrylamide gel matrix following electrophoresis was carried out as reported (Shevchenko *et al*., 2006), a method that is compatible with nano-LC-MS/MS. Briefly, the gel bands were excised and cut into small cubes (~1 mm^3). The gel pieces were shrunk with 500 μl 99.9% (v/v) acetonitrile (Sigma). A 50 μl aliquot of 10 mM dithiothreitol (DTT) in 100 mM ammonium bicarbonate (Sigma) was added to cover the gel pieces completely, and the sample incubated at 56°C in an air thermostat for 30 min to minimize condensation against the underside of the tube cap. The sample was cooled down to room temperature and 50 μl of

55 mM iodoacetamide (Sigma) in 100 mM ammonium bicarbonate was added, and the sample incubated at room temperature for 20 min in the dark. Following reductive alkylation, Coomassie-stained gel pieces were destained for 30 min in 100 μl of 100 mM ammonium bicarbonate/acetonitrile (1:1, v/v) with occasional vortexing. The gel pieces were saturated with trypsin (sequencing grade; Promega) buffer [10 mM ammonium bicarbonate in 10% (v/v) acetonitrile]. The buffer and the enzyme was allowed to seep into the gel matrix for 90 min on ice, and the enzymatic digestion then allowed at 37°C overnight. Peptides were extracted from the gel matrix in 100 μl extraction buffer [5% (v/v) formic acid (Merck), 60% (v/v) acetonitrile] at room temperature and gently shaken at 30°C for 30 min. The liquid extract was dried completely in a rotary evaporator (Savant) and peptides resuspended in 20 μl, 5% (v/v) formic acid for MS analysis.

4.2.2. Peptide Analysis Using Nano-LC-MS/MS

Digested peptides were separated by nanoflow HPLC (Agilent model 1200). Samples (5 μl) were concentrated and desalted on a 300μm × 5mm Zorbax 300SB-C18, trapping column with 5 μm particle size (Agilent). The peptides were separated on a 150 mm × 75 μm Zorbax 300SB-C18, column with 3.5 μm particle size. The following step-wise gradient profile was used at a flow-rate of 0.35μl/min: 10 min, 0% B; 15 min, 10% B; 95 min, 25% B; 100 min 50% B; 101 min, 90% B; 120 min 90% B. Solvent A consisted of 1% (v/v) acetonitrile, 0.1% (v/v) formic acid. Solvent B consisted of 95% (v/v) acetonitrile, 0.1% (v/v) formic acid. Positive ions were generated by nano-ESI and the 4000 QTRAP was operated in "Information Dependent Acquisition" (IDA) mode. For routine protein and peptide identification enhanced mass spectrometry (EMS) scans of 3 sec were carried out in the 400-1400 *m/z* range. The three most abundant peaks at intensities greater than 1000 cps were selected for fragmentation by collision induced dissociation (CID) in quadrupole 2. Quadrupole 1 and 3 were set as the only resolving units. An enhanced resolution (ER) scan

of these peaks was then recorded to determine the charge state of the fragment, followed by a CID product-ion scan. A mass tolerance of 1Da was selected and a rolling collision energy of 10-80 eV was applied. All analyses were performed using mono-isotopic masses.

For identification of acetylation sites precursor-ion scans of 2 sec duration were initially carried out in the 400-1400 *m/z* range. Peaks at intensities greater than 1000 cps that had lost a 126 Da fragment during collision induced dissociation (CID) fragmentation in quadrupole 2 were selected. An enhanced resolution scan of these peaks was then recorded to determine the charge state of the fragment, followed by a CID product-ion scan. A mass tolerance of 1Da was selected and a rolling collision energy of 10-80 eV was applied. All analyses were performed using mono-isotopic masses.

4.2.3. Protein Identification and Modification Discovery by Database Search

MS/MS spectra from the 4000 QTRAP were generated using Analyst v1.2 (Applied Biosystems) and were submitted to the Mascot version 2.1 (Matrix Science) searching was done using a local copy of the Swiss-Prot (v 51.6) database. Precursor and product ion tolerance were 2.4 and 1.2 Da, respectively, which is appropriate for the accuracy of the 4000 QTRAP. Acetylation of lysine was specified as a variable modification and up to six missed cleavages by trypsin were allowed. Proteins and peptides were confidently identified when matches had high ion score (> 20) and statistically significant [low E value(< 3)].

4.3. Results

We set out to identify the residues that were acetylated in core histones of *S. cerevisiae* in stationary and exponential phase. We started by verifying our detection technique, using acetylated BSA (Promega). The protein was separated by SDS-PAGE (Figure 4.1 A), and a

band that contained the protein was cut from the gel (Figure 4.1 B). The protein in the gel matrix was digested with trypsin, the peptides eluted, and analysed by MS.

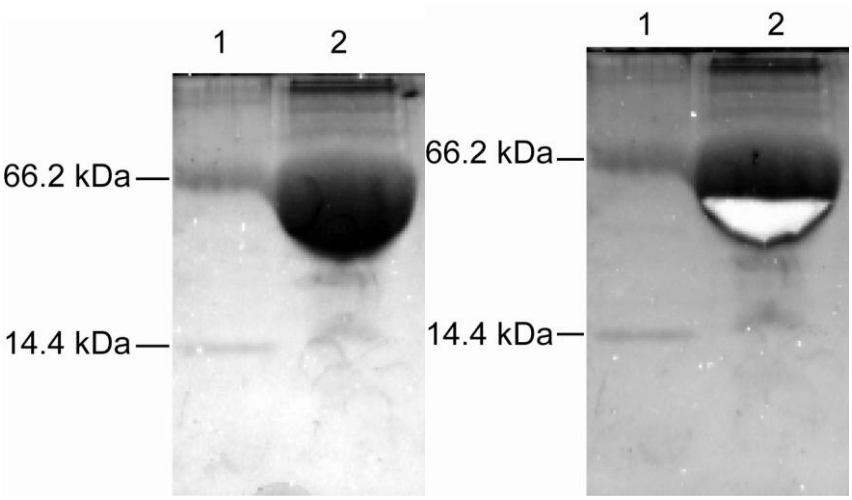

Figure 4.1. Separation of bovine serum albumin (BSA). Acetylated BSA (Promega) was resolved on a 15% SDS-PAGE gel and visualized by Coomassie stain (A). The gel band that contained acetylated BSA was excised, lane 2 (B).

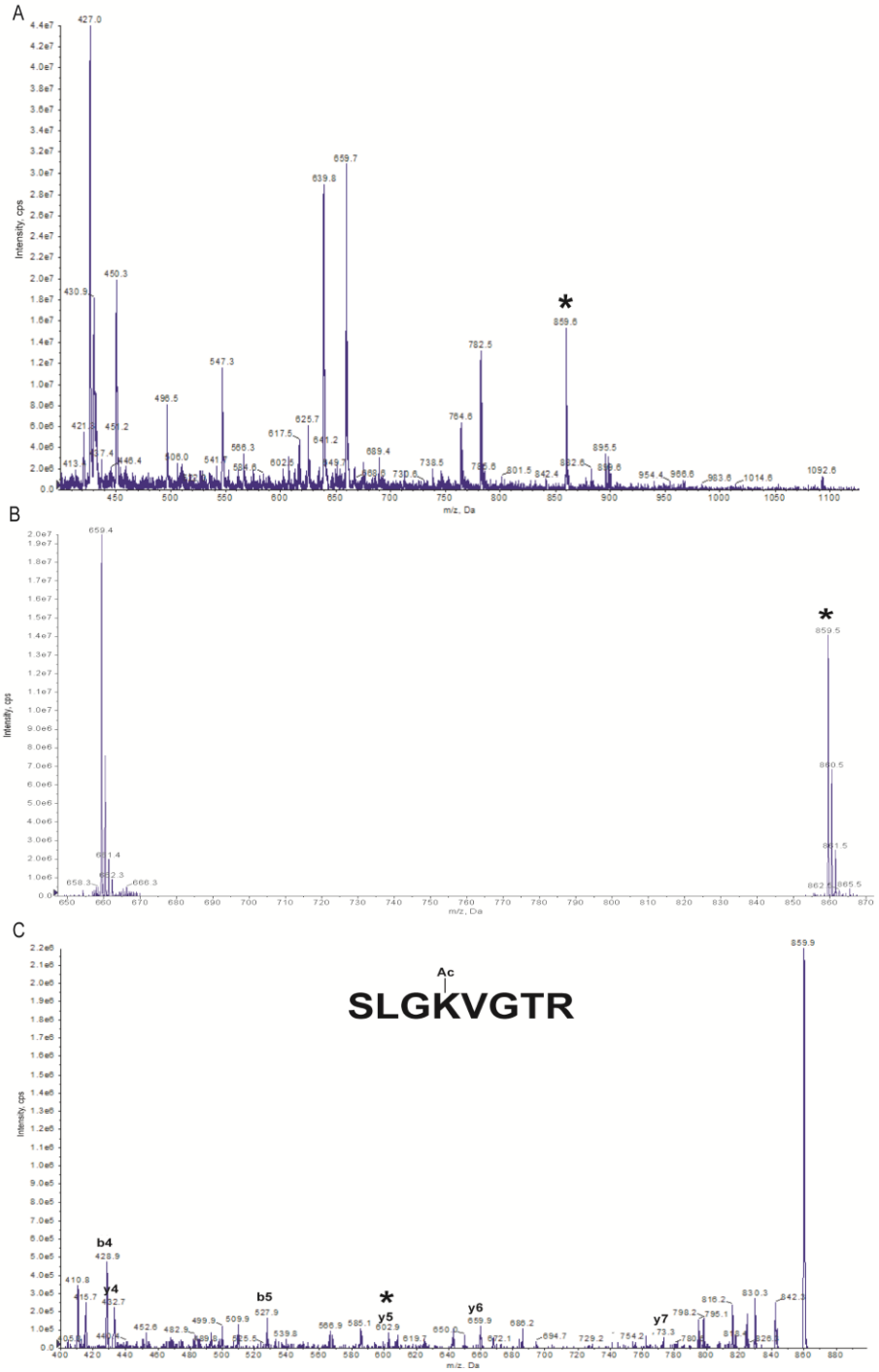

Order	b	Seq.	y	Order
1	88.0393	S		8
2	201.1234	L	772.4676	7
3	258.1448	G	659.3835	6
4	428.2504	K	602.3620	5
5	527.3188	V	432.2565	4
6	584.3402	G	333.1881	3
7	685.3879	T	276.1666	2
8		R	175.1190	1

Figure 4.2.1.1 K455 acetylation was detected in acetylated BSA without performing precursor-ion scan at 126Da. A tryptic digest of acetylated BSA isolated was analyzed by MS. The enhanced mass spectrometry spectrum (A), an enhanced resolution spectrum (B) and CID fragmentation spectrum of the peptide that resolved at 859.5 Da (singly charged), indicated by the asterisk in panel A, is shown (C). The partial y-ion and b-ion series visible in the fragmentation spectrum are indicated, and the y5 peak, representing a terminal lysine residue shifted by 42 Da, indicated by asterisk. The fragmentation peak list is shown (C) with the peaks that could be assigned to the identified peptide with a Mascot search of the Swiss-Prot database indicated in red, and the peaks that were observed in the fragmentation spectrum, underlined.

The enhanced mass spectrometry scan as described in Materials and Methods followed by fragmentation of the eluting acetylated BSA peptides was performed. Enhanced resolution scans of the resulting fragment ions were performed to confirm the charge state and to better resolve the fragment ions. The generated MS/MS spectrum was searched on Mascot search engine against Swiss-Prot database. An eight residues long mono-acetylated peptide was identified with an E value of 4.5 and a Mowse score of 32. The overall Mowse score of the protein was 77. Looking at the EMS (Fig.4.2.1.1A.) and ER (Fig. 4.2.1.1B) spectra the peptide was identified to be a doubly charged peptide of 859.5 Da. To unambiguously locate the site of mono-acetylation at position K455 of the full length acetylated BSA the MS/MS spectrum (Fig.4.2.1.1C) was studied. There is only one possible site of acetylation in this peptide, therefore, looking at the y-series ion peak list table it is clear that the difference between y5 (602.3620Da) and y4 (432.2565Da) is 170.1055Da which is equal to a single lysine residue plus an acetyl group.

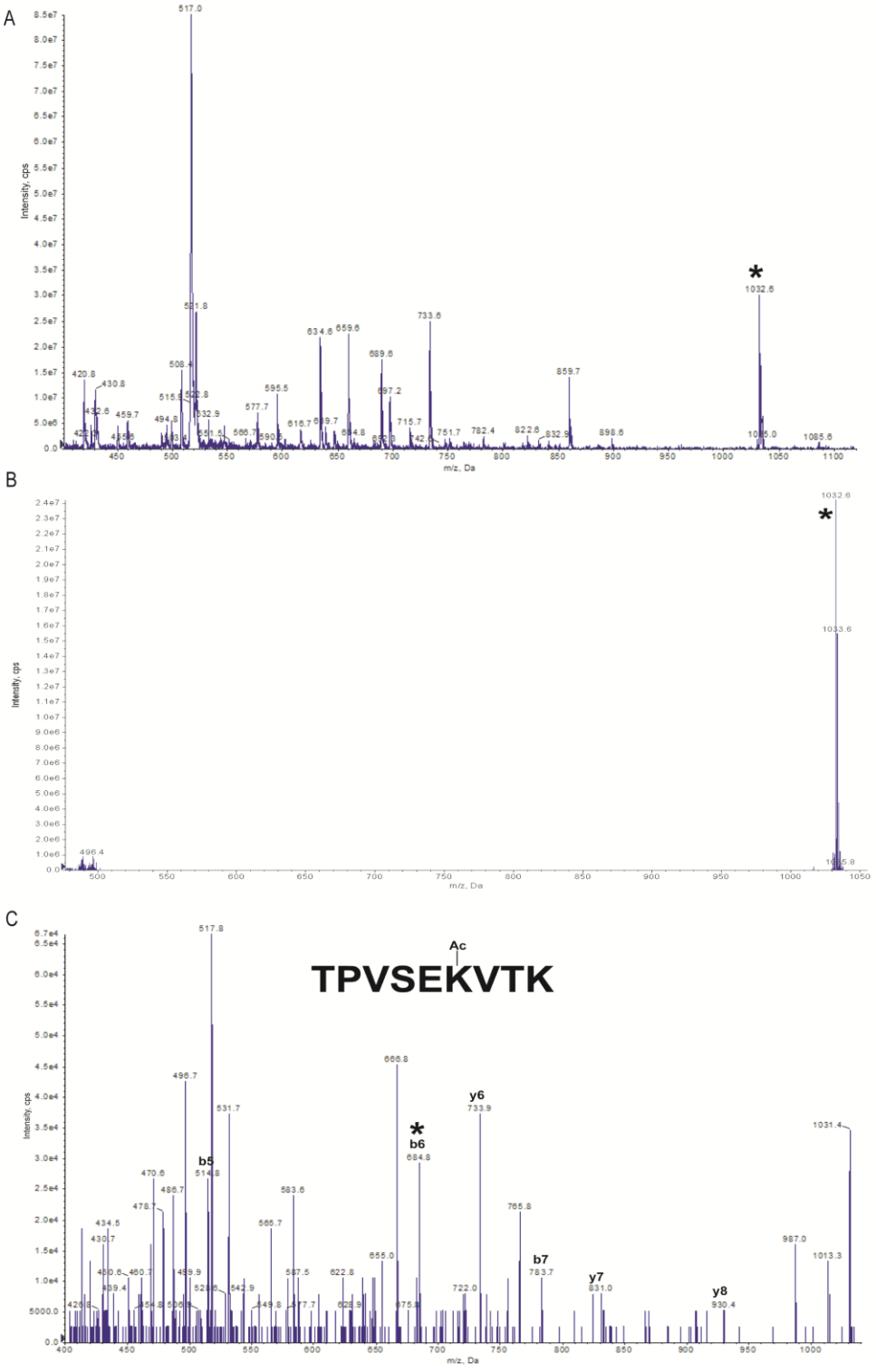
A
B
C
Intensity, cps
m/z, Da
517.0
1032.6
733.6
634.8
659.6
689.6
859.7
697.2
595.5
577.7
420.8
430.8
508.4
515.5
522.8
532.9
459.7
494.8
715.7
751.7
782.4
822.6
832.9
898.8
1085.6
1033.6
496.4
517.8
Ac
TPVSEKVTK
666.8
496.7
531.7
y6
733.9
b6
684.8
b5
514.8
470.6
486.7
583.6
478.7
434.5
430.7
565.7
655.0
765.8
b7
783.7
y7
831.0
y8
930.4
987.0
1013.3
1031.4
722.0

Order	b	Seq.	y	Order
1	102.0550	T		9
2	199.1077	P	929.5302	8
3	298.1761	V	832.4775	7
4	385.2082	S	733.4090	6
5	514.2508	E	646.3770	5
6	684.3563	K	517.3344	4
7	783.4247	V	347.2289	3
8	884.4724	T	248.1605	2
9		K	147.1128	1

Figure 4.2.1.2. K495 acetylation was detected in acetylated BSA without performing precursor-ion scan at 126Da. A tryptic digest of acetylated BSA isolated was analyzed by MS. The enhanced mass spectrometry spectrum (A), an enhanced resolution spectrum (B) and CID fragmentation spectrum of the peptide that resolved at 1032.6 Da (singly charged), indicated by the asterisk in panel A, is shown (C). The partial y-ion and b-ion series visible in the fragmentation spectrum are indicated, and the b6 peak, representing a terminal lysine residue shifted by 42 Da, indicated by asterisk. The fragmentation peak list is shown (C) with the peaks that could be assigned to the identified peptide with a Mascot search of the Swiss-Prot database indicated in red, and the peaks that were observed in the fragmentation spectrum, underlined.

Upon performing enhanced mass spectrometry scan without precursor-ion scan for identification and discovery of acetylation sites in the 607 residues acetylated BSA as described above, it was observed that K455 was not the only site of acetylation detected. K455 and seven more other sites of acetylation were identified. On submitting the generated fragmentation spectra to Mascot search database against a Swiss-Prot database, a nine residue long peptide from position 490-498 was also detected to contain a mono-acetylation site at K495. EMS spectrum (Fig. 4.2.1.2A) and ER spectrum (Fig. 4.2.1.2B.) when considered identified the peptide to be a singly charged peptide of 1032.6Da which is within 1.9 amu of the expected peptide. The ion score and the E value of the peptide was 39 and

0.94, respectively. Since there are two possible site of acetylation in the peptide the MS/MS spectrum (Fig. 4.2.1.2C) and the peak list table was considered for location of the acetylation site. By looking at the N-terminus lysine, the mass difference between the observed b6 and b5 ions, where K495 is located is 684.3563 – 514.2508 = 170.1055Da, which is equal to an acetylated lysine. Trypsin was shown to be hampered from cleaving to the C-terminus of a modified lysine, therefore, trypsin only cleaves unmodified lysine residues. In conclusion, the acetylated BSA was only acetylated in K495 and not K498.

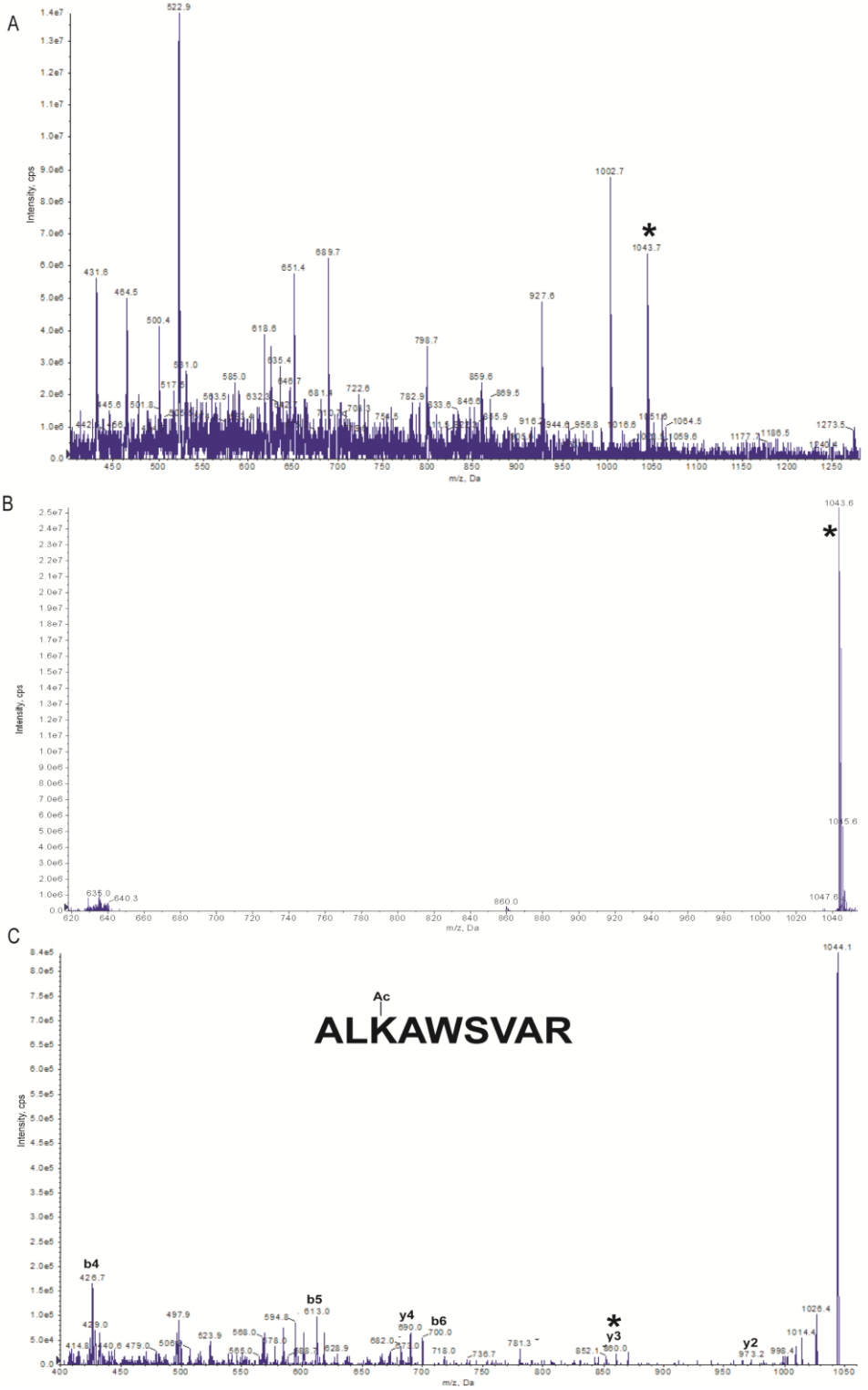
A
Intensity, cps
m/z, Da
522.9
1002.7
1043.7
689.7
651.4
431.6
464.5
500.4
927.6
618.6
799.7
B
Intensity, cps
m/z, Da
1043.6
1045.6
635.0
640.3
860.0
1047.6
C
Ac
ALKAWSVAR
Intensity, cps
m/z, Da
1044.1
b4
426.7
b5
613.0
y4
690.0
b6
700.0
y3
860.0
y2
973.2
1026.4
1014.4

Order	b	Seq.	y	Order
1	72.0444	A		1
2	185.1285	L	972.5625	2
3	355.2340	K	859.4785	3
4	426.2711	A	689.3729	4
5	612.3504	W	618.3358	5
6	699.3824	S	432.2565	6
7	798.4508	V	345.2245	7
8	869.4880	A	246.1561	8
9		R	175.1190	9

Figure 4.2.1.3. K235 acetylation was detected in acetylated BSA without performing precursor-ion scan at 126Da. A tryptic digest of acetylated BSA isolated was analyzed by MS. The enhanced mass spectrometry spectrum (A), an enhanced resolution spectrum (B) and CID fragmentation spectrum of the peptide that resolved at 1043.7 Da (singly charged), indicated by the asterisk in panel A, is shown (C). The partial y-ion and b-ion series visible in the fragmentation spectrum are indicated, and the y3 peak, representing a terminal lysine residue shifted by 42 Da, indicated by asterisk. The fragmentation peak list is shown (C) with the peaks that could be assigned to the identified peptide with a Mascot search of the Swiss-Prot database indicated in red, and the peaks that were observed in the fragmentation spectrum, underlined.

Lysine 235 of the acetylated BSA was found to be acetylated. The peptide's E value was 1.8 and the MOWSE score was 36. EMS spectrum (Fig.4.2.1.3A) identified the peptide to be 1043.7Da and ER spectrum (fig 4.2.1.3B) identified the charge state to be a singly charged peptide. On the MS/MS spectrum (fig 4.2.1.3C) the acetylated lysine (y3) was marked by an asterix. The position of the site of acetylation was confirmed by looking at the peak list table. The mass difference between the observed y3 and y4 ions, were the only lysine residue is located is 859.4785 - 689.3729 = 170.1056Da, which is equal to a single acetylated lysine residue. Therefore, this strengthens the fact that K235 was acetylated.

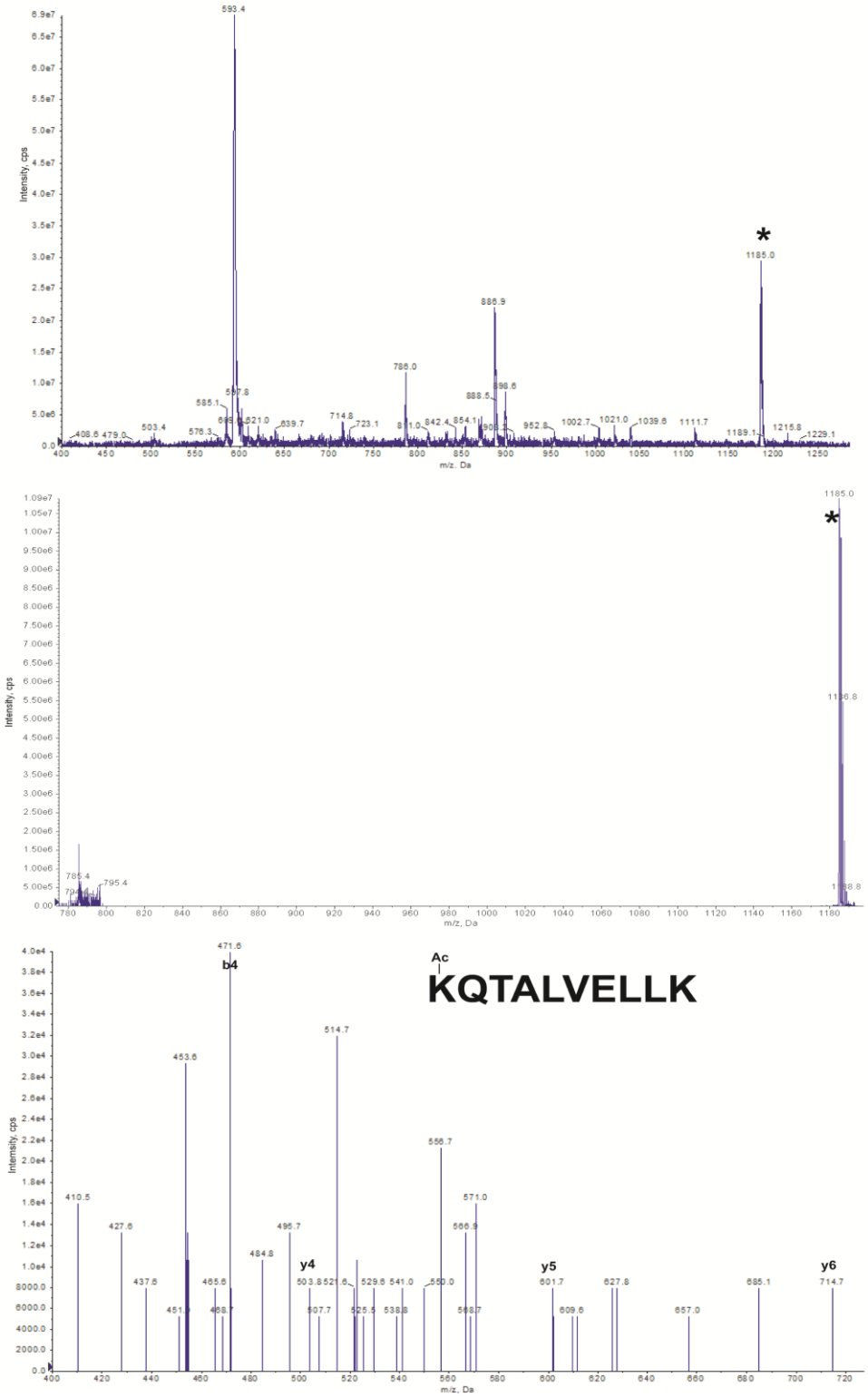
Intensity, cps
m/z, Da
*
1185.0
593.4
888.9
786.0
Ac
KQTALVELLK
b4
y4
y5
y6
471.6
514.7
453.6
556.7
571.0
410.5
427.6
495.7
484.8
437.6
601.7
627.8
685.1
714.7
657.0

Order	b	Seq.	y	Order
1	171.1128	K		10
2	299.1714	Q	1014.6194	9
3	400.2191	T	886.5608	8
4	471.2562	A	785.5131	7
5	584.3402	L	714.4760	6
6	683.4086	V	601.3919	5
7	812.4512	E	502.3235	4
8	925.5353	L	373.2809	3
9	1038.6194	L	260.1969	2
10		K	147.1128	1

Figure 4.2.1.4. K548 acetylation was detected in acetylated BSA without performing precursor-ion scan at 126Da. A tryptic digest of acetylated BSA isolated was analyzed by MS. The enhanced mass spectrometry spectrum (A), an enhanced resolution spectrum (B) and CID fragmentation spectrum of the peptide that resolved at 1185.0 Da (singly charged), indicated by the asterisk in panel A, is shown (C). The partial y-ion and b-ion series visible in the fragmentation spectrum are indicated. The fragmentation peak list is shown (C) with the peaks that could be assigned to the identified peptide with a Mascot search of the Swiss-Prot database indicated in red, and the peaks that were observed in the fragmentation spectrum, underlined.

A ten residue long peptide was detected with one site of acetylation at lysine 548. Enhanced mass spectrometry (Fig. 4.2.1.4A) and Enhanced resolution spectrum (Fig. 4.2.1.4B) when considered confirmed the peptide to be singly charged, 1185.0Da big, which was within 0.2 amu of the expected mass. The E value was 0.0013 and a MOWSE score of 67. In this ten residue long peptide there are two possible sites of acetylation, as seen in the fragmentation spectrum (Fig. 4.2.1.4C), one at the beginning of the N-terminus and the other one on the end of the C-terminus end. The lysine at the end of the C-terminus is unmodified since trypsin can only cut to the C-terminus of an unmodified lysine. This then only leaves the lysine at the beginning of the N-terminus, looking at the fragmentation ion peak list the lysine

resolved below the detectable mass range (400-1400 *m/z*). However, looking at the peak list the, b4 ion, a quadri-peptide KTQA was observed at 471.2562Da, which had a 42 Da mass shift compared to the predicted mass. This then unambigiuosly locates the acetyl group at lysine 548.

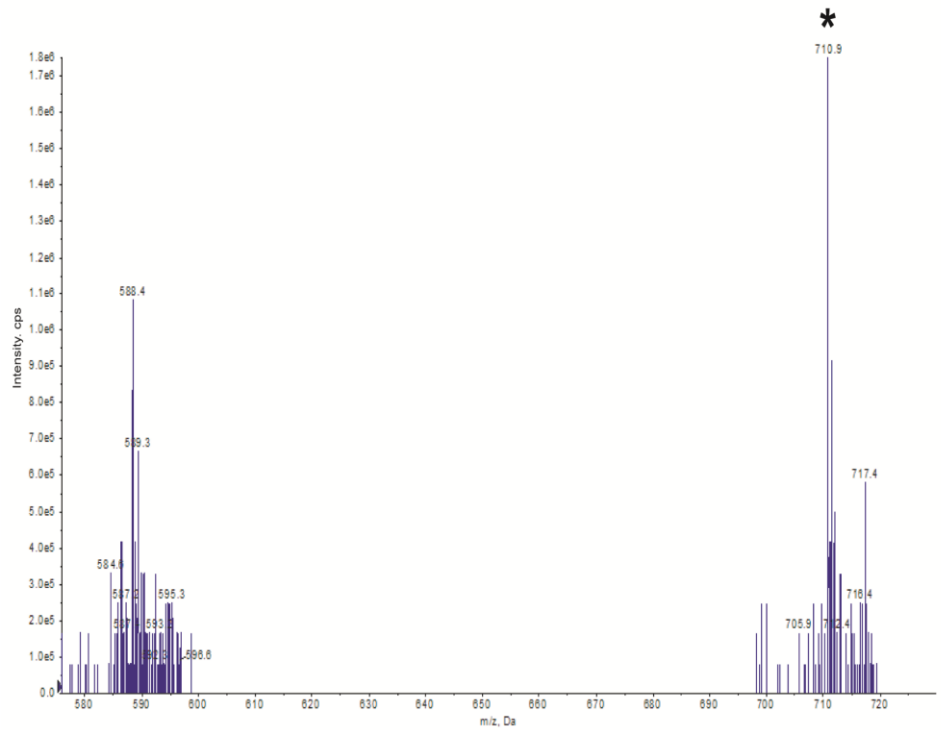
*
710.9
588.4
589.3
717.4
584.4
595.3
716.4
705.9
596.6
Intensity, cps
m/z, Da

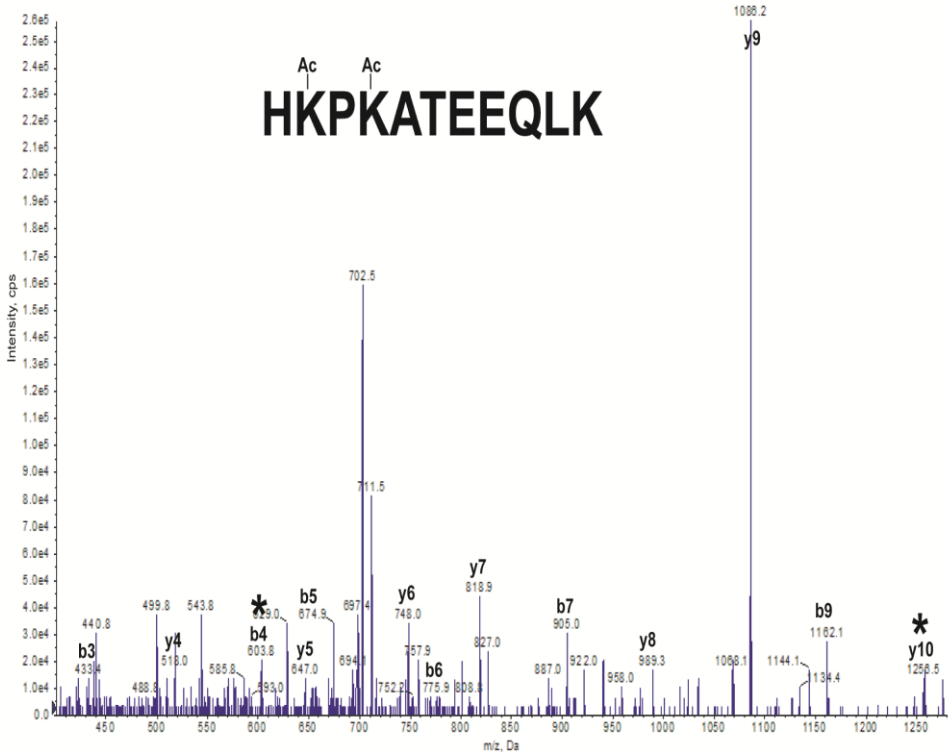
Ac
Ac
HKPKATEEQLK
1088.2
y9
702.5
711.5
y7
818.9
b7
905.0
y6
748.0
b5
674.9
b4
603.8
y5
647.0
b6
775.9
y4
518.0
b3
433.4
y8
989.3
b9
1162.1
y10
1256.5
Intensity, cps
m/z, Da

Order	b	Seq.	y	Order
1	166.0975	H		11
2	336.2030	K	1255.6892	10
3	433.2558	P	1085.5837	9
4	603.3613	K	988.5309	8
5	674.3984	A	818.4254	7
6	775.4461	T	747.3883	6
7	904.4887	E	646.3406	5
8	1033.5313	E	517.2980	4
9	1161.5899	Q	388.2554	3
10	1274.6739	L	260.1969	2
11		K	147.1128	1

Figure 4.2.1.5. K559 and K561 acetylation were detected in acetylated BSA without performing precursor-ion scan at 126Da. A tryptic digest of acetylated BSA isolated was analyzed by MS. The enhanced resolution spectrum (A) and CID fragmentation spectrum of the peptide that resolved at 710.9 Da (doubly charged), indicated by the asterisk in panel A, is shown (B). The partial y-ion and b-ion series visible in the fragmentation spectrum are indicated, and the b4 and y10 peaks, representing terminal lysine residues shifted by 42 Da, indicated by asterisks. The fragmentation peak list is shown (C) with the peaks that could be assigned to the identified peptide with a Mascot search of the Swiss-Prot database indicated in red, and the peaks that were observed in the fragmentation spectrum, underlined.

A di-acetylated peptide was also identified. The ion score was 54 and the E value was 0.0025. Upon studying the enhanced resolution spectrum (Fig. 4.2.1.5A) the peptide was identified to be 710.9Da (doubly charged). Since, the full length of the peptide (1419.7721Da) is over the mass cut off (400-1400 *m/z*) the EMS scan could not be captured. To confirm the di-acetylation assignment, the CID fragmentation spectrum (Fig.4.2.1.5B) and the peak list (Fig.4.2.1.5C) was taken into account. Looking at the sequence, there are three possible sites of acetylation, however, the lysine residue at the end of the N-terminus can not be modified since trypsin cleaved to its C-terminus group. Now, we only left with two

sites, looking at the y-ion series, the mass difference between y10 and y9: 1255.6892 - 1085.5837 = 170.1055, which is equal to an acetylated lysine residue. Similarly, the mass difference between the observed y8 and y7: 988.5309 – 818.4254 = 170.1055, which is equal to an acetylated lysine residue. This then strongly suggest that the acetylated BSA peptide from position 558-568 is di-acetylated at position K559 and K561 but not K568.

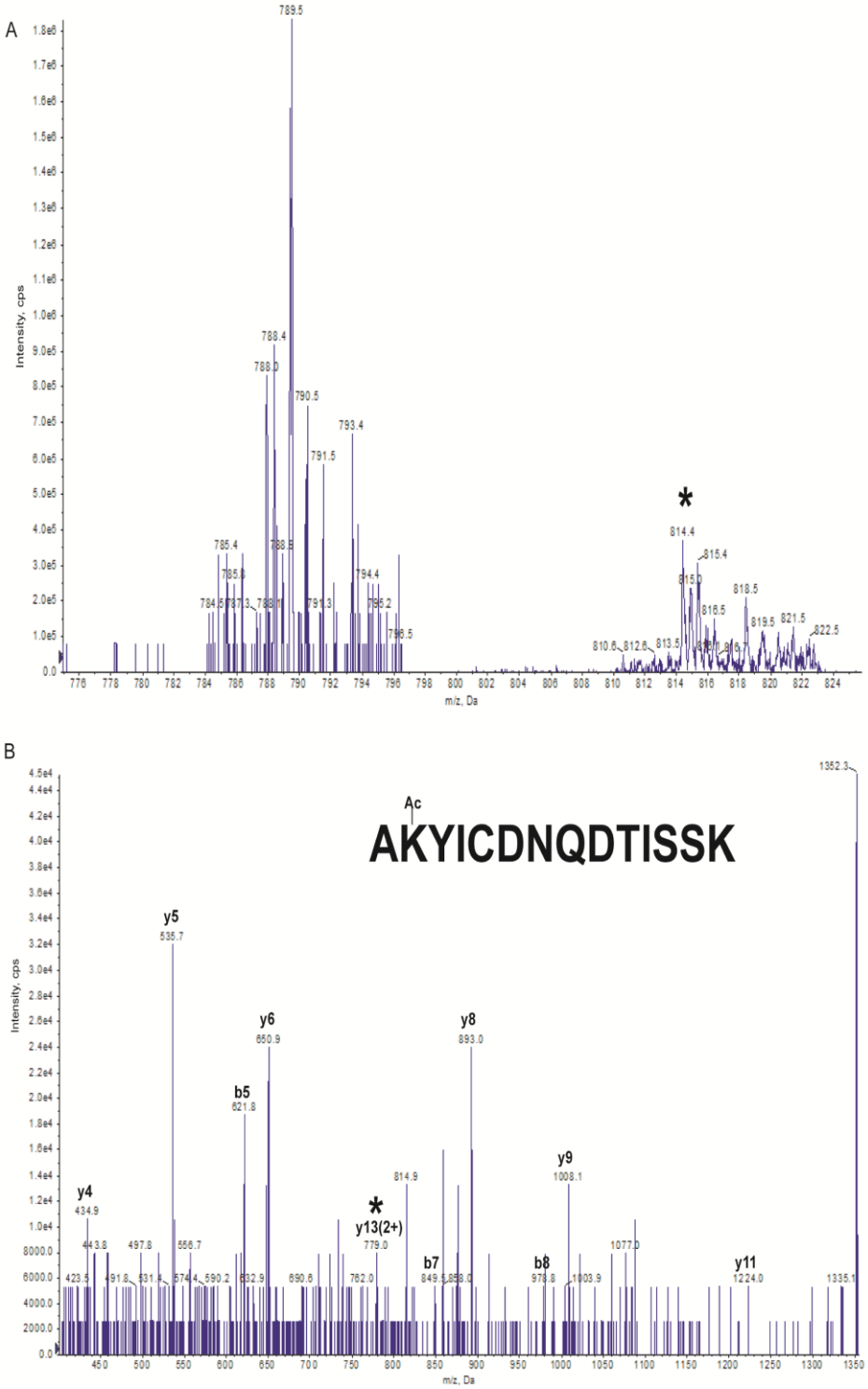
A
Intensity, cps
m/z, Da
B
Ac
AKYICDNQDTISSK
y5
535.7
y6
650.9
y8
893.0
b5
621.8
y9
1008.1
y4
434.9
y13(2+)
779.0
b7
b8
y11
1224.0
1352.3
Intensity, cps
m/z, Da

Order	b	b^{++}	Seq.	y	y^{++}	Order
1	72.0444	36.5258	A			14
2	242.1499	121.5786	K	1556.7261	778.8667	13
3	405.2132	203.1103	Y	1386.6206	693.8139	12
4	518.2973	259.6523	I	1223.5572	612.2823	11
5	621.3065	311.1569	C	1110.4732	555.7402	10
6	736.3334	368.6704	D	1007.4640	504.2356	9
7	850.3764	425.6918	N	892.4371	446.7222	8
8	978.4349	489.7211	Q	778.3941	389.7007	7
9	1093.4619	547.2346	D	650.3355	325.6714	6
10	1194.5096	597.7584	T	535.3086	268.1579	5
11	1307.5936	654.3004	I	434.2609	217.6341	4
12	1394.6257	697.8165	S	321.1769	161.0921	3
13	1481.6577	741.3325	S	234.1448	117.5761	2
14			K	147.1128	74.0600	1

Figure 4.2.1.6. K285 acetylation was detected in acetylated BSA without performing precursor-ion scan at 126Da. A tryptic digest of acetylated BSA isolated was analyzed by MS. The enhanced resolution spectrum (A) and CID fragmentation spectrum of the peptide that resolved at 814.4 Da (doubly charged), indicated by the asterisk in panel A, is shown (B). The partial y-ion and b-ion series visible in the fragmentation spectrum are indicated, and the $y^{++}13$ peak, representing a terminal lysine residue shifted by 42 Da, indicated by asterisk. The fragmentation peak list is shown (C) with the peaks that could be assigned to the identified peptide with a Mascot search of the Swiss-Prot database indicated in red, and the peaks that were observed in the fragmentation spectrum, underlined. The b^{++} and y^{++} columns indicate b-ion and y-ion fragments that are doubly charged.

A doubly charged, 14 residue long peptide was identified to be mono-acetylated at lysine 285. The MOWSE score was 57 the E value was 0.0015. Enhanced resolution spectrum (Fig. 4.2.1.6A) confirmed the peptide to be 814.4Da (doubly charged). Since the full mass of the peptide (1626.7559Da) is outside the window (400-1400 *m/z*) used for capturing enhanced mass spectrometry scans, EMS spectrum could not be retrieved. The fragmentation spectrum (Fig. 4.2.1.6B) and the peak list table substantiated the fact that

there's an acetyl group added to lysine 285. Looking at the peak list it is evident that the mass difference between observed y^{++} 13 peak and the predicted $y^{++}12$ ion: 2 x (778.8667 – 693.8139) = 170.1056, which is equal to an acetylated lysine residue. Therefore, this strengthens the fact that lysine 285 of the acetylated BSA might be acetylated.

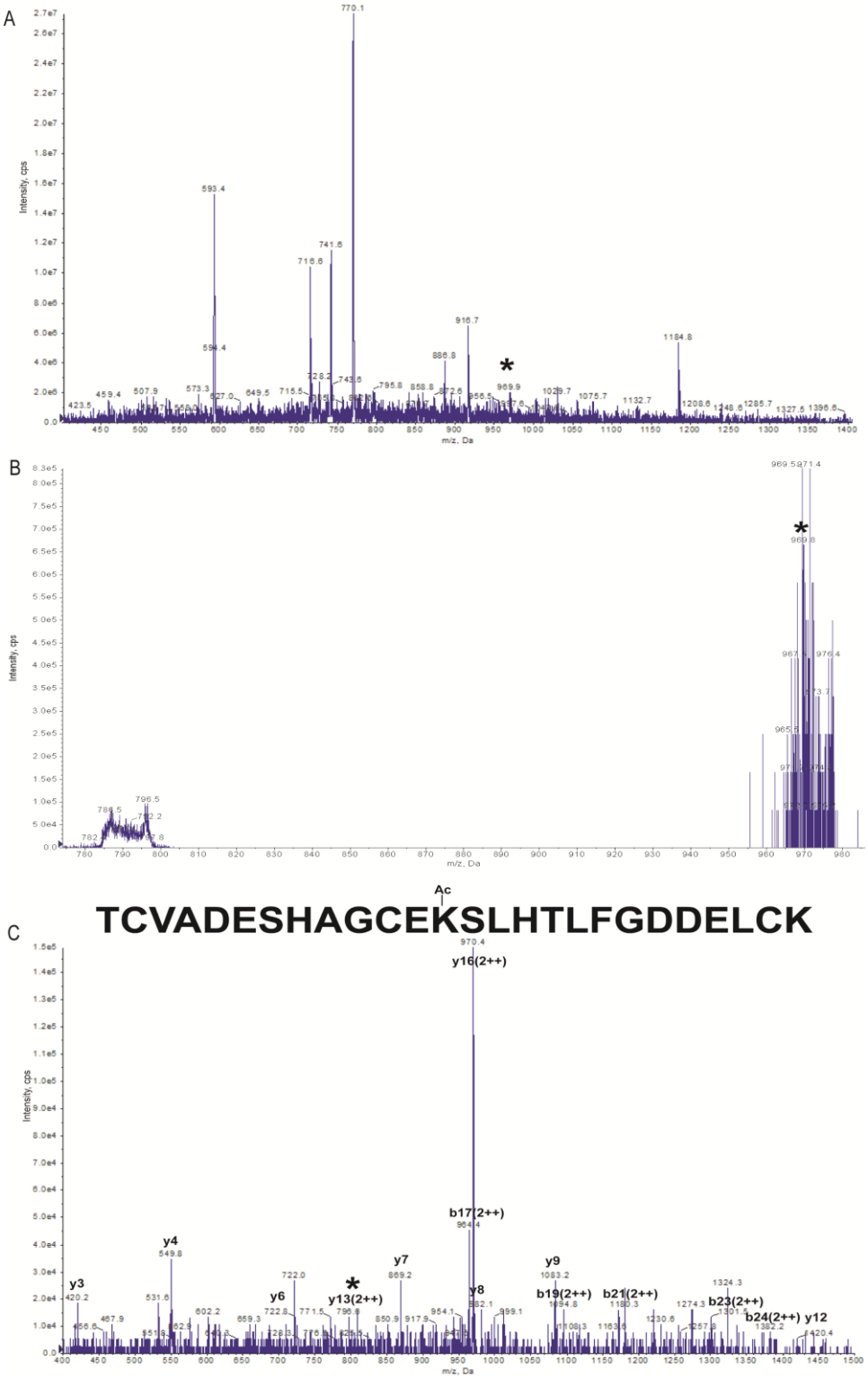

Order	b	b^{++}	Seq.	y	y^{++}	Order
1	102.0550	51.5311	T			25
2	263.0696	132.0384	C	2808.1797	1404.5935	24
3	362.1380	181.5727	V	2647.1651	1324.0862	23
4	433.1751	217.0912	A	2548.0966	1274.5520	22
5	548.2021	274.6047	D	2477.0595	1239.0334	21
6	677.2447	339.1260	E	2362.0326	1181.5199	20
7	764.2767	382.6420	S	2232.9900	1116.9986	19
8	901.3356	451.1714	H	2145.9580	1073.4826	18
9	972.3727	486.6900	A	2008.8990	1004.9532	17
10	1029.3942	515.2007	G	1937.8619	969.4346	16
11	1190.4089	595.7081	C	1880.8405	940.9239	15
12	1319.4515	660.2294	E	1719.8258	860.4165	14
13	1489.5570	745.2821	K	1590.7832	795.8952	13
14	1576.5890	788.7981	S	1420.6777	710.8425	12
15	1689.6731	845.3402	L	1333.6457	667.3265	11
16	1826.7320	913.8696	H	1220.5616	610.7844	10
17	1927.7797	964.3935	T	1083.5027	542.2550	9
18	2040.8637	1020.9355	L	982.4550	491.7311	8
19	2187.9321	1094.4697	F	869.3709	435.1891	7
20	2244.9536	1122.9804	G	722.3025	361.6549	6
21	2359.9805	1180.4939	D	665.2811	333.1442	5
22	2489.0231	1245.0152	E	550.2541	275.6307	4
23	2602.1072	1301.5572	L	421.2115	211.1094	3
24	2763.1219	1382.0646	C	308.1275	154.5674	2
25			K	147.1128	74.0600	1

Figure 4.2.1.7. K309 acetylation was detected in acetylated BSA without performing precursor-ion scan at 126Da. A tryptic digest of acetylated BSA isolated was analyzed by MS. The enhanced mass spectrometry spectrum (A), an enhanced resolution spectrum (B) and CID fragmentation spectrum of the peptide that resolved at 969.9 Da (triply charged), indicated by the asterisk in panel A, is shown (C). The partial y-ion and b-ion series visible in the fragmentation spectrum are indicated, and the $y^{++}13$ peak, representing a terminal lysine residue shifted by 42 Da, indicated by an asterisk. The fragmentation peak list is shown (C) with the peaks that could be assigned to the identified peptide with a Mascot search of the Swiss-Prot database indicated in red, and the peaks that were observed in the fragmentation spectrum, underlined. The b^{++} and y^{++} columns indicate b-ion and y-ion fragments that are doubly charged.

Finally, K309 acetylation was the last modification detected when EMS scan followed by CID fragmentation without precursor-ion scan was performed. On submitting the CID fragmentation spectrum for search in Mascot database against Swiss-Prot database a predicted mono-acetylated peptide with a mass of 969.7689Da (triply charged) was identified. The ion score was 69 and the Evalue was.0.00025. The above assignment was substantiated by considering the EMS spectrum (Fig. 4.2.1.7A) which reported a peak at 909.9Da and the ER spectrum confirmed the triply charged state of the observed peak at 909.8Da. The MS/MS spectrum (Fig. 4.2.1C) was taken into account in order to locate the acety group that was added to lysine 309, looking at the peak list it is clear that the mass difference between $y^{++}13$ and y12: 2x(795.8952) – 1420.6777 = 171.1127Da, which is within 1Da of the predicted mass of a single acetylated lysine residue.

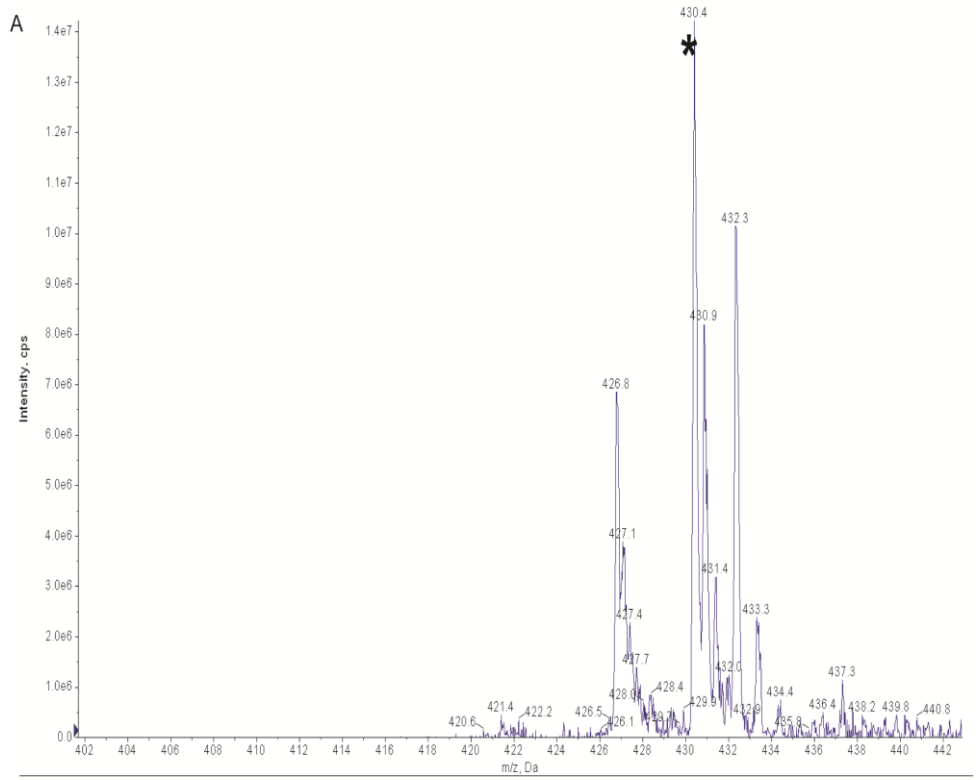
A
Intensity, cps
m/z, Da
430.4
*
432.3
430.9
426.8
427.1
431.4
427.4
433.3
427.7
432.0
437.3
428.4
428.0
434.4
429.9
436.4
438.2
439.8
440.8
421.4
422.2
426.5
426.1
420.6

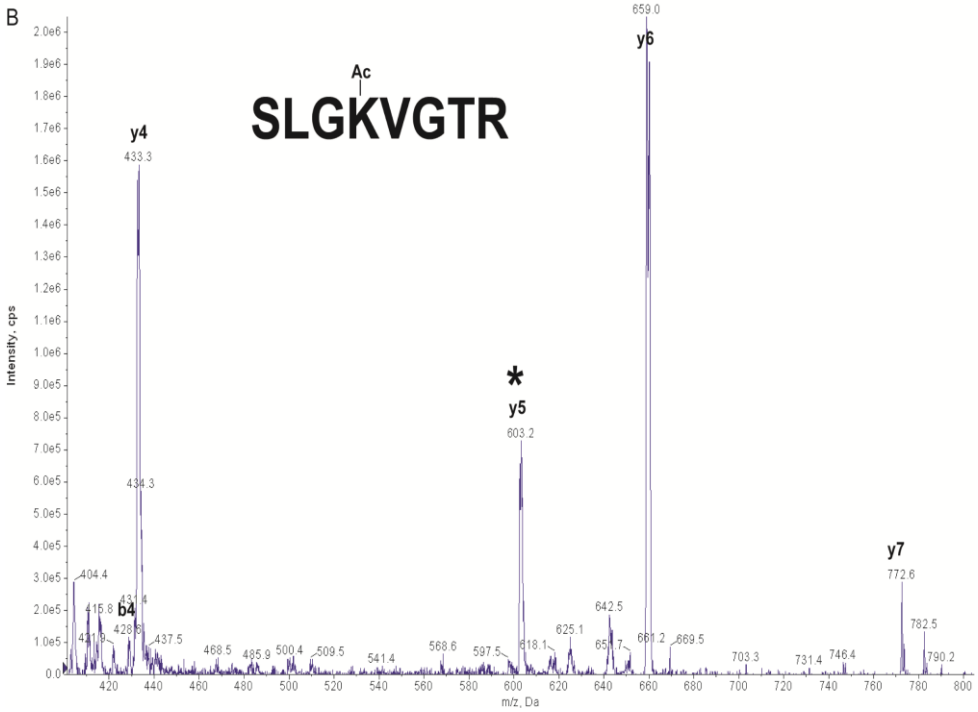
B
Intensity, cps
m/z, Da
Ac
SLGKVGTR
659.0
y6
y4
433.3
*
y5
603.2
434.3
y7
772.6
404.4
415.8
b4
642.5
782.5
625.1
661.2
669.5
790.2
746.4
703.3
731.4
437.5
468.5
485.9
500.4
509.5
541.4
568.6
597.5
618.1

Order	b	Seq.	y	Order
1	88.0393	S		8
2	201.1234	L	772.4676	7
3	258.1448	G	659.3835	6
4	428.2504	K	602.3620	5
5	527.3188	V	432.2565	4
6	584.3402	G	333.1881	3
7	685.3879	T	276.1666	2
8		R	175.1190	1

Figure 4.2.2.1. K455 acetylation was detected in acetylated BSA upon performing precursor ion scan at 126Da. A tryptic digest of acetylated BSA isolated was analyzed by MS. The enhanced resolution spectrum (A) and CID fragmentation spectrum of the peptide that resolved at 430.4 Da (doubly charged), indicated by the asterisk in panel A, is shown (B). The partial y-ion and b-ion series visible in the fragmentation spectrum are indicated, and the y5 peak, representing a terminal lysine residue shifted by 42 Da, indicated by an asterisk. The fragmentation peak list is shown (C) with the peaks that could be assigned to the identified peptide with a Mascot search of the Swiss-Prot database indicated in red, and the peaks that were observed in the fragmentation spectrum, underlined.

It was previously shown that the immonium ion of acetylated lysine, $[HN.CH.[(CH_2)_4.NH.CO.CH_3]+H]^+$ often loses an ammonia moiety, resulting in the immonium ion sub-fragment $[HN.CH.[(CH_2)_4.NH.CO.CH_3]+H]^+$ with a mono-isotopic mass of 126.0919 Da (Trelle and Jensen, 2008). This immonium ion sub-fragment was previously used as a diagnostic ion to detect acetylated lysine residues in peptides during CID fragmentation (Trelle and Jensen, 2008). We therefore performed precursor-ion scans during elution to identify all peptides that lose approximately 126 Da during CID fragmentation.

These peptides were selected and a product-ion scan of each recorded. All product ion scans were submitted to an in-house copy of the Mascot search engine, which matched the experimental MS/MS spectra against the generated theoretical spectra in the Swiss-Prot

database. The result is shown in Fig. 4.2.2.1. The ion score for the total acetylated BSA protein was 219 in this analysis. The Mascot results view page reported a mono-acetylated peptide at lysine 455 with a predicted mass of 430.4303Da (doubly charged). The expected value and the ion score of this particular peptide was 3.9 and 35, respectively The enhanced resolution spectrum (Fig. 4.2.2.1A) confirmed this assignment with a peak at 430.4Da. The MS/MS spectrum (Fig.4.2.2.B) substantiated the location of the added acetyl group, looking at the peak list it is clear that the mass difference between the observed peaks y5 and y4: 602.3620 – 432.2565 = 170.1055, which is equal to a single acetylated lysine residue

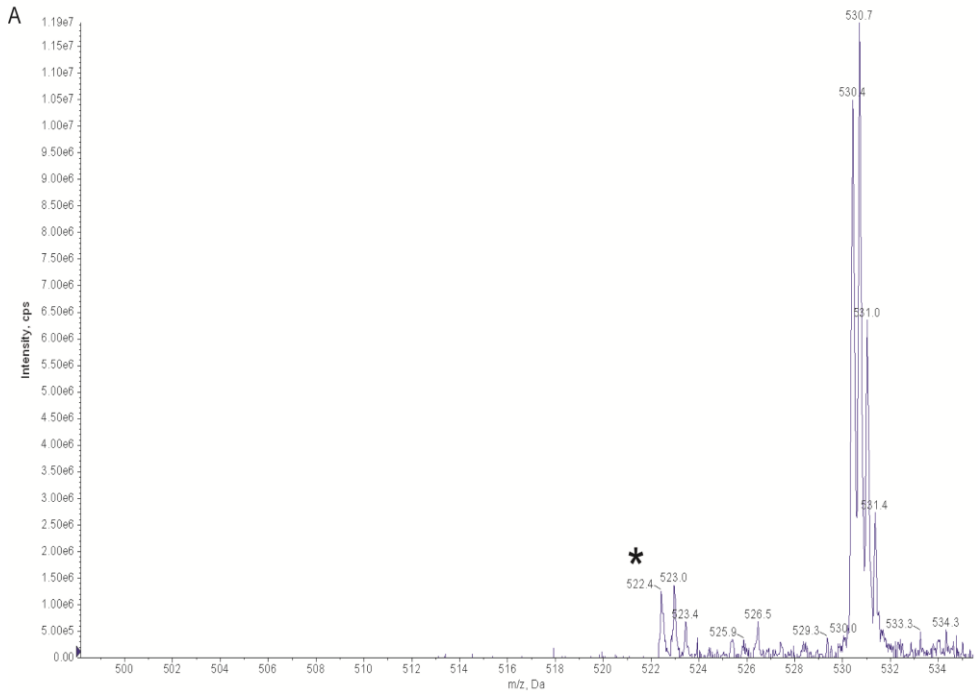
A
Intensity, cps
m/z, Da
530.7
530.4
531.0
531.4
522.4
523.0
523.4
525.9
526.5
529.3
533.3
534.3

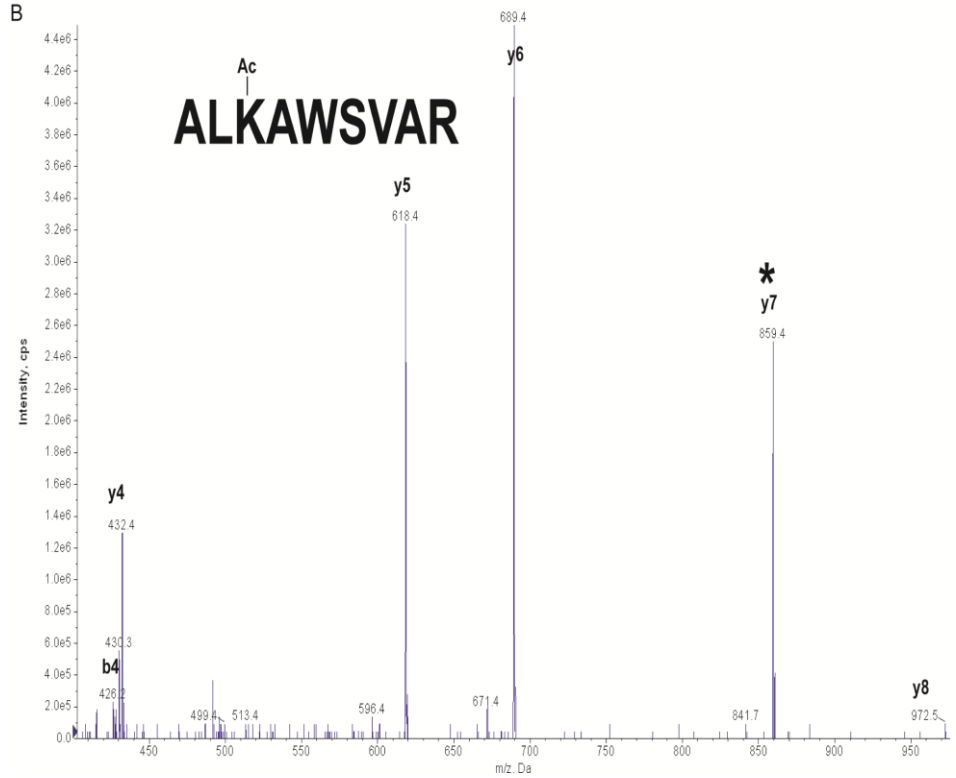
B
Intensity, cps
m/z, Da
Ac
ALKAWSVAR
689.4
y6
y5
618.4
y7
859.4
y4
432.4
430.3
b4
426.2
499.4
513.4
596.4
671.4
841.7
y8
972.5

Order	b	Seq.	y	Order
1	72.0444	A		9
2	185.1285	L	972.5625	8
3	355.2340	K	859.4785	7
4	426.2711	A	689.3729	6
5	612.3504	W	618.3358	5
6	699.3824	S	432.2565	4
7	798.4508	V	345.2245	3
8	869.4880	A	246.1561	2
9		R	175.1190	1

Figure 4.2.2.2. K235 acetylation was detected in acetylated BSA upon performing precursor ion scan at 126Da. A tryptic digest of acetylated BSA isolated was analyzed by MS. The enhanced resolution spectrum (A) and CID fragmentation spectrum of the peptide that resolved at 522.4Da (doubly charged), indicated by the asterisk in panel A, is shown (B). The partial y-ion and b-ion series visible in the fragmentation spectrum are indicated, and the y7 peak, representing a terminal lysine residue shifted by 42 Da, indicated by an asterisk. The fragmentation peak list is shown (C) with the peaks that could be assigned to the identified peptide with a Mascot search of the Swiss-Prot database indicated in red, and the peaks that were observed in the fragmentation spectrum, underlined.

After comparing the generated MS/MS spectra with the theoretical spectra generated by Mascot. A ten residue long peptide beginning from position 233-239 was found to have lost a diagnostic ion of 126Da at K235. The ion score was reported to be 42 and the expectancy value was 0.75. The resultant ER identified a peptide with a mass of 522.4 Da (doubly charged) which is within 0.0015 Da of the predicted mass. The site of acetylation was confirmed by considering the enhanced product ion spectrum (EPI) (Fig. 4.2.2.2B), it is clearly that the difference between the observed peaks y7 and y6: 859.4785 – 689.3729 = 170.1056 Da, is equal to an acetylated lysine residue.

Looking at Figure 4.2.2.3., Mascot algorithm probability scoring predicted the peptide FKDLGEEHFK to be acetylated at position K37 with an ion score of 45 and an E value of 45. The mass of the peptide was 431.4356Da (triply charged). By taking a closer look at the enhanced resolution spectrum (Fig. 4.2.2.3A) verified the identity of the peptide to be 431.4Da (triply charged) which is within 0.04 of the predicted mass. By taking into account the CID fragmentation spectrum it could also be substantiated that the peptide was acetylated at posion K37. Studying the peak list table it is evident that mass shift between the observed peak $y^{++}9$ and $y^{++}8$: 2x(572.7853 – 487.7325) = 170.1056, is equal to an acetylated lysine residue.

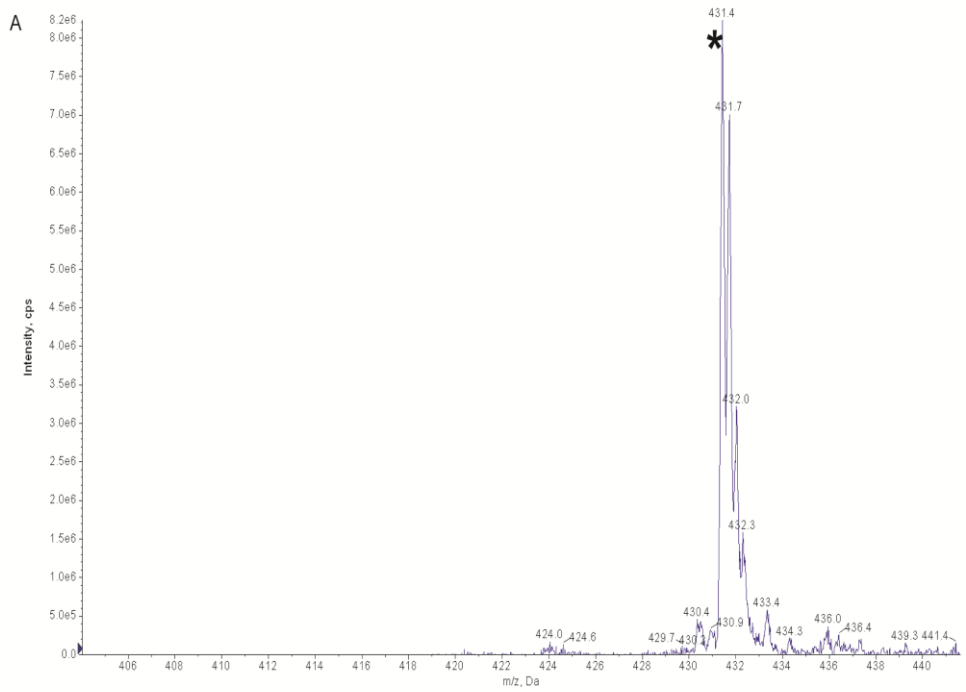
A
Intensity, cps
m/z, Da
431.4
431.7
432.0
432.3
433.4
430.4
430.9
434.3
436.0
436.4
424.0
424.6
429.7
439.3
441.4

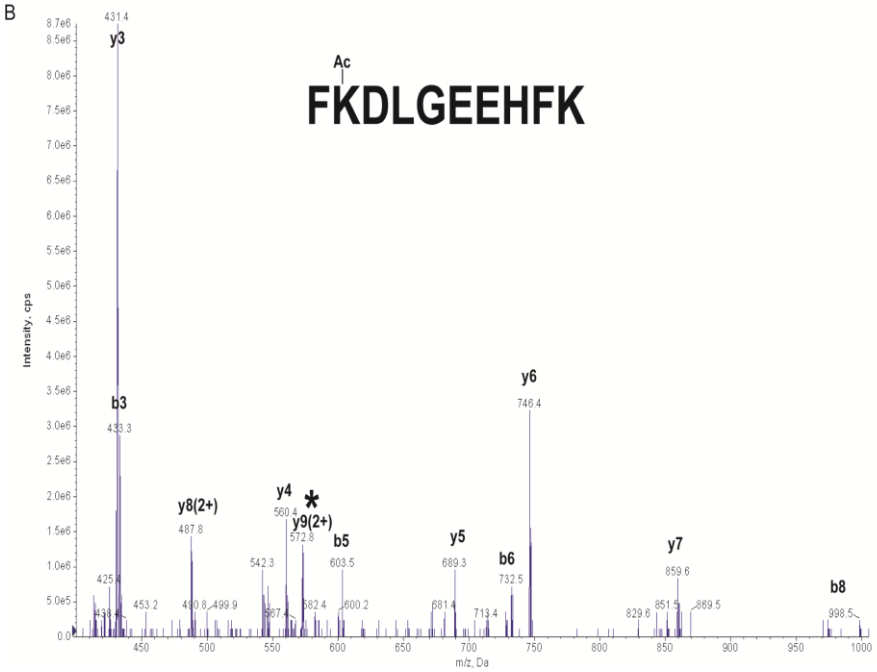
B
Ac
FKDLGEEHFK
Intensity, cps
m/z, Da
y3
b3
y8(2+)
y4
y9(2+)
b5
y5
b6
y6
y7
b8

Order	b	b^{++}	Seq.	y	y^{++}	Order
1	148.0757	74.5415	F			10
2	318.1812	159.5942	K	1144.5633	572.7853	9
3	433.2082	217.1077	D	974.4578	487.7325	8
4	546.2922	273.6497	L	859.4308	430.2191	7
5	603.3137	302.1605	G	746.3468	373.6770	6
6	732.3563	366.6818	E	689.3253	345.1663	5
7	861.3989	431.2031	E	560.2827	280.6450	4
8	998.4578	499.7325	H	431.2401	216.1237	3
9	1145.5262	573.2667	F	294.1812	147.5942	2
10			K	147.1128	74.0600	1

Figure 4.2.2.3 K37 acetylation was detected in acetylated BSA upon performing precursor ion scan at 126 Da. A tryptic digest of acetylated BSA isolated was analyzed by MS. The enhanced resolution spectrum (A) and CID fragmentation spectrum of the peptide that resolved at 431.4 Da (triply charged), indicated by the asterisk in panel A, is shown (B). The partial y-ion and b-ion series visible in the fragmentation spectrum are indicated, and the $y^{++}9$ peak, representing a terminal lysine residue shifted by 42 Da, indicated by an asterisk. The fragmentation peak list is shown (C) with the peaks that could be assigned to the identified peptide with a Mascot search of the Swiss-Prot database indicated in red, and the peaks that were observed in the fragmentation spectrum, underlined. The b^{++} and y^{++} columns indicate b-ion and y-ion fragments that are doubly charged.

Looking at figure 4.2.2.4, precursor-ion scan identified a peptide that had a double loss of 126Da diagnostic ion. A search of the Swiss-Prot database with the CID fragmentation spectrum of this peak, using the Mascot search engine, predicted a pepide that was di-acetylated at position K559 and K561 with a precursor mass of 696.3873Da (doubly charged) which had an ion score of 39 and an E value of 2.2. Studying next at the EPI spectrum, partial b-ion and y-ion series are evident (see Fig. 4.2.2.4B). The mass difference between y10 and y9 where the lysine 559 at the N-terminal end is situated is: 1255.6892 – 1085.5837 = 170.1055, which is equal to an acetylated lysine. Similarly, the mass difference between y8 and y7 where lysine 561 is located is: 988.5309 – 818.4254 = 170.1055, also

equal to an acetylated lysine residue. This strongly supports the fact that the peptide (HKPKATEEQLK) is indeed di-acetylated at K559 and K561.

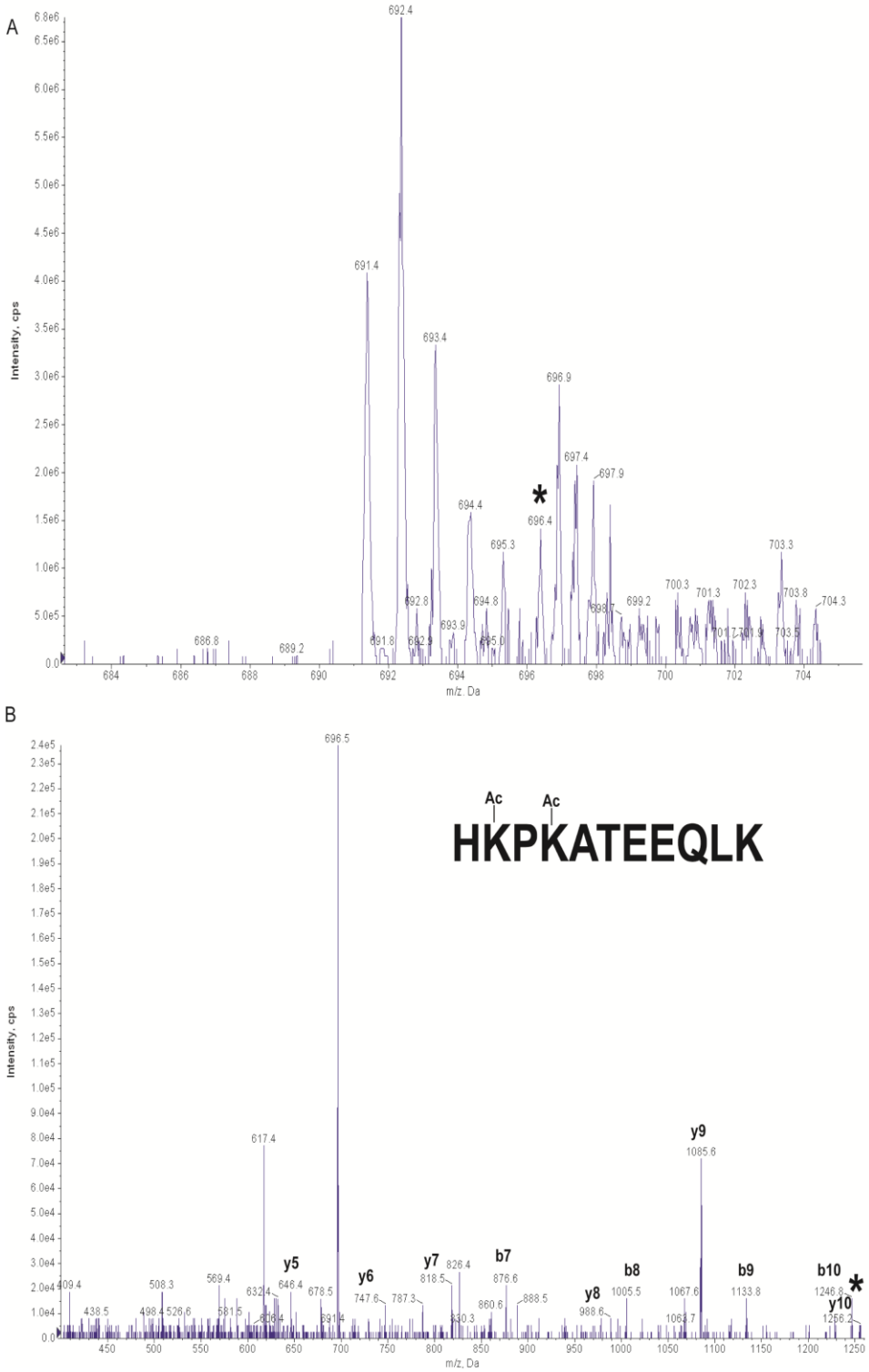

Order	b	Seq.	y	Order
1	138.0662	H		11
2	308.1717	K	1255.6892	10
3	405.2245	P	1085.5837	9
4	575.3300	K	988.5309	8
5	646.3671	A	818.4254	7
6	747.4148	T	747.3883	6
7	876.4574	E	646.3406	5
8	1005.5000	E	517.2980	4
9	1133.5586	Q	388.2554	3
10	1246.6426	L	260.1969	2
11		K	147.1128	1

Figure 4.2.2.4 K559 and K561 acetylation was detected in acetylated BSA upon performing precursor ion scan at 126 Da. A tryptic digest of acetylated BSA isolated was analyzed by MS. The enhanced resolution spectrum (A) and CID fragmentation spectrum of the peptide that resolved at 696.9 Da (doubly charged), indicated by the asterisk in panel A, is shown (B). The partial y-ion and b-ion series visible in the fragmentation spectrum are indicated, and the y8 and y10 peaks, representing terminal lysine residues shifted by 42 Da, indicated by asterisks. The fragmentation peak list is shown (C) with the peaks that could be assigned to the identified peptide with a Mascot search of the Swiss-Prot database indicated in red, and the peaks that were observed in the fragmentation spectrum, underlined.

The precursor ion scan of the tryptic digest of the acetylated BSA identified the 126 Da diagnostic ion in a 477.7979Da peptide (Fig 4.2.2.5A). A Mascot search of the Swiss-Prot database with the fragmentation spectrum of this peptide identified the sequence GACLLPKIETMR, located at sequence position 198-209 of the BSA. The ion score and expectancy value was 55 and 0.056, respectively. The observed mass of 477.8 Da is for the triply charged peptide. This peptide had a mass shift of 42 Da which is consistent with the presence of a single acetyl group in the peptide, which may be located on K204. The fragmentation spectrum (Fig. 4.2.2.5B) shows the presence of the y3, y4, y5, y6, y7 b5 and

b6 fragments. Thus, the difference between observed y6 and y5 where lysine 204 is located is: 819.4393 – 649.3338 = 170.1055 which is equal to a single acetylated Thus, the single acetyl group detected in the fragment is present on K204.

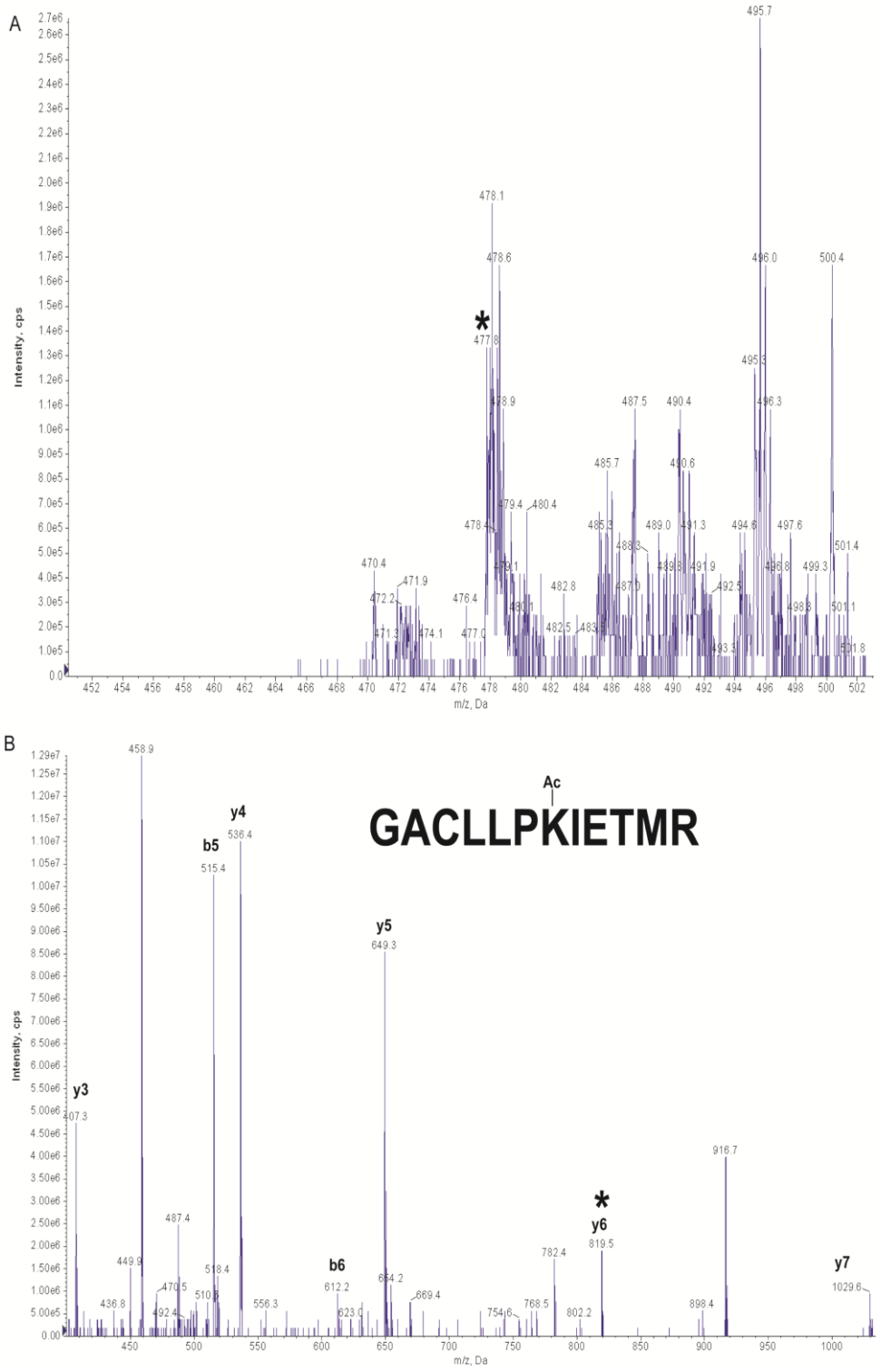
A
Intensity, cps
m/z, Da
B
Ac
GACLLPKIETMR
y4
536.4
b5
515.4
y5
649.3
y3
y6
819.5
b6
y7
1029.6

Order	b	Seq.	y	Order
1	58.0287	G		12
2	129.0659	A	1373.7280	11
3	289.0965	C	1302.6908	10
4	402.1806	L	1142.6602	9
5	515.2646	L	1029.5761	8
6	612.3174	P	916.4921	7
7	782.4229	K	819.4393	6
8	895.5070	I	649.3338	5
9	1024.5496	E	536.2497	4
10	1125.5973	T	407.2071	3
11	1256.6377	M	306.1594	2
12		R	175.1190	1

Figure 4.2.2.5 K204 acetylation was detected in acetylated BSA upon performing precursor ion scan at 126 Da. A tryptic digest of acetylated BSA isolated was analyzed by MS. The enhanced resolution spectrum (A) and CID fragmentation spectrum of the peptide that resolved at 477.8 Da (triply charged), indicated by the asterisk in panel A, is shown (B). The partial y-ion and b-ion series visible in the fragmentation spectrum are indicated, and the y6 peak, representing a terminal lysine residue shifted by 42 Da, indicated by an asterisk. The fragmentation peak list is shown (C) with the peaks that could be assigned to the identified peptide with a Mascot search of the Swiss-Prot database indicated in red, and the peaks that were observed in the fragmentation spectrum, underlined.

The precursor-ion scan detected a fragment ion loss of approximately 126Da from peptide GACLLPKIETMR. A search of the Swiss-Prot database with the CID fragmentation spectrum of this peak, using the Mascot search engine, predicted a pepide that was acetylated at position K160 with a precursor mass of 477.7979Da (triply charged) which had an ion score of 55 and an E value of 0.056. Studying the EPI spectrum, partial b-ion and y-ion series are evident (Fig. 4.2.2.6B). The mass difference between y8 and y7 where the lysine 160 is

situated is: 1097.5990 – 927.4934 = 170.1056, which is equal to an acetylated lysine. This strongly supports the fact that the peptide (GACLLPKIETMR) is indeed acetylated at K160.

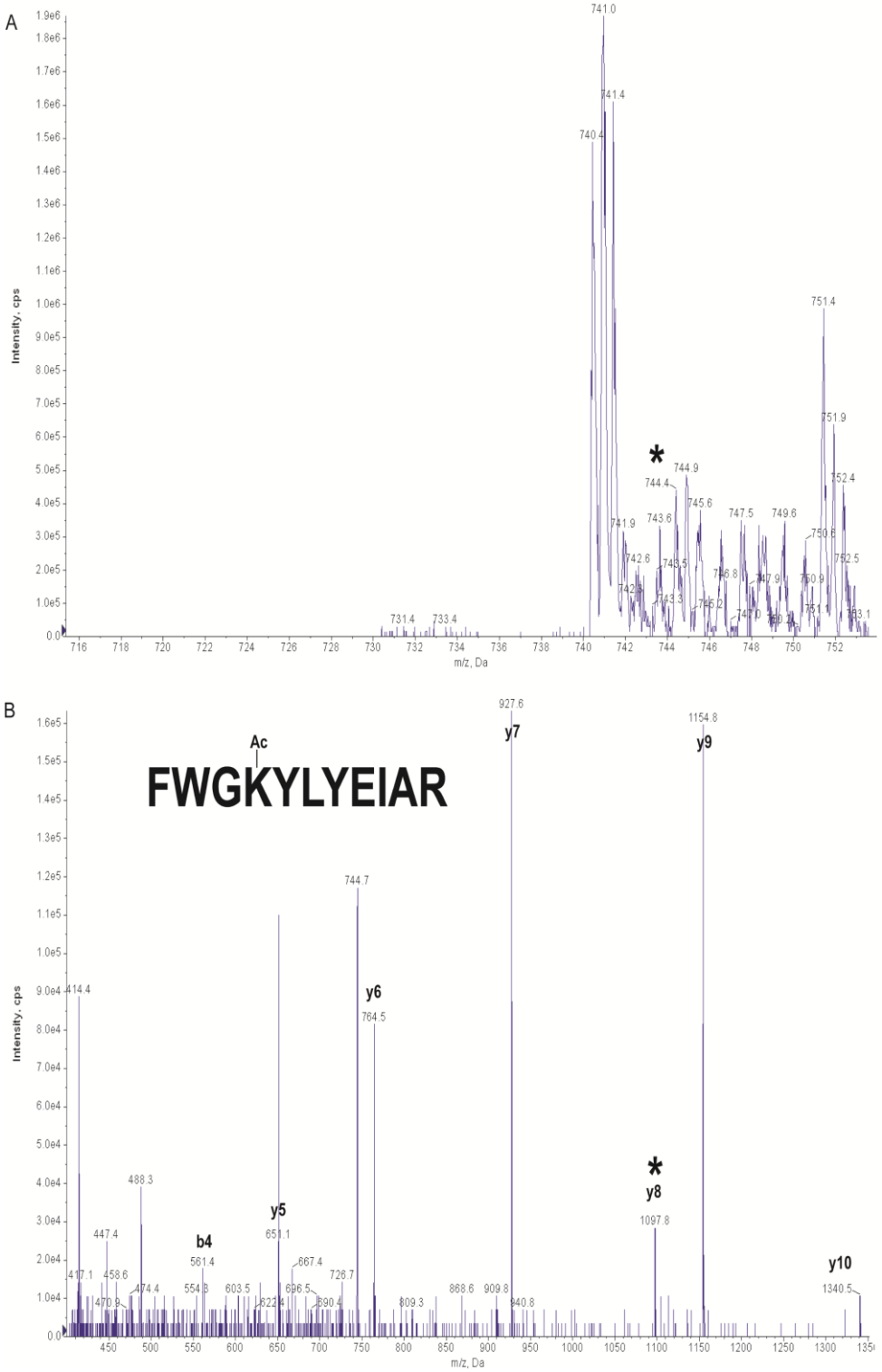

Order	b	Seq.	y	Order
1	148.0757	F		11
2	334.1550	W	1340.6997	10
3	391.1765	G	1154.6204	9
4	561.2820	K	1097.5990	8
5	724.3453	Y	927.4934	7
6	837.4294	L	764.4301	6
7	1000.4927	Y	651.3461	5
8	1129.5353	E	488.2827	4
9	1242.6194	I	359.2401	3
10	1313.6565	A	246.1561	2
11		R	175.1190	1

Figure 4.2.2.6 K160 acetylation was detected in acetylated BSA upon performing precursor ion scan at 126 Da. A tryptic digest of acetylated BSA isolated was analyzed by MS. The enhanced resolution spectrum (A) and CID fragmentation spectrum of the peptide that resolved at 744.4 Da (doubly charged), indicated by the asterisk in panel A, is shown (B). The partial y-ion and b-ion series visible in the fragmentation spectrum are indicated, and the y8 peak, representing a terminal lysine residue shifted by 42 Da, indicated by an asterisk. The fragmentation peak list is shown (C) with the peaks that could be assigned to the identified peptide with a Mascot search of the Swiss-Prot database indicated in red, and the peaks that were observed in the fragmentation spectrum, underlined

Looking at figure 4.2.2.7, it is evident that K401 was acetylated. The precursor ion scan identified the peptide LKHLVDEPQNLIK to may have lost a diagnostic ion of approximately 126Da. When the CID fragmentation spectrum was submitted to Mascot search engine to search against Swiss-Prot database, a peptide of the mass of 530.4008Da (triply charged) was predicted. The ion score of the peptide was 52 with an expectancy value of 0.11. Figure 4.2.2.7A, an enhanced resolution spectrum, was considered to confirm the charge state and the mass of the precursor ion (530.4Da), which was within 0.0008 Da of the predicted peptide. The location of the acetyl group on the peptide was verified by studying the

fragmentation spectrum (Fig. 4.2.2.7B) and the peak list table. It was evident from the table that the mass shift between the observed $y^{++}12$ and the predicted y11, where the only possible site of acetylation is located is: 2x (738.9065 – 653.8537) = 170.1056, is equal to a single acetyl group. Therefore, this further strengthens the possibility that the peptide LKHLVDEPQNLIK may be acetylated at K401.

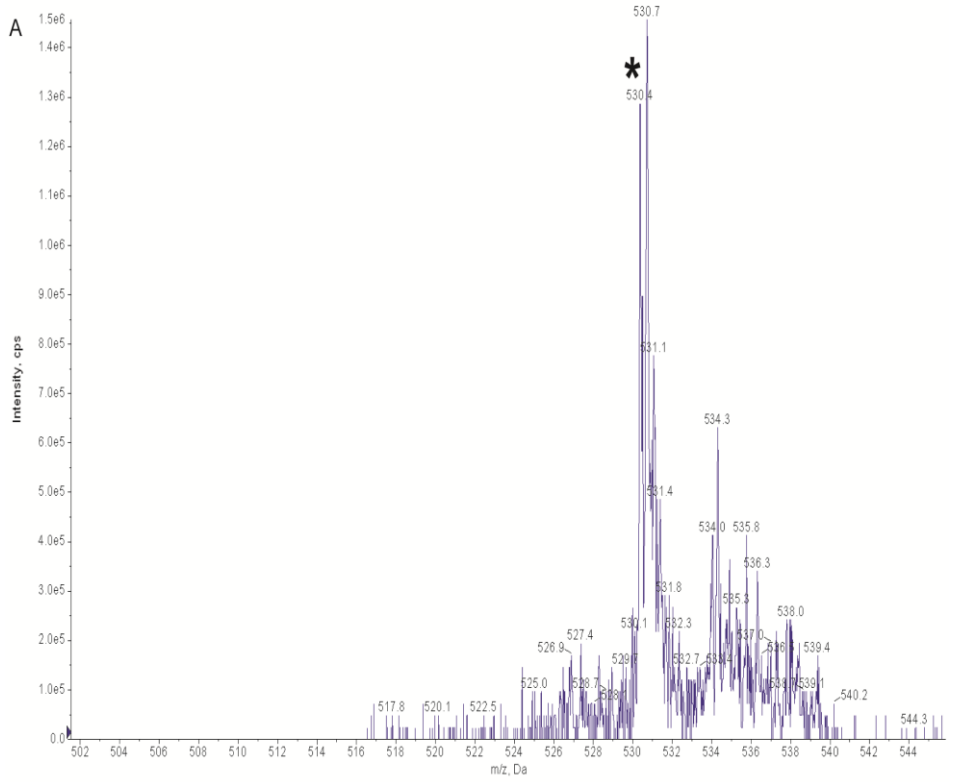
A
Intensity, cps
m/z, Da
530.7
530.4
531.1
534.3
531.4
534.0
535.8
536.3
531.8
535.3
538.0
530.1
532.3
527.4
526.9
537.0
539.4
529.7
532.7
525.0
539.1
540.2
517.8
520.1
522.5
544.3

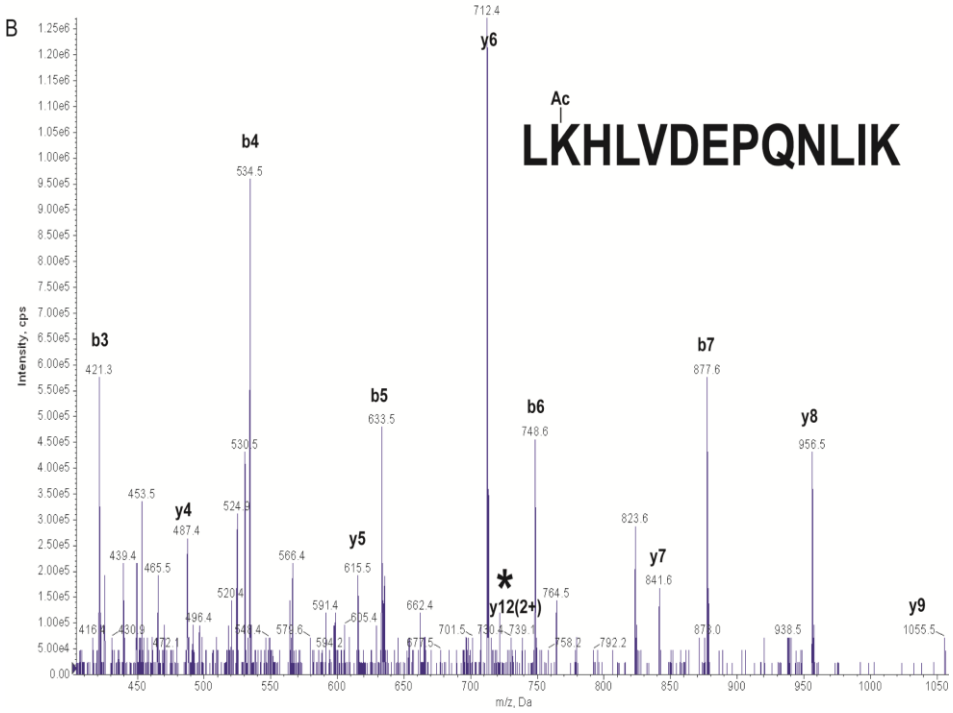
B
Intensity, cps
m/z, Da
712.4
y6
Ac
LKHLVDEPQNLIK
b4
534.5
b3
421.3
b5
633.5
b6
748.6
b7
877.6
y8
956.5
530.5
453.5
y4
487.4
524.3
y5
615.5
566.4
823.6
y7
841.6
439.4
465.5
y12(2+)
764.5
591.4
662.4
y9
1055.5
496.4
520.4
605.4
758.2
792.2
938.5

Order	b	b^{++}	Seq.	y	y^{++}	Order
1	114.0913	57.5493	L			13
2	284.1969	142.6021	K	1476.8057	738.9065	12
3	421.2558	211.1315	H	1306.7001	653.8537	11
4	534.3398	267.6736	L	1169.6412	585.3242	10
5	633.4083	317.2078	V	1056.5572	528.7822	9
6	748.4352	374.7212	D	957.4887	479.2480	8
7	877.4778	439.2425	E	842.4618	421.7345	7
8	974.5306	487.7689	P	713.4192	357.2132	6
9	1103.5731	552.2902	Q	616.3664	308.6869	5
10	1217.6161	609.3117	N	487.3239	244.1656	4
11	1330.7001	665.8537	L	373.2809	187.1441	3
12	1443.7842	722.3957	I	260.1969	130.6021	2
13			K	147.1128	74.0600	1

Figure 4.2.2.7 K401 acetylation was detected in acetylated BSA upon performing precursor ion scan at 126Da. A tryptic digest of acetylated BSA isolated was analyzed by MS. The enhanced resolution spectrum (A) and CID fragmentation spectrum of the peptide that resolved at 530.4 Da (triply charged), indicated by the asterisk in panel A, is shown (B). The partial y-ion and b-ion series visible in the fragmentation spectrum are indicated, and the $y^{++}12$ peak, representing a terminal lysine residue shifted by 42 Da, indicated by an asterisk. The fragmentation peak list is shown (C) with the peaks that could be assigned to the identified peptide with a Mascot search of the Swiss-Prot database indicated in red, and the peaks that were observed in the fragmentation spectrum, underlined. The b^{++} and y^{++} columns indicate b-ion and y-ion fragments that are doubly charged.

The precursor ion scan also identified a peptide located in third region of the BSA called Albumin domain, which contains five or six internal di-sulphide bonds (Hilger *et al*., 2001), to have lost a double diagnostic ion with mass of 126Da. A search of the Swiss-Prot database with the CID fragmentation spectrum of this peak, using the Mascot search engine, predicted a peptide that was di-acetylated at position K547 and K548 with a precursor mass of 798.5706Da (doubly charged) which had an ion score of 54 and an E value of 0.073. Looking at the CID fragmentation spectrum, partial b-ion and y-ion series are evident (Fig.

4.2.2.8B). There are two possible sites of acetylation. The mass difference between y11 and y10 where the lysine 547 is situated is: 1354.8304 – 1184.7249 = 170.1055, which is equal to an acetylated lysine. Similarly, the mass difference between y10 and y9, where the second possible site of acetylation is immediately located is: 1184.7249 – 1014.6194 = 170.1055, which is equal to a single acetylated. This strongly supports the fact that the peptide (QIKKQTALVELLK) is indeed di-acetylated at K547 and K548.

In the first region of the Albumin domain located at the N-terminal region of BSA, precursor ion scan detected a loss of the diagnostic ion 126Da. Mascot probability algorithms predicted a peptide with a mass of 663.3691Da (triply charged). The ion socre was 61 and E value of 0.019. Looking at the ER spectrum (see Fig. 4.2.2.9A), a precursor ion peak with a mass of 663.2Da which is within 0.2Da of the predicted mass, was identified. By studying the enhanced product ion (see Fig. 4.2.29B), the difference between the observed peaks y6 and y5, where the lysine 100 is situated is: 715.4461 – 545.3406 = 170.1055Da, which is equal to a single acetylated lysine residue.

Looking at figure 4.2.2.10, a precursor ion scan detected a peptide with four sites of acetylation with three sites already been identified. Mascot search predicted a peptide with mass of 724.2234Da (triply charged). The predicted sites of acetylation were K547, K548, both already identified (see Fig.4.2.2.8), K559, already identified in Fig. 4.2.2.4, and finally K557 which is the unique modification in this overlapping peptide. Looking at the enhanced resolution (Fig. 4.2.2.10A), it is evident that a precursor ion peak with a mass of 724.2Da (triply charged) which is within 0.02Da of the predicted mass. To verify the location of the unique modification site in this peptide the fragmentation spectrum and the peak list was considered, whereby it was observed that the mass difference between the observed peaks y5 and y4, where the unidentified lysine acetylated is located is: 721.4355 – 551.3300 = 170.1055, which is equal to a single acetylated lysine residue.

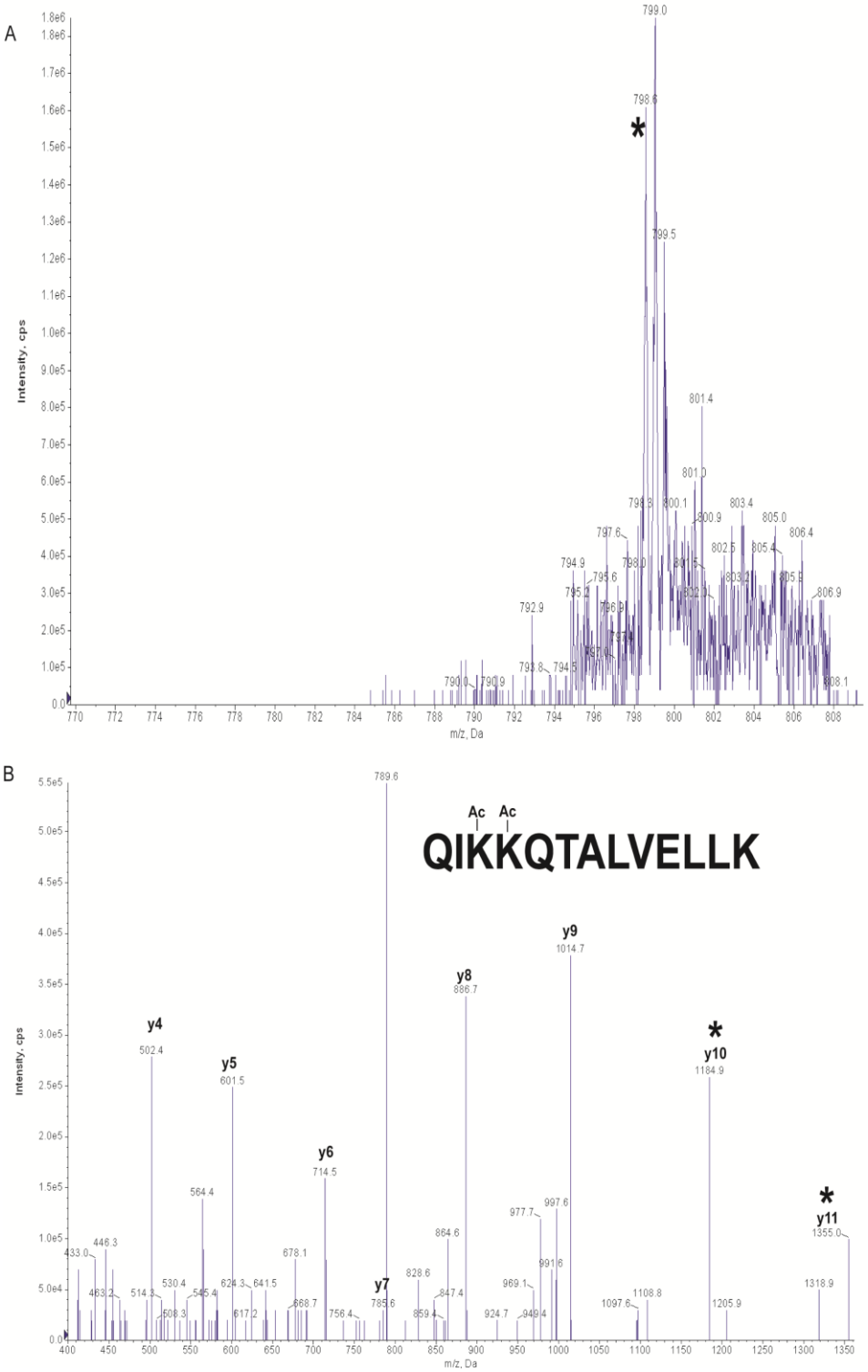
A
Intensity, cps
m/z, Da
B
Ac Ac
QIKKQTALVELLK
y4
502.4
y5
601.5
y6
714.5
y7
785.6
y8
886.7
y9
1014.7
y10
1184.9
y11
1355.0
Intensity, cps
m/z, Da

Order	b	Seq.	y	Order
1	129.0659	Q		13
2	242.1499	I	1467.9145	12
3	412.2554	K	1354.8304	11
4	582.3610	K	1184.7249	10
5	710.4195	Q	1014.6194	9
6	811.4672	T	886.5608	8
7	882.5043	A	785.5131	7
8	995.5884	L	714.4760	6
9	1094.6568	V	601.3919	5
10	1223.6994	E	502.3235	4
11	1336.7835	L	373.2809	3
12	1449.8675	L	260.1969	2
13		K	147.1128	1

Figure 4.2.2.8 K547 and K548 acetylation was detected in acetylated BSA upon performing precursor ion scan at 126Da. A tryptic digest of acetylated BSA isolated was analyzed by MS. The enhanced resolution spectrum (A) and CID fragmentation spectrum of the peptide that resolved at 798.6 Da (doubly charged), indicated by the asterisk in panel A, is shown (B). The partial y-ion and b-ion series visible in the fragmentation spectrum are indicated, and the y10 and y11 peaks, representing terminal lysine residues shifted by 42 Da, indicated by asterisks. The fragmentation peak list is shown (C) with the peaks that could be assigned to the identified peptide with a Mascot search of the Swiss-Prot database indicated in red, and the peaks that were observed in the fragmentation spectrum, underlined.

Finally, a loss of the diagnostic ion (126Da) was also detected on a peptide located at the N-terminal of the acetylated BSA. A search of the Swiss-Prot database with the CID fragmentation spectrum of this peak, using the Mascot search engine, predicted a 31 residue long peptide that was acetylated at position K65 with a precursor mass of 1227.0394Da (triply charged) which had an ion score of 85 and an E value of 0.00017. Looking at the CID fragmentation spectrum, partial b-ion and y-ion series are evident (Fig. 4.2.2.11B). There is only one possible site of acetylation. The mass difference between y11

and y10 where the lysine 547 is situated is: 1333.7362 – 1163.6307 = 170.1055, which is equal to an acetylated lysine.

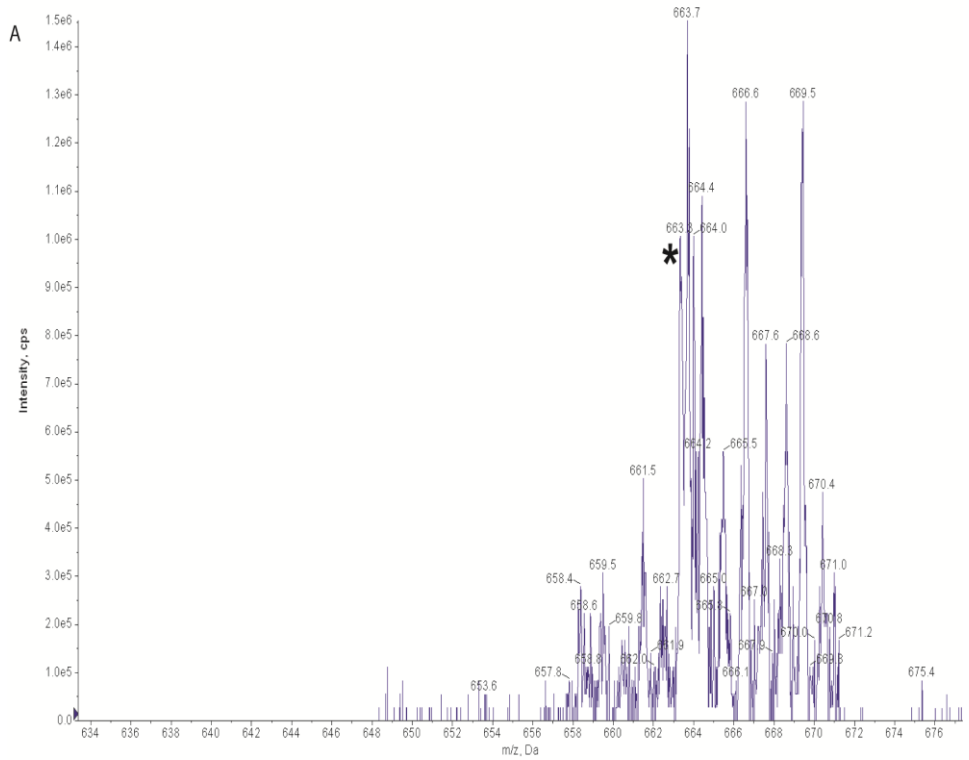
A
Intensity, cps
m/z, Da
663.7
666.6
669.5
664.4
664.0
*
667.6
668.6
664.2
665.5
661.5
670.4
659.5
658.4
662.7
668.3
671.0
658.6
659.8
671.2
657.8
653.6
675.4

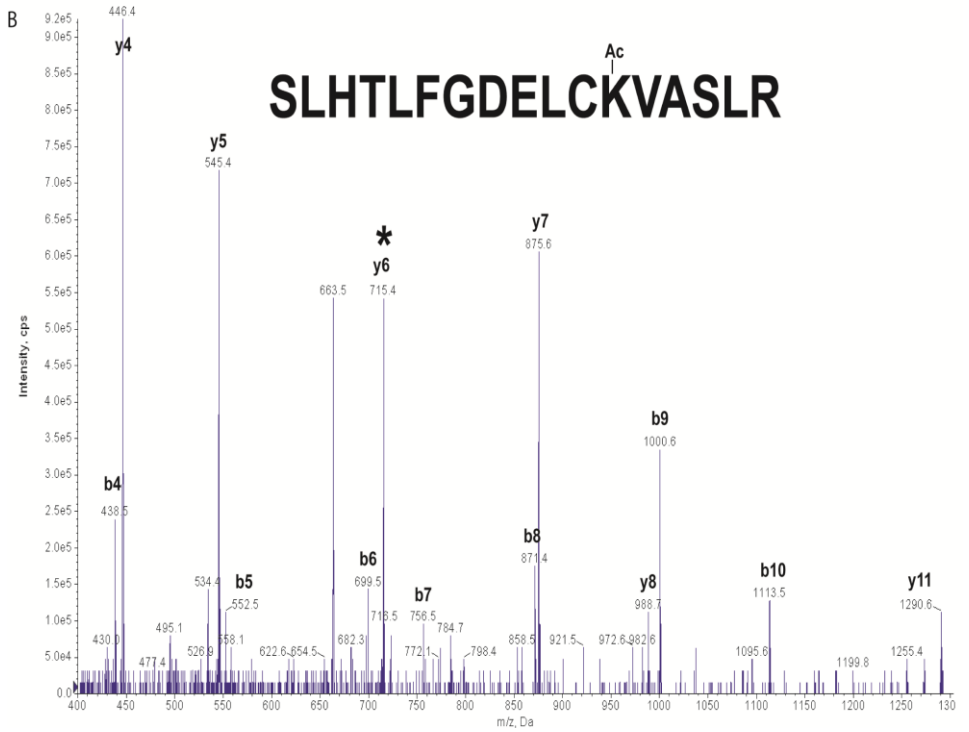
B
SLHTLFGDELCKVASLR
Ac
Intensity, cps
m/z, Da
446.4
y4
y5
545.4
y7
875.6
*
y6
663.5
715.4
b9
1000.6
b4
438.5
b8
871.4
b6
699.5
b5
552.5
b7
y8
988.7
b10
1113.5
y11
1290.6

Order	b	Seq.	y	Order
1	88.0393	S		17
2	201.1234	L	1900.9949	16
3	338.1823	H	1787.9109	15
4	439.2300	T	1650.8520	14
5	552.3140	L	1549.8043	13
6	699.3824	F	1436.7202	12
7	756.4039	G	1289.6518	11
8	871.4308	D	1232.6303	10
9	1000.4734	E	1117.6034	9
10	1113.5575	L	988.5608	8
11	1273.5882	C	875.4767	7
12	1443.6937	K	715.4461	6
13	1542.7621	V	545.3406	5
14	1613.7992	A	446.2722	4
15	1700.8312	S	375.2350	3
16	1813.9153	L	288.2030	2
17		R	175.1190	1

Figure 4.2.2.9 K100 acetylation was detected in acetylated BSA upon performing precursor ion scan at 126Da. A tryptic digest of acetylated BSA isolated was analyzed by MS. The enhanced resolution spectrum (A) and CID fragmentation spectrum of the peptide that resolved at 663.8Da (triply charged), indicated by the asterisk in panel A, is shown (B). The partial y-ion and b-ion series visible in the fragmentation spectrum are indicated, and the y6 peak, representing a terminal lysine residue shifted by 42 Da, indicated by an asterisk. The fragmentation peak list is shown (C) with the peaks that could be assigned to the identified peptide with a Mascot search of the Swiss-Prot database indicated in red, and the peaks that were observed in the fragmentation spectrum, underlined.

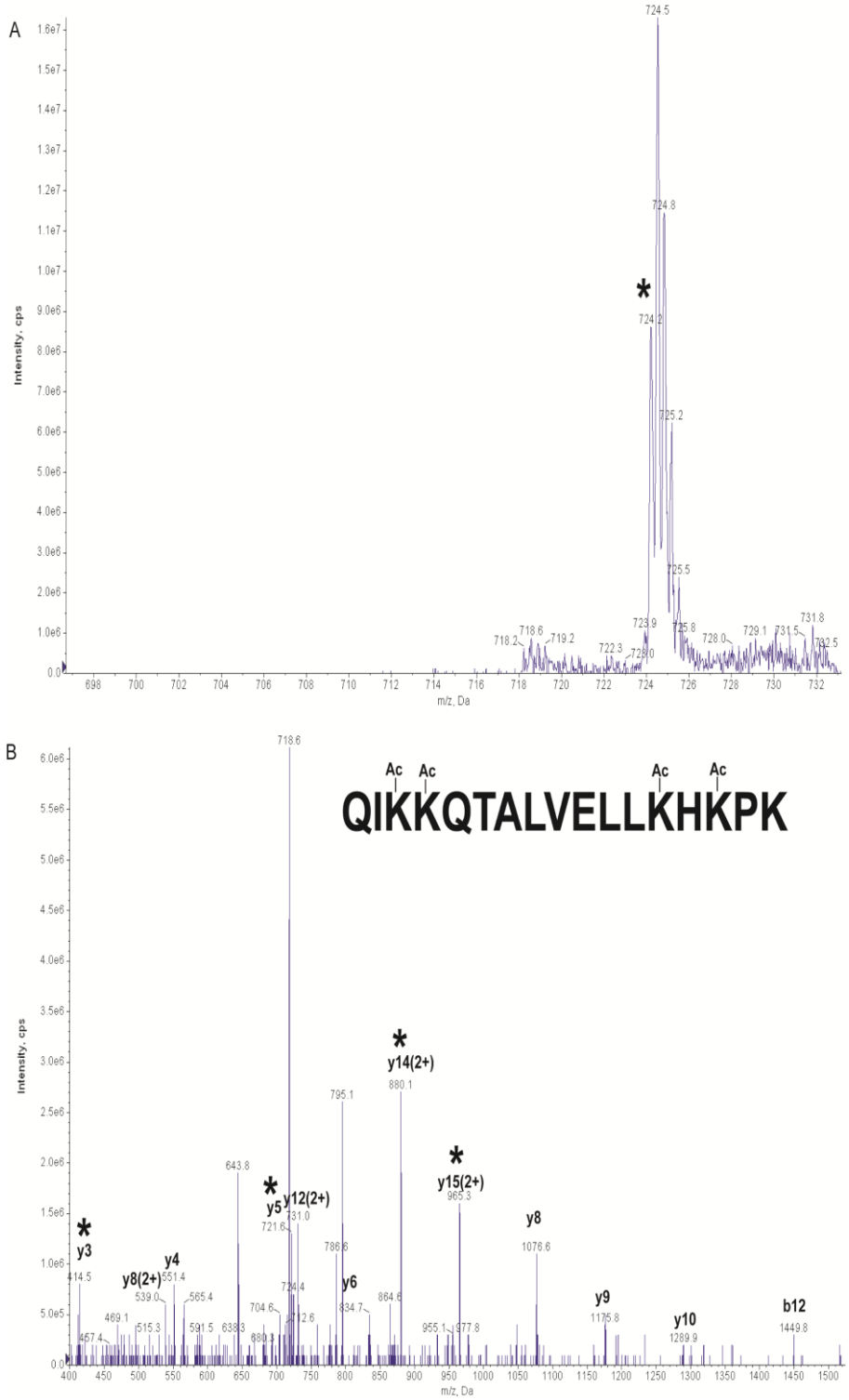
A
Intensity, cps
m/z, Da
724.5
724.8
724.2
725.2
725.5
B
QIKKQTALVELLKHKPK
Ac
Ac
Ac
Ac
y14(2+)
y15(2+)
y12(2+)
y5
y3
y4
y8(2+)
y6
y8
y9
y10
b12
Intensity, cps
m/z, Da

Order	b	b^{++}	Seq.	y	y^{++}	Order
1	129.0659	65.0366	Q			17
2	242.1499	121.5786	I	2043.2212	1022.1142	16
3	412.2554	206.6314	K	1930.1371	965.5722	15
4	582.3610	291.6841	K	1760.0316	880.5195	14
5	711.4035	356.2054	Q	1589.9261	795.4667	13
6	812.4512	406.7293	T	1460.8835	730.9454	12
7	883.4883	442.2478	A	1359.8358	680.4216	11
8	996.5724	498.7898	L	1288.7987	644.9030	10
9	1095.6408	548.3240	V	1175.7147	588.3610	9
10	1224.6834	612.8453	E	1076.6462	538.8268	8
11	1337.7675	669.3874	L	947.6037	474.3055	7
12	1450.8515	725.9294	L	834.5196	417.7634	6
13	1620.9571	810.9822	K	721.4355	361.2214	5
14	1758.0160	879.5116	H	551.3300	276.1686	4
15	1928.1215	964.5644	K	414.2711	207.6392	3
16	2025.1743	1013.0908	P	244.1656	122.5864	2
17			K	147.1128	74.0600	1

Figure 4.2.2.10 K547, K548, K557 and K559 acetylation was detected in acetylated BSA upon performing precursor ion scan at 126Da. A tryptic digest of acetylated BSA isolated was analyzed by MS. The enhanced resolution spectrum (A) and CID fragmentation spectrum of the peptide that resolved at 724.2 Da (triply charged), indicated by the asterisk in panel A, is shown (B). The partial y-ion and b-ion series visible in the fragmentation spectrum are indicated, and the y3, y5, $y^{++}14$ and $y^{++}15$ peak, representing terminal lysine residues shifted by 42 Da, indicated by asterisks. The fragmentation peak list is shown (C) with the peaks that could be assigned to the identified peptide with a Mascot search of the Swiss-Prot database indicated in red, and the peaks that were observed in the fragmentation spectrum, underlined. The b^{++} and y^{++} columns indicate b-ion and y-ion fragments that are doubly charged.

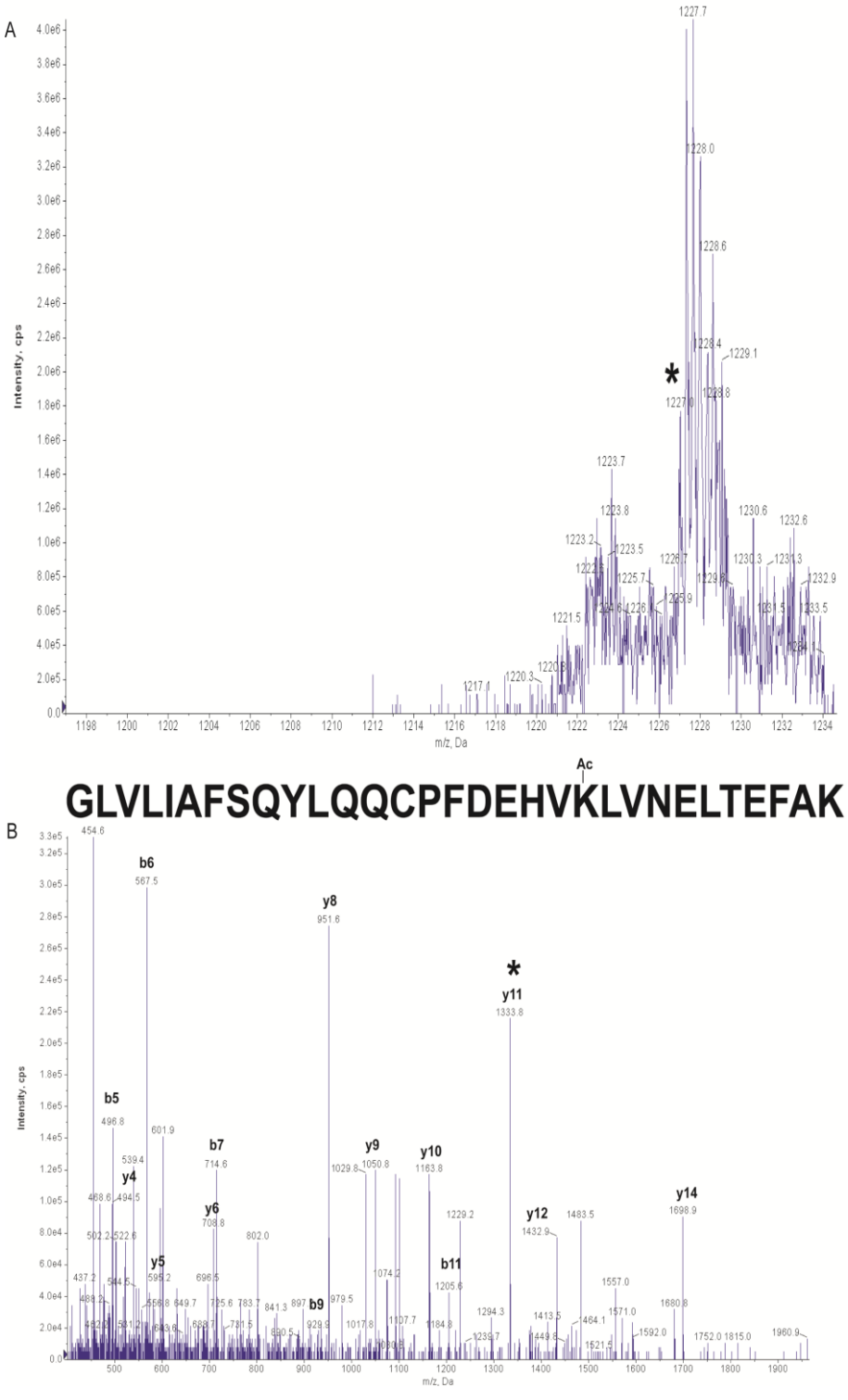
A
Intensity, cps
m/z, Da
Ac
GLVLIAFSQYLQQCPFDEHVKLVNELTEFAK
B
Intensity, cps
m/z, Da
b5
b6
b7
y4
y5
y6
y8
y9
y10
y11
y12
b9
b11
y14

Order	b	Seq.	y	Order
1	58.0287	G		31
2	171.1128	L	3623.8342	30
3	270.1812	V	3510.7501	29
4	383.2653	L	3411.6817	28
5	496.3493	I	3298.5976	27
6	567.3865	A	3185.5136	26
7	714.4549	F	3114.4765	25
8	801.4869	S	2967.4081	24
9	929.5455	Q	2880.3760	23
10	1092.6088	Y	2752.3174	22
11	1205.6929	L	2589.2541	21
12	1334.7355	Q	2476.1701	20
13	1463.7780	Q	2347.1275	19
14	1623.8087	C	2218.0849	18
15	1720.8615	P	2058.0542	17
16	1867.9299	F	1961.0015	16
17	1982.9568	D	1813.9330	15
18	2111.9994	E	1698.9061	14
19	2249.0583	H	1569.8635	13
20	2348.1267	V	1432.8046	12
21	2518.2323	K	1333.7362	11
22	2631.3163	L	1163.6307	10
23	2730.3847	V	1050.5466	9
24	2844.4277	N	951.4782	8
25	2973.4703	E	837.4353	7
26	3086.5543	L	708.3927	6
27	3187.6020	T	595.3086	5
28	3316.6446	E	494.2609	4
29	3463.7130	F	365.2183	3
30	3534.7501	A	218.1499	2
31		K	147.1128	1

Figure 4.2.2.11 K65 acetylation was detected in acetylated BSA upon performing precursor ion scan at 126Da. A tryptic digest of acetylated BSA isolated was analyzed by MS. The enhanced resolution spectrum (A) and CID fragmentation spectrum of the peptide that resolved at 1227.0Da (triply charged), indicated by the asterisk in panel A, is shown (B). The partial y-ion and b-ion series visible in the fragmentation spectrum are indicated, and the y11 peak, representing a terminal lysine residue shifted by 42 Da, indicated by an asterisk. The fragmentation peak list is shown (C) with the peaks that could be assigned to the identified peptide with a Mascot search of the Swiss-Prot

database indicated in red, and the peaks that were observed in the fragmentation spectrum, underlined.

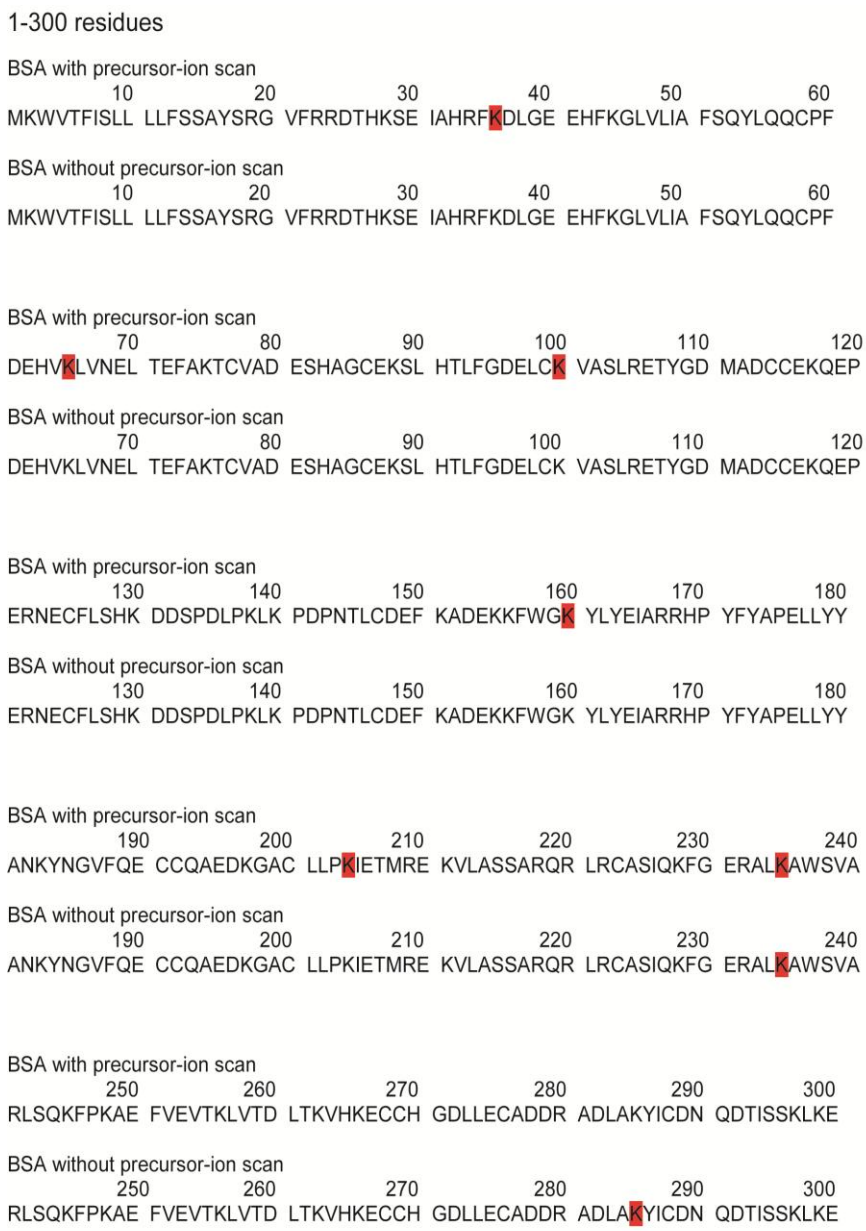

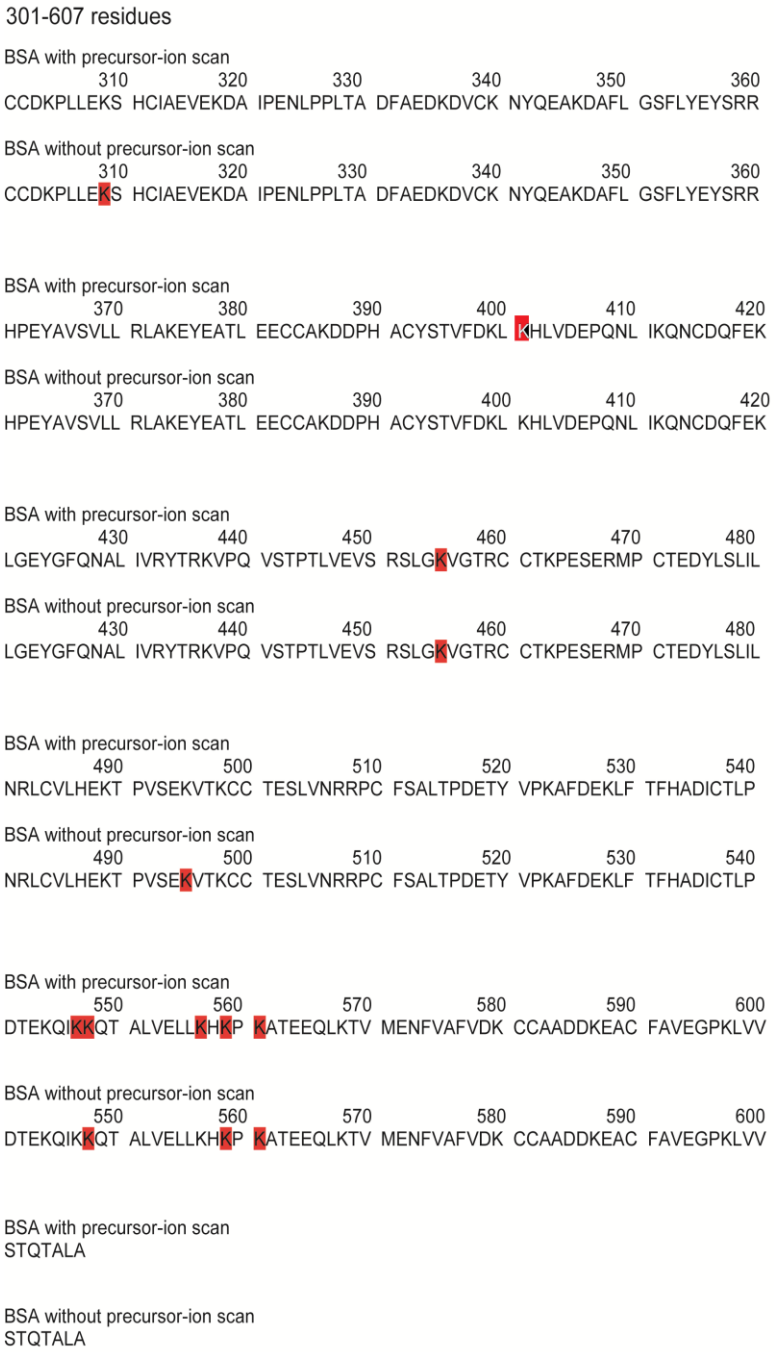

Figure 4.3. Comparison of acetylation state of full length sequence acetylated BSA (Promega) with precursor-ion scan and without precursor-ion scan. Sites of acetylation are indicated by red rectangles.

In bottom-up tandem MS, acetylated lysines are localised by the presence of a 170Da gap (acetyl-lysine residue) between consecutive b- and y-ions and through the presence of "diagnostic" ions. The derivative of immonium ion of acetyl-lysine that has lost ammonia (Im – NH_3,126.0913Da) were reported as MS/MS marker ions for the presence of acetylated lysine (Trelle and Jensen, 2008). Here, we used acetylated BSA (Promega), which has been reported to enhance the performance of restriction enzymes, to test the effectivity and specificity of the targeted discovery of modified peptides (precursor – ion scan). To understand the degree to which the precursor ion scan can improve the identification of modified peptides in LC-MS/MS, we compared the MS/MS analysis of acetylated BSA proteins using precursor ion scan and without precursor ion scan, in which case the target discovery approach was replaced with broader survey scans (enhanced mass scans).

Looking at Figure 4.3, there were 13 sites of acetylation that were discovered by precursor ion scan with an overall protein ion score of 219 as compared to 7 sites of acetylation detected by the un-targeted enhanced MS method with an overall protein ion score of 77. The precursor ion scan method had 8 sites of acetylation that were unique, whereas, the enhanced MS method had only 2 sites of acetylation that were unique. Both these methods had 5 overlapping sites of acetylation. It can be suggested, therefore, that the data dependant and targeted approach of precursor ion scan may increase the discovery of modified peptides by two folds.

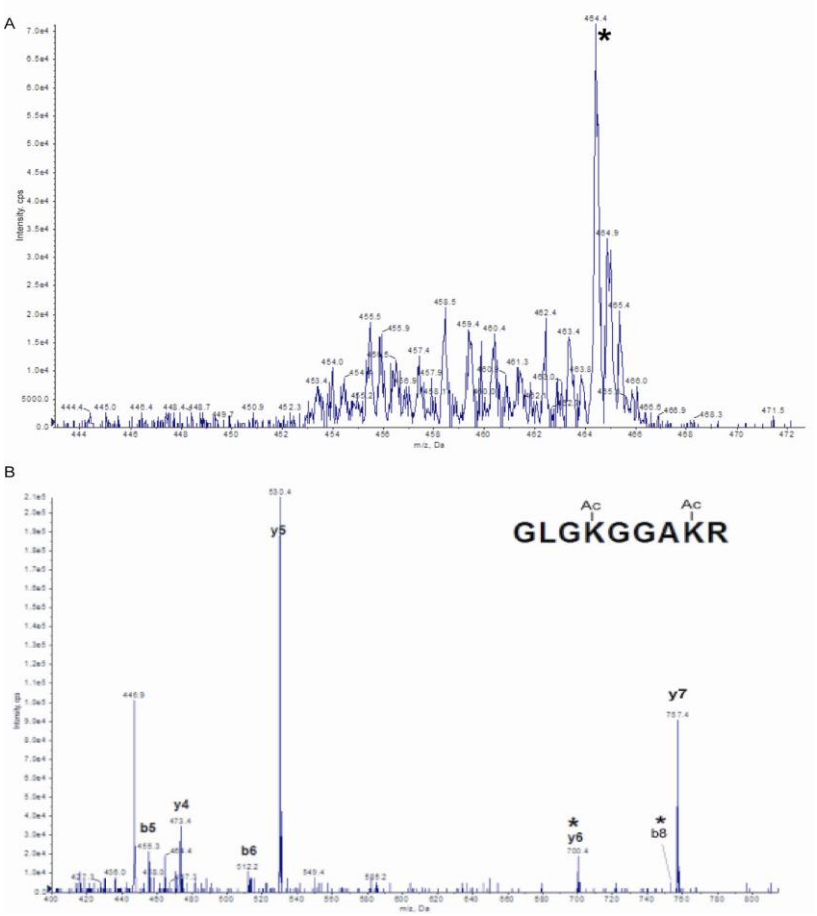

Order	b	Seq.	y	Order
1	58.0287	G		9
2	171.1128	L	870.5156	8
3	228.1343	G	757.4315	7
4	398.2398	K	700.4100	6
5	455.2613	G	530.3045	5
6	512.2827	G	473.2831	4
7	583.3198	A	416.2616	3
8	753.4254	K	345.2245	2
9		R	175.1190	1

Figure 4.4. K12 and K16 of histone H4 are acetylated in exponential phase. A tryptic digest of histone H4 isolated from exponential phase yeast cells was analyzed by MS. The enhanced resolution ion spectrum (A) and CID fragmentation spectrum of the peptide that resolved at 464.4 Da (doubly charged), indicated by the asterisk in panel A, is shown (B). The partial y-ion and b-ion series visible in the fragmentation spectrum are indicated, and the y6 and b8 peaks, representing terminal lysine residues shifted by 42 Da, indicated by asterisks. The fragmentation peak list is shown (C) with the peaks that could be assigned to the identified peptide with a Mascot search of the Swiss-Prot database indicated in red, and the peaks that were observed in the fragmentation spectrum, underlined.

After establishing that we can successfully detect acetylated lysine residues in bovine serum albumin, histone H4 was isolated from exponential phase *S. cerevisiae* cells using the Zymolyase method, resolved by SDS-PAGE electrophoresis, the H4 containing gel slice excised, the histone digested with trypsin in the gel slice, and the resulting peptides eluted and subjected to MS analysis.

Of all the peptides generated by tryptic cleavage of H4, only the peptide from position 9-17 produced a diagnostic ion at approximately 126 Da, indicative of at least one acetylated lysine residue. A di-acetylated H4 fragment with an E-value of 0.66 and a MOWSE score of 40 was identified when performing a Mascot search with the fragmentation spectrum of this peptide against the Swiss-Prot database. Note that the reported expectancy value and MOWSE score are for the peptide fragment only, not the whole H4 protein, which was identified with a MOWSE score of 196. This assignment is supported by the precursor ion mass of 464.3723 Da (see Fig. 4.4 A), recorded by the enhanced resolution scan of the ion. This is within approximately 0.6 Da of the expected mass of the peptide GLGKGGAKR with a mass of 843.5159 for the $[M+H]^+$ ion and 42.0106 Da for each of the acetyl groups, where

the peptide is in a doubly charged state. This result provides very strong evidence that the peptide fragment from 9-17 of H4 is di-acetylated. Since this fragment contains only two lysine residues, it is very likely that both K12 and K16 were acetylated. To confirm this assignment, the CID fragmentation spectrum was also considered.

Partial b- and y-ion fragmentation series could be identified (see Fig. 4.4 B). Looking first at the y-ion series, the y4, y5, y6 and y7 fragments were visible. Histone H4 lysine 12 will thus correspond to the N-terminal residue in the y6 fragment. The mass difference between the y5 and y6 fragment is 170.1055 Da. This is within 0.1 Da of the mass of an acetylated lysine residue, which is equal to 128.09 Da plus 42.0106 Da. This result demonstrates that lysine 12 of H4 is acetylated in exponential phase *S. cerevisiae* cells.

Looking next at the b-ion series (Fig. 4.4 B), the b5, b6 and b8 ions could be identified. Lysine 16 would be the C-terminal residue in the b8 fragment. Since the b7 fragment was not observed, possibly due to the lower proton affinity of this fragment, it was not possible to directly calculate the mass of the C-terminal residue in b8. However, the difference in mass of the b6 (512.2827 Da) and b8 (753.4254 Da) fragments was 241.1427 Da. The mass of the di-peptide AK with the lysine acetylated is 241.13, within 0.1 Da of the observed mass. This provides very strong evidence that the second acetyl group is present on K16 of the H4 fragment.

To investigate the acetylation state of histone H4 in semi-quiescent *S. cerevisiae*, we isolated H4 from stationary phase yeast cells using the Zymolyase method, performed a tryptic digest of the sample resolved on an SDS-PAGE gel, and analyzed the eluted peptide fragments by MS.

We could not detect the diagnostic ion at 126 Da, a sub-fragment formed by loss of ammonia from the immonium ion of acetylated lysine, during a precursor-ion scan of all peptides generated by tryptic cleavage of H4. This result suggested that H4 was not acetylated in yeast in stationary phase. However, since ion-suppression in different samples may influence the generation of the immonium ion sub-fragment, we also studied the fragmentation spectra of the peptides. The result is shown in Fig. 4.5.

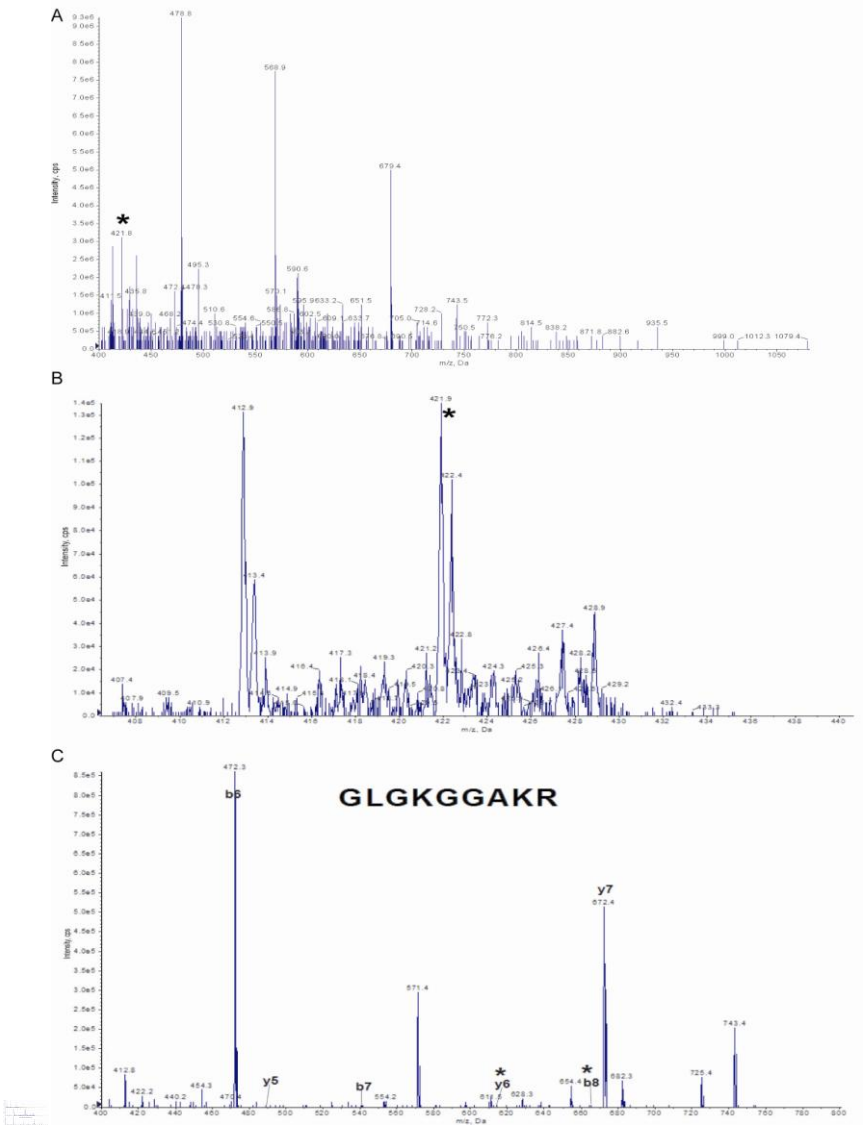

Order	b	Seq.	y	Order
1	58.0295	G		9
2	171.1135	L	786.5192	8
3	228.1350	G	673.4351	7
4	356.2299	K	616.4136	6
5	413.2514	G	488.3187	5
6	470.2729	G	431.2972	4
7	541.3100	A	374.2757	3
8	669.4050	K	303.2386	2
9		R	175.1437	1

Figure 4.5. K12 and K16 of histone H4 are non-acetylated in stationary phase. A tryptic digest of histone H4 isolated from stationary phase yeast cells was analyzed by MS. The enhanced product ion spectrum (A) and CID fragmentation spectrum of the peptide that resolved at 421.9 Da (doubly charged), indicated by the asterisk in panel A, is shown (B). The partial y-ion and b-ion series visible in the fragmentation spectrum are indicated, and the y6 and b8 peaks, representing a terminal lysine residue, indicated by asterisks. The expected fragmentation peak list is shown (C) with the peaks that were observed in the fragmentation spectrum, underlined.

Looking first at the GLGKGGAKR peptide from position 9-17 of H4, found to be di-acetylated in exponential phase, a precursor peak at 421.9 Da is visible (see Fig. 4.5 A and B). In addition, the MOWSE score of the full length stationary phase histone H4 identified by Mascot was 114. A search of the Swiss-Prot database with the CID fragmentation spectrum of this precursor peptide peak, using the Mascot search engine, could not identify the H4 fragment from position 9-17. However, upon manually searching the Analyst v1.2 (AB/SCIEX) peak list, the fragment was observed. The mass at which this peak resolved (421.9 Da) is consistent (within 0.4 Da) with the doubly charged peptide GLGKGGAKR with none of the lysines acetylated. Looking next at the MS/MS spectrum, partial b-ion and y-ion series are visible (see Fig. 4.5 C). The mass difference between y5 and y6, where lysine 12 is present as the N-terminal residue, is 616.4136 - 488.3187 = 128.0949, within 0.1Da of the

mono-isotopic mass of unmodified lysine. Lysine 16 is the C-terminal residue of the b8 ion. The mass difference between b7 and b8 is 669.4050 - 541.3100 = 128.095, also within 0.1 Da of the mass of an unacetylated lysine residue. This result demonstrated that, in contrast to exponential phase, both lysine 12 and 16 were not acetylated in stationary phase. Although it is a formal possibility that low levels of the acetylated peptide were present, no evidence of a mono- or di-acetylated peptide containing K12 and K16 were observed.

We next asked whether the acetylation state of histone H3 also differed between exponential and stationary phase in yeast. Histone H3 was isolated from exponential and stationary phase yeast cells, resolved by SDS-PAGE, the gel fragment excised and the histone digested with trypsin in the gel matrix. The eluate was finally analyzed by MS. The digest was separated on a C-18 HPLC nano column, and a precursor-ion scan performed on the eluate. Where a 126 Da precursor ion, indicative of acetylated lysine, was detected, the fragmentation spectrum of the eluting peptide was also recorded. We detected two acetylated peptides in histone H3 isolated from exponential phase, a di-acetylated peptide (Fig. 4.6) and a mono-acetylated peptide (Fig.4.8). A Mascot search of the Swiss-Prot database with the MS/MS spectrum identified the di-acetylated peptide KSTGGKAPR (residue position 9-17) (Expectancy value=0.014; MOWSE score=44). In its un-acetylated form this peptide has a predicted mass of 451.26 Da in its doubly charged state. The enhanced resolution scan of this di-acetylated peptide revealed a mass of 493.4 for the doubly charged state (Fig. 4.6A), a difference of 42.14, consistent with the presence of two acetyl groups on this peptide. Looking at the fragmentation spectrum (Fig. 4.6B) partial y-ion and b-ion series are visible. It was not possible to directly view the N-terminal lysine residue, since the b1 ion resolved below the lower mass cut-off of the fragmentation spectrum. However, the y8 ion was detected at 815.437 Da. Thus the mass difference between the full peptide (986.8 Da for the singly charged state) and the y8 ion is 171.363 Da, which is most consistent with an acetylated lysine residue (170.1 Da). Neither the y3 nor b6 ions were

observed in the fragmentation spectrum, it is therefore not possible to directly calculate the mass of K14. However, we note that the mass predicted for the y2 ion of the KSTGGKAPR peptide was 343.2088 Da (Fig. 4.6C). The y4 ion, which was observed, had a mass of 513.3144 Da. Thus, the N-terminal residue of the y4 fragment had a mass of 170.1056 Da, consistent with an acetylated lysine residue. Furthermore, the mass difference between the predicted b6 and observed b5 ions is 643.3410 - 473.2354 = 170.1056, again consistent with an acetylated lysine residue. We therefore conclude that K9 and K14 is acetylated in histone H3 in exponential phase yeast cells.

To investigate whether these residues were also acetylated in semi-quiescent stationary phase in yeast, histone H3 was isolated from stationary phase cells and analyzed as above. The precursor-ion scan did not identify any acetylated peptides in the tryptic digest of histone H3 isolated from stationary phase. We therefore performed an enhanced MS scan to identify the KSTGGKAPR peptide. A 450.5 Da peak was identified (Fig. 4.7A), within 0.76 Da of a mass of 451.26 Da which is expected for the doubly charged peptide. Searching the fragmentation spectrum of the peptide that eluted in this peak against the Swiss-Prot database with Mascot, indeed we identified the un-acetylated KSTGGKAPR peptide as the best match (Expectancy value=2.2; MOWSE score=21) Looking at the fragmentation spectrum of this peptide (Fig. 4.7C) partial b-ion and y-ion series are visible. Again, the b1 ion, containing the N-terminal K9, is below the mass cut-off of the scan (Fig. 4.7C). The mass difference between the full-length peptide (902.58 Da; singly charged) and y8 ion (773.4264 Da) is 129.1536 Da, within 1 Da of the mass of an un-acetylated lysine residue. Looking next at K14, a b5 (431.2249 Da) and $b6^0$ (541.3093 Da) fragment were observed, the latter having lost a water molecule (18 Da). Thus, the observed mass of K14 is 541.3093 - 431.2249 + 18 = 128.0844 Da, within 0.1 Da of the mass of an un-acetylated lysine residue. Neither the y3 nor the y4 fragment, or any neutral loss sub-fragment thereof, was observed, not allowing calculation of the mass of K14 from the y-ion fragmentation series.

However, the MS evidence presented above clearly indicated that both K9 and K14 were un-acetylated in histone H3 isolated from stationary phase yeast cells.

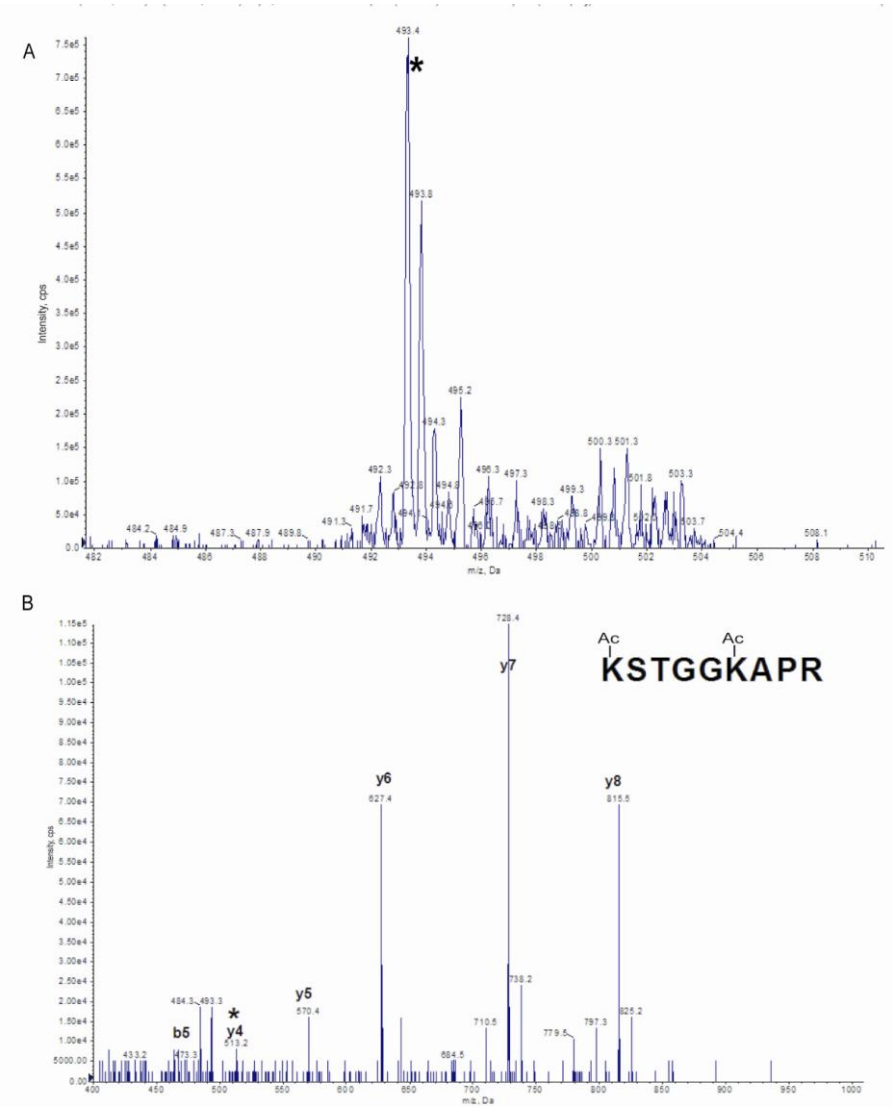

Order	b	Seq.	y	Order
1	171.1128	K		9
2	258.1448	S	815.4370	8
3	359.1925	T	728.4050	7
4	416.2140	G	627.3573	6
5	473.2354	G	570.3358	5
6	643.3410	K	513.3144	4
7	714.3781	A	343.2088	3
8	811.4308	P	272.1717	2
9		R	175.1190	1

Figure 4.6. K9 and K14 of histone H3 are acetylated in exponential phase. A tryptic digest of histone H3 isolated from exponential phase yeast cells was analyzed by MS. The enhanced product ion spectrum (A) and CID fragmentation spectrum of the peptide that resolved at 493.4 Da, indicated by the asterisk in panel A, is shown (B). The partial y-ion and b-ion series visible in the fragmentation spectrum are indicated, and the y4 peak, shifted by 42 Da, indicated by the asterisk. The fragmentation peak list is shown (C) with the peaks that could be assigned to the identified peptide with a Mascot search of the Swiss-Prot database indicated in red, and the peaks that were observed in the fragmentation spectrum, underlined.

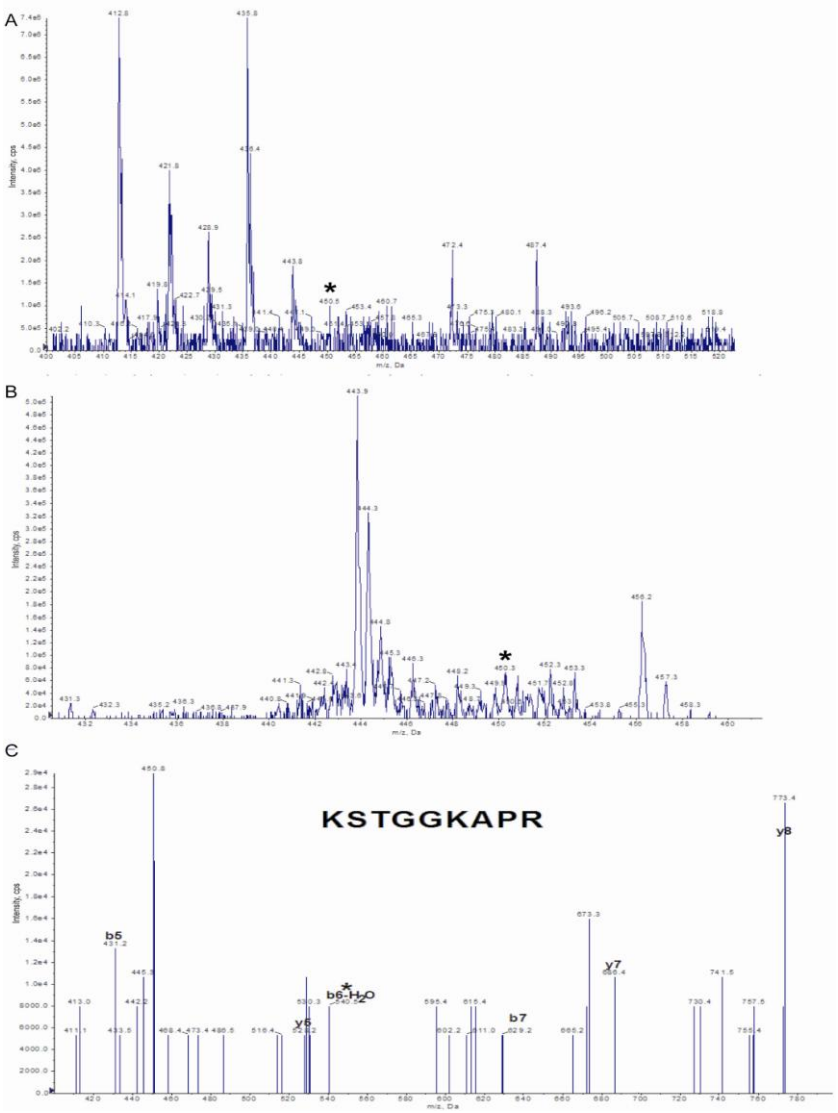

Order	b	b^0	Seq.	y	y^0	Order
1	129.1022		K			9
2	216.1343	198.1237	S	773.4264	755.4159	8
3	317.1819	299.1714	T	686.3944	668.3838	7
4	374.2034	356.1928	G	585.3467		6
5	431.2249	413.2143	G	528.3253		5
6	559.3198	541.3093	K	471.3038		4
7	630.3570	612.3464	A	343.2088		3
8	727.4097	709.3991	P	272.1717		2
9			R	175.1190		1

Figure 4.7. K9 and K14 of histone H3 are un-acetylated in stationary phase. A tryptic digest of histone H3 isolated from stationary phase yeast cells was analyzed by MS. The enhanced product ion spectrum (A) and CID fragmentation spectrum of the peptide that resolved at 493.4 Da, indicated by the asterisk in panel A, is shown (B). The partial y-ion and b-ion series visible in the fragmentation spectrum are indicated, and the y4 peak, shifted by 42 Da, indicated by the asterisk. The fragmentation peak list is shown (C) with the peaks that could be assigned to the identified peptide with a Mascot search of the Swiss-Prot database indicated in red, and the peaks that were observed in the fragmentation spectrum, underlined. The b^0 and y^0 columns indicate b-ion and y-ion fragments that formed after loss of a water molecule (18 Da).

Apart from the H3 peptide KSTGGKAPR (residue position 9-17), the precursor ion scan of the tryptic digest of H3 isolated from exponential phase yeast cells also identified the 126 Da diagnostic ion in a 455.3 Da peptide (Fig 4.8A). A Mascot search of the Swiss-Prot database with the fragmentation spectrum of this peptide identified the sequence SAPSTGGVKKPHR, located at sequence position 28-40 of yeast H3 (Expectancy value=1.3; MOWSE score=23). The predicted mass of this peptide is 1321.73 Da, 42 Da less than the observed mass of 1363.74 Da (the observed mass of 455.3 Da is for the triply charged peptide). This 42 Da mass difference is consistent with the presence of a single acetyl group in the peptide, which may be located on either K36 or K37. The fragmentation spectrum (Fig. 4.8B) shows the

presence of the y3, y8, y9, y10 and y11 fragments. However, none of these fragments allow the direct calculation of the mass for either K36 or K37. On the other hand, the b9 ion, observed at 827.4258 Da (see the asterisk in Fig. 4.8B), contains K36 as the C-terminal residue. The predicted mass of b8, which contains a residue that is not acetylatable, is 657.3202 Da (Fig. 4.8C). Thus, the difference between b8 and the observed b9 fragment is 170.1056 Da, which is within 0.1 Da of an acetylated lysine residue. Thus, the single acetyl group detected in the fragment is present on K36 of H3. K37 is not acetylated.

We note that K27 precedes the H3 peptide SAPSTGGVKKPHR. It is well-documented that acetylation of lysine abolished the ability of trypsin to hydrolyze the peptide backbone C-terminal to the modified residue (Bloxham *et al*., 1981). Thus, the SAPSTGGVKKPHR peptide fragment could only have been generated from an H3 molecule that was not acetylated at residue K27. Furthermore, no fragment containing acetylated K27 was detected in the precursor ion scan for the 126 Da diagnostic ion in the tryptic digest of H3. We therefore conclude that K27, unlike K36, was not acetylated in histone H3 in exponential phase.

We next performed a precursor ion scan on the tryptic digest of histone H3 isolated from stationary phase yeast cells, but could not detect the 126 Da diagnostic ion in any eluted fragment, suggesting that not all of the H3 peptides contained an acetyl group. We then performed an enhanced MS scan, and identified the peptide KSAPSTGGVK at 523.4 Da with a Mascot search of the fragmentation spectrum against the Swiss-Prot database (Fig. 4.9 C) (Expectancy value=0.11; MOWSE score=39). The predicted mass for the doubly charged peptide is 466.23 Da. Thus, in its singly charged state, the peak identified as KSAPSTGGVK is approximately 114 Da more massive than predicted. Nevertheless, the y-ion series, of which 70% of the fragmentation products were matched by Mascot, and 40% of the products observed, gave mass differences corresponding to the expected sequence.

The entire series, intriguingly, is shifted by 112.052 Da, suggesting that the y1 lysine is modified by an adduct of this mass. A search of the UniMod database of post-translational protein modifications (Creasy and Cottrell, 2004) for any modification within 1 Da of this mass, revealed a singly entry, acrolein, with the systematic name prop-2-enal. It is a highly nucleophilic aldehyde that is a product of lipid metabolism, but also forms with thermal decomposition of acrylamide, and was previously shown to form adducts by reacting with the ε-amino of lysine and with cysteine residues (Furuhata *et al*., 2003; Beretta *et al.*, 2008). However, acrolein has a molecular mass of 56 Da, suggesting that two acrolein adducts formed per lysine residue in the peptide above. Beretta and colleagues previously showed that two such adducts indeed formed on the single lysine residue of the GHK tri-peptide, followed by intra-molecular aldol condensation and dehydration to form N-(3-formyl-3,4-dehydropiperidino) lysine (Beretta *et al*., 2008). The proposed reaction scheme is shown in Fig. 4.10

Since it is unlikely that trypsin would have cleaved a peptide C-terminal to such a modification, we suggest that the di-acroleination of the C-terminal lysine of KSAPSTGGVK occurred during electrophoresis in the polyacrylamide gel, where acrolein may have been present. We therefore propose that this modification did not occur *in vivo*. Importantly, we found no evidence for acetylation of this lysine residue (K36), unlike the equivalent residue of H3 in exponential phase. The *m/z* value of the observed b6-ion (572.3039 Da) also showed that K27, N-terminal in the KSAPSTGGVK peptide, was not acetylated in H3 of *S. cerevisiae* stationary phase.

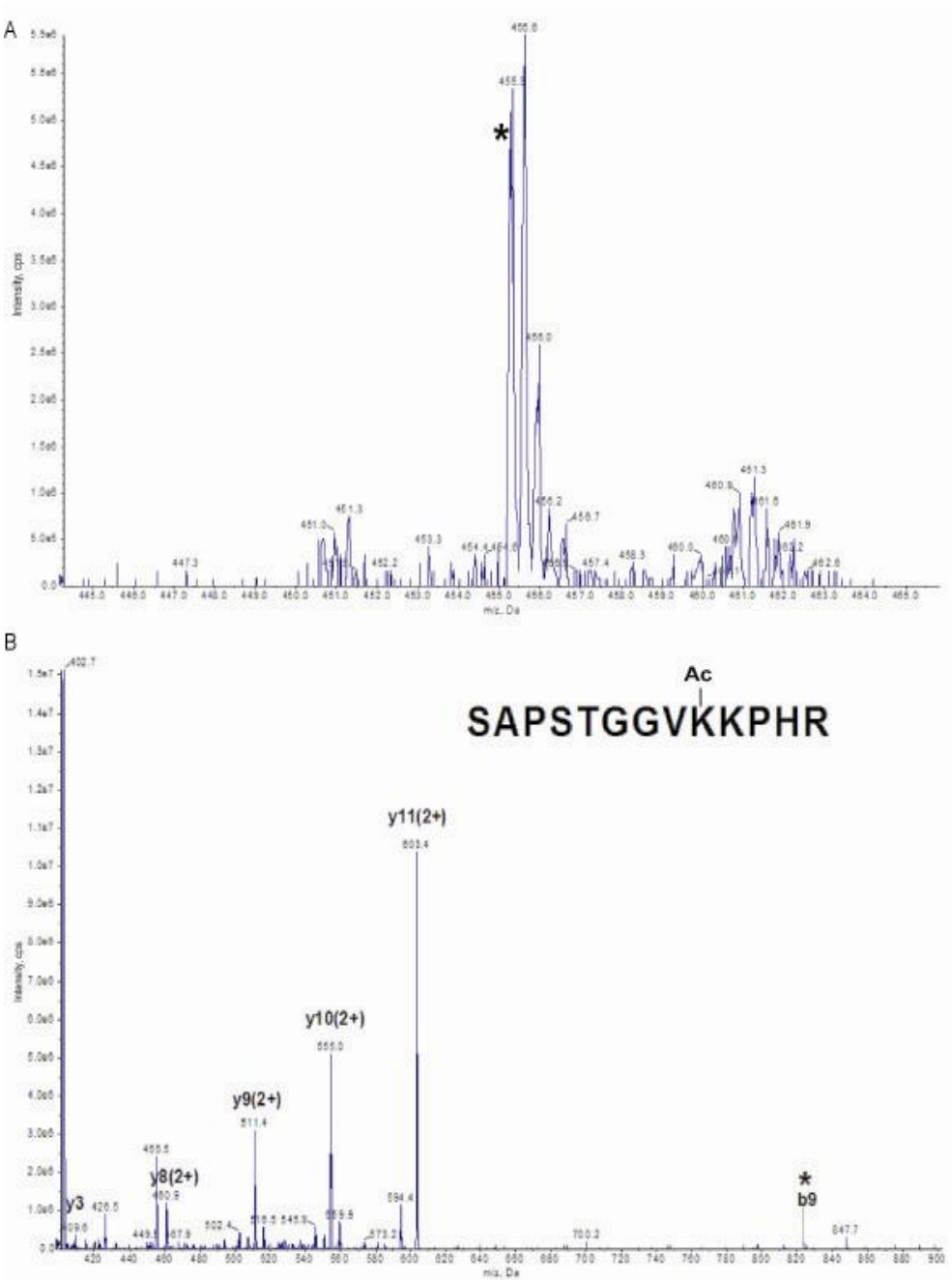
A
B
Ac
SAPSTGGVKKPHR
y11(2+)
y10(2+)
y9(2+)
y8(2+)
y3
b9
Intensity, cps
m/z, Da

Order	b	b^{++}	Seq.	y	y^{++}	Order
1	88.0393	44.5233	S			13
2	159.0764	80.0418	A	1276.7120	638.8597	12
3	256.1292	128.5682	P	1205.6749	603.3411	11
4	343.1612	172.0842	S	1108.6222	554.8147	10
5	444.2089	222.6081	T	1021.5901	511.2987	9
6	501.2304	251.1188	G	920.5425	460.7749	8
7	558.2518	279.6295	G	863.5210	432.2641	7
8	657.3202	329.1638	V	806.4995	403.7534	6
9	827.4258	414.2165	K	707.4311	354.2192	5
10	955.5207	478.2640	K	537.3256	269.1664	4
11	1052.5735	526.7904	P	409.2306	205.1190	3
12	1189.6324	595.3198	H	312.1779	156.5926	2
13			R	175.1190	88.0631	1

Figure 4.8. Histone H3 K36, but not K37, is acetylated in exponential phase. A tryptic digest of histone H3 isolated from exponential phase yeast cells was analyzed by MS. The enhanced product ion spectrum (A) and CID fragmentation spectrum of the peptide that resolved at 455.3 Da, indicated by the asterisk in panel A, is shown (B). The partial y-ion and b-ion series visible in the fragmentation spectrum are indicated, and the b9 peak, shifted by 42 Da relative to the mass of lysine, indicated by the asterisk. The fragmentation peak list is shown (C) with the peaks that could be assigned to the identified peptide with a Mascot search of the Swiss-Prot database indicated in red, and the peaks that were observed in the fragmentation spectrum, underlined. Superscript "++" indicate doubly charged fragments.

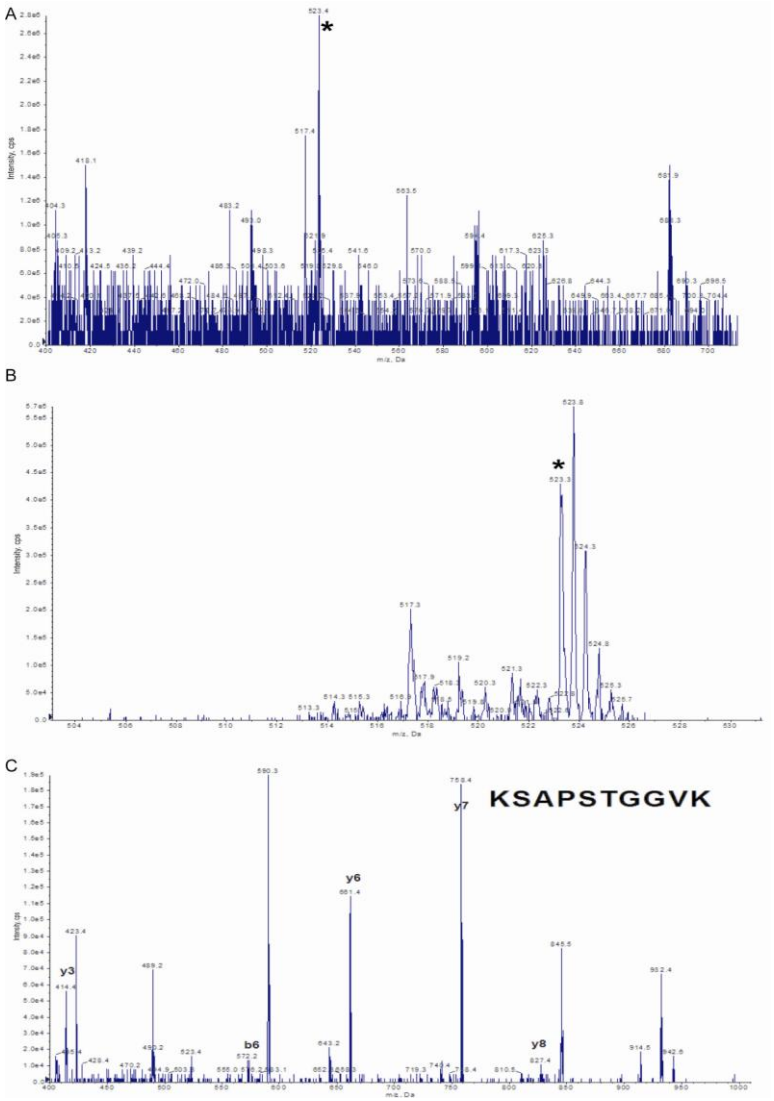

Order	b	Seq.	y	Order
1	129.1022	K		10
2	216.1343	S	915.4782	9
3	287.1714	A	828.4462	8
4	384.2241	P	757.4090	7
5	471.2562	S	660.3563	6
6	572.3039	T	573.3243	5
7	629.3253	G	472.2766	4
8	686.3468	G	415.2551	3
9	785.4152	V	358.2336	2
10		K	259.1652	1

Figure 4.9. Histone H3 K27 and K36 are not acetylated in stationary phase. A tryptic digest of histone H3 isolated from stationary phase yeast cells was analyzed by MS. The enhanced product ion spectrum (A) and CID fragmentation spectrum of the peptide that resolved at 523.4 Da, indicated by the asterisk in panel A, is shown (B). The partial y-ion and b-ion series visible in the fragmentation spectrum are indicated. The fragmentation peak list is shown (C) with the peaks that could be assigned to the identified peptide with a Mascot search of the Swiss-Prot database indicated in red, and the peaks that were observed in the fragmentation spectrum, underlined. Note that the y-ion series is shifted by 112.056 Da due to the presence of an adduct of this mass on y1.

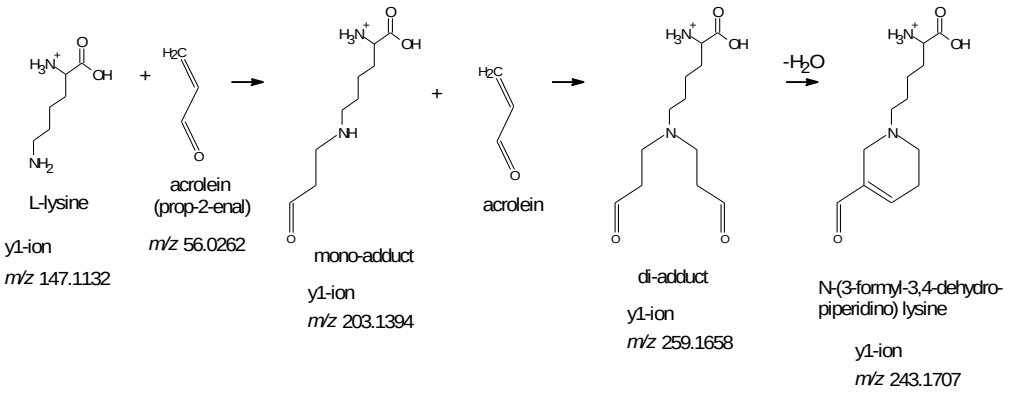

Figure 4.10. Proposed reaction scheme for the formation of an acrolein adduct on the ε-amino group of lysine. (Adapted from Beretta *et al.*, 2008). The predicted *m/z* values of the different modified y1-ions are indicated.

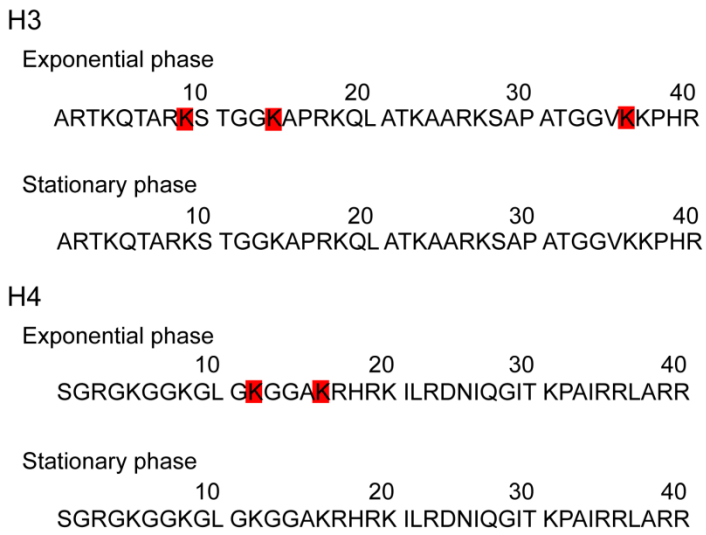

Figure. 4.11. Acetylation state of the N-terminal tail sequences of *Saccharomyces cerevisiae* histones H3 and H4 in exponential and stationary phase. Sites of acetylation are indicated by red rectangles.

4.4. Discussion and Conclusions

Of the modifications studied, histone acetylation has been the most studied and appreciated. Propelled, in part, by the discovery of the various enzyme complexes and the compelling evidence that acetylation of specific lysine residues in the N-termini of the core histones plays a fundamental role in transctription regulation (Struhl, 1998).

In 1964 Allfrey and colleagues showed histone H3 and H4 inhibited RNA synthesis in calf nuclei *in vitro*, and that acetylation of the arginine-rich histones alleviated this repressive effect. This initial report saw the birth of epigenetics and an understanding that covalent modifications of histones may provide a mechanism whereby DNA function may be regulated. In recent years post-translational modifications of histones have been shown to underlie gene transcription.

Over a decade ago, a plethora of work has been done in trying to understand the type of modifications on histone N-terminal tails and the possible physiological function inside the living cell. A histone acetyltransferase was found to be responsible for acetylation of all four nucleosomal histone H4 lysine residues (K5, K8, K12 and K16) and in histone H2A *in vitro* is Esa1 which is part of the NuA4 complex (Clarke *et al*., 1999; Allard *et al*., 1999). In our work we have shown that in exponential histone H4 lysine 12 and 16 are both acetylated. Lysine 12 is strongly associated with gene transcription in actively growing cells (Johnson *et al*., 1998). Whereas, lysine 16 performs a more structural function in chromatin organisation. It was illustrated that nucleosomal cores that were uniformly acetylated at lysine 16 hampered the ability of chromatin to form cross-fibre interactions which lead to a more “relaxed” state of chromatin (Shogren-Knaak, 2006). On the other hand, the stationary phase H4 was not acetylated at neither lysine 12 and 16.

We have shown in exponential phase that histone H3 is acetylated at lysine 9, 14 and 36. In addition, enhanced product ion spectrum (fig. 4.8) showed that some of the H3 lysine 27 peptides were not acetylated as trypsin cleaved after this residue. Peptides of the yeast histone H3 in stationary phase were not acetylated at lysine 9, 14, 27, 36 and 37 (Figs 4.7 and 4.9). Some groups (Kuo *et al*., 1996; Utley *et al*., 1998; Zhang *et al*., 1998) have showed that the yeast Gcn5 catalyses, among others, histone H3 K9 and K14 acetylation. Furthermore, Chip-Chip studies showed that acetylation of histone H3 at lysine 9 and 14 peaks at predicted start sites of expressed genes and that this modification was associated with genome-wide transcription rates (Pokholok *et al*., 2005).

Additional level of functional complexity in the acetylation or methylation of histone lysine residues surfaced from the finding that lysine residues can be targeted for both acetylation or methylation but not simultaneously. The interchange between acetylation, deacetylation and methylation at the same sites illustrates a dynamic relationship between gene expression and repression that has the potential to occur at other histone lysine residues. Recent studies have described lysine 36 of histone H3 as a site of methylation mediated by the methyltransferase Set2 in the budding yeast *S. cerevisiae* (Strahl *et al*., 2002). In its methylated form, H3 K36 functions in the process of transcriptional elongation and occurs prevalently in the coding regions of genes (Shilatifard, 2004). In addition to being a site of methylation, H3 K36 can also be a target for acetylation (Morris *et al*., 2007). In Fig.4.8, we have showed that histone H3 was acetylated at lysine 36. Morris and colleagues demonstrated that acetylation of H3 at K36 is conserved in mammals and, in yeast, is localized predominantly to the promoters of RNA polymerase II-transcribed genes (Morris *et al*., 2007). It was also demonstrated that the Gcn5-tethered SAGA complex particularly acetylates H3 K36 *in vitro* and is required for H3 K36ac *in vivo*. Jointly, these results suggest that H3 K36 acetylation maybe conserved and likely functions in transcription.

4.5. Reference List

S. Allard, R. T. Utley, J. Savard, A. Clarke, P. Grant, C. J. Brandl, L. Pillus, J. L. Workman, and J. Cote. NuA4, an essential transcription adaptor/histone H4 acetyltransferase complex containing Esa1p and the ATM-related cofactor Tra1p. *EMBO J* 18 (18):5108-5119, 1999.

V.G. Allfrey, R. Faulkner, and A. E. Mirsky. Acetylation and methylation of histones and their possible role in the regulation of RNA synthesis. *Proc.Natl.Acad.Sci.U.S.A* 51 (5): 786-794, 1964.

G. Beretta, E. Arlandini, R. Artali, J. M. Anton, and Facino R. Maffei. Acrolein sequestering ability of the endogenous tripeptide glycyl-histidyl-lysine (GHK): characterization of conjugation products by ESI-MSn and theoretical calculations. *J.Pharm.Biomed.Anal.* 47 (3):596-602, 2008.

D. P. Bloxham, D. C. Parmelee, S. Kumar, R. D. Wade, L. H. Ericsson, H. Neurath, K. A. Walsh, and K. Titani. Primary structure of porcine heart citrate synthase. *Proc.Natl.Acad.Sci.U.S.A* 78 (9):5381-5385, 1981.

A. S. Clarke, J. E. Lowell, S. J. Jacobson, and L. Pillus. Esa1p is an essential histone acetyltransferase required for cell cycle progression. *Mol.Cell Biol.* 19 (4):2515-2526, 1999.

D. M. Creasy and J. S. Cottrell. Unimod: Protein modifications for mass spectrometry. *Proteomics* 4 (6):1534-1536, 2004.

A. Furuhata, T. Ishii, S. Kumazawa, T. Yamada, T. Nakayama, and K. Uchida. N(epsilon)-(3-methylpyridinium)lysine, a major antigenic adduct generated in acrolein-modified protein. *J.Biol.Chem.* 278 (49):48658-48665, 2003.

J. C. Hansen, C. Tse, and A. P. Wolffe. Structure and function of the core histone N-termini: more than meets the eye. *Biochemistry* 37 (51):17637-17641, 1998.

C. A. Johnson, L. P. O'Neill, A. Mitchell, and B. M. Turner. Distinctive patterns of histone H4 acetylation are associated with defined sequence elements within both heterochromatic and euchromatic regions of the human genome. *Nucleic Acids Res.* 26 (4):994-1001, 1998.

T. Kouzarides. Chromatin modifications and their function. *Cell* 128 (4):693-705, 2007.

S. A. Morris, B. Rao, B. A. Garcia, S. B. Hake, R. L. Diaz, J. Shabanowitz, D. F. Hunt, C. D. Allis, J. D. Lieb, and B. D. Strahl. Identification of histone H3 lysine 36 acetylation as a highly conserved histone modification. *J Biol.Chem.* 282 (10):7632-7640, 2007.

D. K. Pokholok, C. T. Harbison, S. Levine, M. Cole, N. M. Hannett, T. I. Lee, G. W. Bell, K. Walker, P. A. Rolfe, E. Herbolsheimer, J. Zeitlinger, F. Lewitter, D. K. Gifford, and R. A. Young. Genome-wide map of nucleosome acetylation and methylation in yeast. *Cell* 122 (4):517-527, 2005.

G. Schäfer, C. R. McEvoy, and H. G. Patterton. The *Saccharomyces cerevisiae* linker histone Hho1p is essential for chromatin compaction in stationary phase and is displaced by transcription. *Proc.Natl.Acad.Sci.U.S.A* 105 (39):14838-14843, 2008.

A. Shilatifard. Transcriptional elongation control by RNA polymerase II: a new frontier. *Biochim.Biophys.Acta* 1677 (1-3):79-86, 2004.

M. Shogren-Knaak, H. Ishii, J. M. Sun, M. J. Pazin, J. R. Davie, and C. L. Peterson. Histone H4-K16 acetylation controls chromatin structure and protein interactions. *Science* 311 (5762):844-847, 2006.

B. D. Strahl, R. Ohba, R. G. Cook, and C. D. Allis. Methylation of histone H3 at lysine 4 is highly conserved and correlates with transcriptionally active nuclei in *Tetrahymena*. *Proc.Natl.Acad.Sci.U.S.A* 96 (26):14967-14972, 1999.

B. D. Strahl, P. A. Grant, S. D. Briggs, Z. W. Sun, J. R. Bone, J. A. Caldwell, S. Mollah, R. G. Cook, J. Shabanowitz, D. F. Hunt, and C. D. Allis. Set2 is a nucleosomal histone H3-selective methyltransferase that mediates transcriptional repression. *Mol.Cell Biol.* 22 (5):1298-1306, 2002.

K. Struhl. Histone acetylation and transcriptional regulatory mechanisms. *Genes Dev.* 12 (5):599-606, 1998.

G. Vidali, E. L. Gershey, and V. G. Allfrey. Chemical studies of histone acetylation. The distribution of epsilon-N-acetyllysine in calf thymus histones. *J.Biol.Chem.* 243 (24):6361-6366, 1968.

SUMMARY

To date, the most studied post-translational histone modification is lysine acetylation, mainly because of its link to active gene expression. In this study we have used a high-resolution discontinuous TAU gel system to assess histone isoforms differing by a single acetyl group. One way-Anova statistical analyses were used to calculate the average level for each isoform at each time point for the four core histones. We found that the di-acetylated isoform was predominant in H4. The predominance of the di-acetylated H4 isoform have been shown to be indicative of a decondensed chromatin structure, as well as a requirement for deposition in newly replicated chromatin (Chambers and Shaw, 1984). No statistically significant change between the different acetylation isoforms of H4 was observed during exit of stationary phase

In H3, a shift towards higher levels of acetylation was again observed during exit of stationary phase. This tendency, however, was not statistically significant. The ratios between the different acetylation isoforms remained even during exit of stationary phase for both histones H2A and H2B. This was expected since it was demonstrated that the H2A-H2B dimer-tails played a lesser role in chromatin compaction (Krajewski and Ausió, 1996; Dorigo *et al*., 2003; Kan *et al*., 2007).

We were surprised by the fact that the acetylation levels of particularly histones H3 and H4 were not statistically significantly different between exponential and stationary phases, and investigated whether this could be due to a strain-specific effect. However, several genotypically distinct strains gave identical results.

We then extended our study with targeted mass spectrometry. Core histones H3 and H4, were isolated by the conventional zymolyase method, digested in the gel slice with trypsin, the peptides were eluted and analysed by mass spectrometry. We specifically performed a

precursor survey scan to detect the presence of peptides that generated an *m/z* 126 fragment by collision induced dissociation. This fragment was previously shown to allow the unambiguous assignment of a 42 Da mass shift in a fragmentation series to acetylated lysine as opposed to the approximately isobaric tri-methylated lysine. We found that there was a difference in the acetylation state of histone H3 and H4 in stationary and exponential phase in *S. cerevisiae*. The bulk of histone H3 was acetylated at K9, K14 and K36 in exponential phase. Immuno-precipitation studies have shown that histone H3 at lysine 9 and 14 was intensively acetylated at the predicted transcription start sites of induced genes (Pokholok *et al*., 2005).

We have also presented evidence that suggested that in exponential phase histone H4 K12 and K16 were both acetylated.

In the case of the TAU analysis, histones were isolated by a rapid isolation method. For the MS analysis, the histones were isolated by a conventional zymolyase method. A striking difference in the acetylation state of histones H3 and H4 in exponential and stationary phase were observed with the latter method. We propose that the major reason for the inconsistency in the observed acetylation states in the TAU the MS analyses were the two histone isolation methods used.

Reference

S. A. Chambers and B. R. Shaw. Levels of histone H4 diacetylation decrease dramatically during sea urchin embryonic development and correlate with cell doubling rate. *J Biol.Chem.* 259 (21):13458-13463, 1984.

B. Dorigo, T. Schalch, K. Bystricky, and T. J. Richmond. Chromatin fiber folding: requirement for the histone H4 N-terminal tail. *J.Mol.Biol.* 327 (1):85-96, 2003.

P. Y. Kan, X. Lu, J. C. Hansen, and J. J. Hayes. The H3 tail domain participates in multiple interactions during folding and self-association of nucleosome arrays. *Mol.Cell Biol.* 27 (6):2084-2091, 2007.

W. A. Krajewski and J. Ausio. Modulation of the higher-order folding of chromatin by deletion of histone H3 and H4 terminal domains. *Biochem.J.* 316 (Pt 2):395-400, 1996.

D. K. Pokholok, C. T. Harbison, S. Levine, M. Cole, N. M. Hannett, T. I. Lee, G. W. Bell, K. Walker, P. A. Rolfe, E. Herbolsheimer, J. Zeitlinger, F. Lewitter, D. K. Gifford, and R. A. Young. Genome-wide map of nucleosome acetylation and methylation in yeast. *Cell* 122 (4):517-527, 2005.